REGULATION OF LIVER FIBROSIS VIA ALTERATION OF HEPATIC STELLATE CELL ACTIVATION DURING LIVER REPAIR

A Dissertation

by

KELLY MARIE MCDANIEL

Submitted to the Office of Graduate and Professional Studies of
Texas A&M University
in partial fulfillment of the requirements for the degree of

DOCTOR OF PHILOSOPHY

Chair of Committee,	Gianfranco Alpini
Committee Members,	Fanyin Meng
	Shannon Glaser
	Cynthia Meininger
Head of Program,	Warren Zimmer

August 2017

Major Subject: Medical Sciences

ABSTRACT

Cholestatic liver diseases including primary biliary cholangitis (PBC), primary sclerosing cholangitis (PSC) and alcoholic-induced hepatobiliary damage are growing problems in the United States as well as worldwide. There are no successful treatments for these diseases that ultimately develop into cirrhosis and end stage liver diseases with no treatment but liver transplantation. We used the cholestatic bile-duct ligated (BDL) mouse liver to examine treatment with small or large cholangiocytes, a mouse model that mimics some features of PSC to study treatment with stem cell-derived extracellular vesicles and a mouse model of alcoholic liver disease to show the important role of let-7. After treatment, liver tissues/cells were analyzed for fibrosis, inflammation, endodermal markers and hepatic stellate cell activation. Mechanisms of action were evaluated further *in vitro* through the use of hepatic cell lines. We showed that small cholangiocyte treatment reduced fibrosis, biliary mass and stellate cell activation through enhanced expression of FoxA2. We additionally showed that treatment of cultured human stellate cell lines with cholangiocyte supernatants from small cholangiocyte-treated BDL mice showed increased senescence and decreased fibrosis and inflammation. Stem cell-derived extracellular vesicle treatment reduced fibrosis, biliary mass and inflammation while increasing FoxA2 gene expression. Treatment of stellate cells with medium from cultured cholangiocytes treated with stem cell-derived extracellular vesicles decreased inflammatory and fibrosis markers and increased senescence. We further showed that knockdown of Lin28 in mice, increased let-7 expression, reduced fibrosis and steatosis and reduced mesenchymal markers in stellate

cells but increased senescence. Taken together, these studies show that successful treatments can reduce fibrosis through alteration of stellate cell activation. These studies may provide important insights into future treatment options for cholestatic and alcoholic liver disease patients.

ACKNOWLEDGEMENTS

I would like to acknowledge my mentor. Dr. Gianfranco Alpini who encouraged me to continue my education and was tough on me throughout this process. He helped me to grow as a scientist and a person through his guidance. Additionally, I would like to acknowledge Dr. Fanyin Meng for his support and guidance through my time at the laboratories of Drs Alpini and Meng.

I would like to acknowledge and the current and former members of the Alpini and Meng labs who helped with these studies both intellectually and technically. These include, Julie Venter, Sugeily Ramos-Lorenzo, Tami Annable, Tianhao Zhou, Nan Wu, Ying Wan, Konstantina Kyristsi, Keisaku Sato, Thao Giang, and Lindsey Kennedy.

I would also like to acknowledge the investigators of the Baylor Scott and White DDRC, Drs Shannon Glaser and Heather Francis and my committee member, Dr. Cynthia Meininger, who were always available to help and guide me as well as challenge me when I needed them.

Finally, I would like to acknowledge the NIH, Baylor Scott and White and the Veteran's administration for funding these studies. I would also like to acknowledge the Central Texas Veterans Health Care System for providing our lab space and resources to perform these studies.

CONTRIBUTORS AND FUNDING SOURCES

CONTRIBUTORS

Part 1, faculty committee recognition

This work was supervised by a thesis (or) dissertation committee consisting of Distinguished Professor Dr. Gianfranco Alpini [committee chair] of the Department of Internal Medicine, Associate Professor Dr. Fanyin Meng, Associate Professor Dr. Shannon Glaser of the Department of Internal Medicine, and Professor Dr. Cynthia Meininger of the Department of Medical Physiology.

Part 2, student/collaborator contributions

All work for the thesis (or) dissertation was completed by the student, under the supervision of Dr. Gianfranco Alpini, Dr. Fanyin Meng and Dr. Shannon Glaser of the Department of Internal Medicine.

Funding Sources

Graduate study was supported by a fellowship from Texas A&M University, a VA Merit Award (1I01BX001724) to Dr. Meng, a VA Merit award to Dr. Alpini (5I01BX000574), a VA Merit Award (5I01BX002192) to Dr. Glaser, the Dr. Nicholas C. Hightower Centennial Chair of Gastroenterology from Baylor Scott & White, a VA Research Senior Career Scientist Award and, by NIH grants DK058411, DK107310, DK076898, DK095291 and DK062975 to Drs. Alpini, Meng and Glaser. This material is the result

of work supported by resources at the Central Texas Veterans Health Care System. The content is the responsibility of the author(s) alone and does not necessarily reflect the views or policies of the Department of Veterans Affairs or the United States Government.

TABLE OF CONTENTS

LIST OF FIGURES

LIST OF TABLES

1. INTRODUCTION

Liver diseases remain a major health concern in the United States and worldwide. The term "liver disease" includes over 100 etiologies of hepatic and biliary diseases, all of which can ultimately lead to liver failure over time. Currently, liver and biliary cancer combined is the 5th leading cause of death in U.S. men and the 9th leading cause of death in women [1]. Unfortunately, mortality from liver and intrahepatic and extrahepatic bile duct cancer continues to rise and is projected to be the third leading cause of cancer-related deaths in the U.S. by 2030 [2]. Current treatment strategies merely aim to prevent disease progression; therefore, more targets are needed in order to develop curative therapies. Many studies are currently underway to examine the mechanisms of liver and biliary tumorigenesis in an effort to identify novel treatment modalities.

The liver is the largest gland in the body. It is comprised of a right and left lobe divided by the falciform ligament. Blood is supplied to the liver from the inferior side via the hepatic artery which brings blood from the heart, and the portal vein, which brings blood from the gastrointestinal tract to the liver for filtering. Blood drains from the liver via the hepatic vein which connects to the inferior vena cava [3]. Besides filtering blood and producing vital proteins for the body, one of the liver's major functions is production of bile. Bile acids are produced by hepatocytes which when combined with bilirubin, produced from blood waste products, comprise bile which is essential for the breakdown of lipids during digestion [4]. Bile is drained from the liver for secretion into

the small intestine by bile ducts. These ducts are comprised of interconnecting tubules which grow from small to large ducts to make up the biliary tree. Microscopically, the liver is made up of hexagonal lobules which surround a central vein that empties into the hepatic vein. Branches of the hepatic artery, the portal vein and biliary tree surround each central vein and make up the portal triad. Blood is filtered through large-diameter capillaries called sinusoids from the branches of the portal vein and the hepatic vein to the central vein. Inside the sinusoids, Kupffer cells filter out toxins, dead blood cells and other material for excretion or storage in the liver. The sinusoids direct the clean blood to the central vein where it is returned to the heart for oxygenation by the lungs. Bile travels from the hepatocytes through bile canaliculi to the bile ducts where it travels to the gallbladder for storage before secretion into the small intestine when needed for lipid digestion.

There are many forms of acute and chronic liver diseases. The most common types of liver disease affect either the biliary tract or the liver parenchyma. Damage to the liver can occur as a result of substance abuse, overconsumption of fat and/or sugar, autoimmune disease, toxicity or heredity. In most cases, damage to any part of the liver affects the rest of the liver and can eventually lead to liver failure or cancer. In all cases of hepatic disease, a malfunctioning liver will affect the body's ability to produce crucial proteins, detoxify itself or disrupt the liver's ability to produce and release bile. Blockage of the biliary system can cause an obstructive biliary disorder which causes back of bile into the body of the liver and can lead to bile duct proliferation in an effort

by the cholangiocytes to bypass the blockage in addition to hepatic toxicity due to bile acid buildup (cholestasis) [5]. Any change in bile production will affect the body's ability to digest lipids as well as the homeostatic state of the liver.

The liver is remarkably capable of repair and regeneration. Although it is inundated by many toxins and other potentially hazardous substances, it is typically able to remove these impurities and dispose of them via urine. If a portion of the liver is removed, the cells of the liver are able to regenerate the portion that is missing via a compensatory mechanism. In order for the liver to regenerate itself, mature hepatocytes must divide or transform into a more stem-like state in order to produce more hepatocytes to make up for hepatocyte loss. This mechanism is true of cholangiocytes and other cells of the liver as well. In this way, the liver is a plastic organ which is able to respond to outside or internal damages and maintain its own homeostasis.

Cholangiopathies are a form of liver disease that are characterized by inflammation and/or destruction of cholangiocytes, the cells which line the bile ducts [6]. Because of inflammation and/or destruction of cholangiocytes, bile ducts become destroyed and/or obstructed leading to bile blockage, which causes cholestasis. Cholestasis leads to a number of medical problems, including increased liver fibrosis that eventually leads to cirrhosis and ultimately liver failure. The cells that are primary affected in cholangiopathies, cholangiocytes, line the bile ducts and serve as a barrier between the corrosive bile and the surrounding liver tissue [7]. The biliary tree has both small and

large bile ducts which are lined by small and large bile ducts, respectively [8]. It has been speculated that biliary progenitor cells are contained in the small cholangiocyte population and are able to repair and maintain the cholangiocyte population during liver injury [9].

There is a great deal of speculation by many sources about the biliary progenitors and their role in repair of the damaged biliary tree during cholangiopathies. One source of progenitor cells could be in the peribiliary glands, which contain a stem cell niche with cells that express factors expressed in both the liver and pancreas [10]. Additionally, there are the cells contained in the Canals of Herring which contain hepatic progenitors which are thought to be able to differentiate into any of the cells in the liver [11]. Another group has described an "intermediate hepatocyte" that expresses both hepatocyte and cholangiocyte markers and which may have the ability to replenish damaged hepatocytes or cholangiocytes [12]. These intermediate hepatocytes were shown to appear in correlation with increased inflammation and necrosis, indicating that the differentiation of stem cells to this intermediate hepatocyte is related to liver injury [13]. Another area of thought is that small cholangiocytes contain a reservoir of biliary progenitors that are able to repair and maintain the biliary epithelium [9, 14]. We will explore this last idea during these studies.

Because there is various debate about the source of stem cells to repair liver damage, one of the stem cell niches which could be important to repair is the mesenchymal stem cell.

These stem cells have been shown to be beneficial in the treatment of several diseases, such as osteoarthritis, autoimmunity and graft vs host disease [15-18]. Because there is an inflammatory response during cholangiopathies, these cells could be vital to modulating the inflammatory environment during cholestasis. It is thought that mesenchymal stem cells may be able to aid in liver repair [19, 20]. Because these cells don't routinely travel to the liver, transplantation of these cells, or harvesting of extracellular vesicles from these cells for transplantation may be of better therapeutic use.

Extracellular vesicles (EVs) are small membrane bound vesicles that are secreted through exocytosis by all cells in order to communicate with other cells. EVs encompass various sizes of membrane bound vesicles, including exosomes, microvesicles and apoptotic bodies. These EVs could contain various DNAs, RNAs, microRNAs or proteins that allow for these molecules to be transported to other cells. These EVs travel through the circulatory or lymph system to their target cells where the recipient cells receive the messages and change their behavior as a result. EVs could be a mechanism by which stem cells communicate with progenitor cells or other cells capable of becoming progenitor cells in order to repair the liver after injury.

Another serious liver disease that is prevalent worldwide is alcoholic liver disease (ALD). ALD is a widespread disease that affects millions of people worldwide. ALD occurs as a result of excess alcohol consumption over time and is characterized by

steatosis (fatty liver) and the sequelae of injury and inflammation leading to fibrosis (scarring) and eventual cirrhosis and end stage liver failure. Alcohol disrupts NAD+/NADH levels in the liver, which causes the steatosis and leads to further damage. It has been shown that ALD patients are more prone to a second hepatic insult, such as non-alcoholic fatty liver disease or hepatitis infection [21].

The common theme between cholangiopathies and ALD is inflammation that leads to liver fibrosis/cirrhosis. The primary cell type responsible for fibrosis is the hepatic stellate cell (HSC) [22]. In the normal liver, HSCs are quiescent, vitamin A storing cells. When liver injury occurs, HSCs become activated and transform into a myofibroblast phenotype [23]. These activated HSCs move to the site of injury where they lay down extracellular matrix (ECM) for dividing cells to adhere. Unfortunately, when cells do not divide for repair, HSCs secrete excessive amounts of ECM, which forms a scar and causes liver fibrosis [24].

A microRNA (miRNA) is a small non-coding RNA, which influences gene expression independent of any other regulation, typically by direct binding to 3'-UTR sites. These small regulatory RNAs have recently garnered a great deal of attention by the scientific community as potential targets for treating human disease and could be contained within EVs to serve as regulatory messages to other cells to coordinate liver repair. Several miRNAs have been shown to be altered during the progression of liver diseases [25]. One of the first miRNAs discovered, lethal-7 (let-7), is altered in several forms of liver

disease [26]. Additionally, let-7 is a major regulator of cellular differentiation in the developing organism. We have shown that let-7, a member of the miR-181 family, is upregulated in stem-cell-derived EVs compared to hepatocyte-derived EVs (unpublished data).

Lin28 is an RNA binding protein that is important in the regulation of development. [27] It has been shown to be a lineage modifying gene which is vital to maintenance of the stem cell phenotype [28, 29]. Lin28 has been shown to be a direct regulator of members of the let-7 family by direct post transcriptional binding to the microRNA, let-7. [30] Lin28 itself is regulated by miR-125 and let-7 [31-38]. In a see-saw type regulatory mechanism, differentiation is in part controlled by the expression of Lin28 and let-7. An abundance of let-7 correlates with a differentiated phenotype, whereas increased expression of Lin28 indicates an undifferentiated cellular phenotype. Logically, alterations in both let-7 family members and Lin28 have been shown in various cancers where Lin28 is overexpressed in highly aggressive and metastatic tumors. The Lin28/let-7 axis may have importance in the regulation of fibrosis during liver disease.

The studies reported here were designed to evaluate the role of progenitor cells and stem- cell-derived EVs in models of cholangiopathy. Additionally, these studies were designed to evaluate the role of let-7, a miRNA known to be upregulated in stem-cell-derived EVs in a model of ALD.

2. FORKHEAD BOX A2-REGULATED BILIARY HETEROGENEITY AND SENSESCENCE DURING CHOLESTATIC LIVER INJURY*

2.1. Overview

Biliary-committed progenitor cells (small cholangiocytes, SMCCs) from murine small bile ducts are more resistant to hepatobiliary injury than murine large cholangiocytes (LGCCs) from large bile ducts. The definitive endoderm marker, FoxA2, is a key transcriptional factor that regulates cell differentiation and tissue regeneration in systemic tissue. Our aim was to characterize the translational role of FoxA2 during cholestatic liver injury. The mRNA expression of FoxA2 in SMCCs and LGCCs was assessed by PCR array analysis. Liver tissues from Primary Sclerosing Cholangitis (PSC) and Primary Biliary Cholangitis (PBC) patients were tested by real-time PCR for methylation, senescence and fibrosis markers. Bile duct ligation (BDL) and Multidrug resistance type 2 gene (MDR2) knockout mice ($MDR2^{-/-}$) were used as animal models of cholestatic liver injury and were studied with or without healthy transplanted LGCCs or SMCCs. We demonstrate that FoxA2 was notably enhanced in murine liver progenitor cells and SMCCs, and was silenced in human PSC and PBC liver tissues relative to respective controls. The increase in FoxA2 was that are correlated with changes in the epigenetic methylation enzymes DNMT1 and DNMT3B. Serum alanine

aminotransferase (ALT) and aspartate aminotransferase (AST) levels in non-obese diabetic/severe combined immunodeficiency (NOD/SCID) mice engrafted with SMCCs after BDL showed significant changes compared with vehicle-treated mice, along with reduced liver fibrosis. Enhanced expression of FoxA2 was observed in BDL mouse liver after SMCC cell therapy. Furthermore, activation of fibrosis signaling pathways were observed in BDL/MDR2$^{-/-}$ mouse liver, and these signals were ameliorated along with reduced hepatic/enhanced hepatic stellate cellular senescence after SMCC engraft. Our data suggests that the definitive endoderm marker and positive regulator of biliary development, FoxA2, mediates the therapeutic effect of biliary-committed progenitor cells during cholestatic liver injury.

2.2. Introduction

The biliary epithelium is a complex network of interconnected ducts that increase in diameter from small to large bile ducts[39, 40]. The larger portion of the biliary epithelium is lined by mature, cAMP-dependent large cholangiocytes, whereas small (constitutively quiescent) cholangiocytes line small bile ducts [40-42]. Cholangiocytes are supported on a basement membrane and surrounded by connective tissue, extracellular matrix and the peribiliary plexus [43, 44]. These cells are specialized to act as an interface within the harsh environment imposed by bile and are morphologically and functionally heterogeneous, but with phenotypic patterns implicating a single maturational lineage. Small and large cholangiocytes have been characterized in the intrahepatic biliary epithelium of rats and mice and this phenotype is similar in humans as well [40, 41, 45-47]. It has been proposed that small cholangiocytes contain a population of biliary committed progenitors, showing expression of various biliary progenitor markers, and incorporate into neo-bile ducts at the sites of injury [9, 14]. When large cholangiocytes are damaged, small, Ca^{2+}-dependent cholangiocytes are activated, acquiring phenotypic and functional features of large cholangiocytes and resulting in the repopulation of the injured large bile ducts [40, 41, 45, 48].

The definitive endoderm markers FoxA2 and Sox17 are key transcriptional factors of cell differentiation [49, 50]. These transcriptional factors are essential for the establishment of developmental competence in the foregut endoderm and the initiation

of liver specification. Studies have shown that hepatic deletion of FoxA2 causes cholestasis in mice fed a cholic acid–enriched diet (40). In addition, FoxA2 is downregulated in human subjects with primary sclerosing cholangitis (PSC) and biliary atresia [51]. Other studies have demonstrated that FoxA2 and Sox17 are downregulated in the bile duct ligated (BDL) mouse model of obstructive cholestasis [52]. Thus, it seems likely that FoxA2 and Sox17 play a major role in patients with chronic cholestatic disorders. The Notch pathway is necessary for the specification of the biliary epithelium, and Notch pathway ablation results in failure of hepatoblast specification into cholangiocytes, resulting in bile duct paucity, a characteristic of Alagilles syndrome [53]. Furthermore, ectopic activation of the Notch pathway in fetal hepatoblasts by overexpression of the Notch intracellular domain (NICD) results in hyperarborization of biliary ductules [53]. It has been shown that TNFα dephosphorylates FoxA2 through IKKα. This activates Protein numb homolog (NUMB) transcription, which is able to inhibit NCID and prevent further downstream activation [54]. Interestingly, activated Notch signaling can affect the expression of both FoxA2 and Sox17 [55, 56], suggesting a functional link among these three multipotent molecules during the differentiation process.

Hepatocyte growth and proliferation may be blocked under the conditions that occur during severe liver injury [57]. When this occurs, cholangiocytes originating from the portal ductules and canals of Herring are able to initiate phenotypical changes allowing them to express hepatocyte-associated transcription factors [58]. Cholangiocytes can

also acquire stem cell phenotypes and, in turn, become hepatocytes, restoring liver regeneration when hepatocytes fail to proliferate [59]. However, an alternative interpretation is that regeneration after hepatic injury/partial hepatectomy is driven by liver and biliary stem/progenitor cells. Biliary stem/progenitor cells are thought to be located within the canals of Hering and have markers in common with biliary epithelia. Progenitor cells become more widespread in diseased conditions [12]. Therefore, when hepatocytes fail to proliferate in response to hepatobiliary injury, biliary progenitor cells are one of the most important regenerative alternatives. The following study evaluated the possible role of FoxA2-mediated biliary cell restorative therapy during cholestatic liver injury, especially recovery effects on biliary injury and liver fibrosis using BDL animal models (for chronic liver injury) and MDR2$^{-/-}$ mice that develop periportal fibrosis similar to humans with PSC [60].

2.3. Materials and Methods

Reagents

All reagents were purchased from (Sigma-Aldrich, St. Louis, MO) unless otherwise indicated. Antibodies against DNA (cytosine-5)-methyltransferase 1 (DNMT1), DNA (cytosine-5)-methyltransferase 3B (DNMT3B), cadherin 1 (CDH1), cadherin 2 (CDH2) and β-actin were purchased from Cell Signaling Technologies (Danvers, MA). The S100A4 primary antibody was purchased from AbCam (Cambridge, MA). All real-time PCR primers were obtained from Qiagen (Valencia, CA).

Human Subjects

Human samples were obtained from Dr. Pietro Invernizzi (Liver Unit and Center for Autoimmune Liver Diseases, Humanitas Clinical and Research Center, Rozzano, Milan, Italy) under a protocol by the Ethics Committee of the Humanitas Research Hospital; the protocol was also reviewed by the Veterans' Administration IRB and International Research Committee. The use of human tissue was also approved by the Texas A&M HSC College of Medicine Institutional Review Board.

Formalin-fixed, paraffin-embedded liver sections (4-5 μm thick) were obtained from three patients with PSC and three patients with primary biliary cholangitis (PBC). Five patients had advanced stage (3-4) biliary diseases [61] and one patient with PBC had an early stage of disease. The six control livers were obtained from patients undergoing resection of liver metastasis (Please see Table 1 for patients' information).

Table 1. Characteristics of Liver Donors of Normal Controls and PSC and PBC Patients

	Age (Years)	Sex	Pathological Diagnosis	Cirrhosis
PSC Patient 1	94	Female	Advanced stage	Yes
PSC Patient 2	18	Female	Advanced stage	No
PSC Patient 3	88	Male	Advanced stage	No
PBC Patient 1	65	Female	Advanced stage	Yes
PBC Patient 2	63	Female	Early stage	No
PBC Patient 3	55	Female	Advanced stage	Yes
Normal control 1	72	Female	Normal	No
Normal control 2	34	Female	Normal	No
Normal control 3	64	Male	Normal	No

Animal Models

The Animal Care and Use Committee of Baylor Scott & White approved the animal protocols according to the National Research Council's *Guide for the Care and Use of Laboratory Animals*. Male NOD.CB17-*Prkdc*^{scid}/J (NOD/SCID) mice (25-30 gm, 6 to 7 wk of age) were obtained from Jackson Laboratories (Bar Harbor, ME). Mdr2$^{-/-}$ mice were also obtained from Jackson Laboratories (FVB.129P2). BDL or sham surgery was performed as described [62, 63]. In all experimental groups, liver and body weight as well as liver-to-body weight ratio, an index of growth of liver cells (including cholangiocytes) were recorded.

Purified Cholangiocytes and Biliary Cell Lines

Small and large cholangiocytes were isolated by counterflow elutriation followed by immunoaffinity separation [45] with a monoclonal antibody (a gift of Dr. R Faris, Brown University, Providence, RI) against an unidentified antigen expressed by all non-malignant intrahepatic human (H69) (Meng and Alpini, unpublished observations, 2014) and murine cholangiocytes. The *in vitro* studies were performed in H69 cells (a gift from Gregory Gores, Mayo Clinic, Rochester, MN), human hepatic stellate cells (ScienCell, Carlsbad, CA), and our small (SMCCs) and large (LGCCs) murine cholangiocytes [64].

Isolation of Hepatic Stellate Cells by Laser Capture Microdissection

Frozen liver sections were sectioned with a cryostat and affixed to the membrane side of nuclease and human nucleic acid free 2.0mm PEN membrane slides (Leica Microsystems, Wetzlar, Germany). Slides were thawed at room temperature and fixed in ice cold 100% methanol for 3 minutes. Slides were rinsed briefly in ice cold phosphate buffered saline (PBS) and then blocked with 5% goat serum for 2 hours at 4^{o}C. A 1:50 dilution of desmin-specific antibody (Abcam, Cambridge, MA) was applied to the slides and they were incubated overnight at 4°C. Slides were rinsed 4 times in ice cold PBS and an Alexa Fluor® Plus 488 (ThermoFisher, Waltham, MA) fluorescent secondary antibody was applied overnight at 4^{o}C. Slides were rinsed 4 times with ice cold PBS. A laser capture microdissection (LCM) system LMD7000 (Leica, Buffalo Grove, IL) was then used to capture desmin-positive cells and collect them in a thin walled PCR tube. The collected cells were then used to isolate RNA with the Arcturus Pico Pure RNA Isolation Kit (Applied Biosystems, Foster City, CA) according to the manufacturer's instructions. The complementary DNA was made and qPCR was performed as described above.

Cell Transfections

Transfections were performed using the Lipofectamine transfection reagent (Life Technologies, ThermoFisher, Waltham, MA), the SiTran1.0 reagent (Origene, Rockville, MD) or the Turbofectin 8.0 reagent (Origene, Rockville, MD), according to the manufacturers' guidelines. Transfection conditions for each hepatobiliary cell line were first optimized to result in 20%-30% transfection efficiency with a cell viability of more than 80%. The transfection efficiency of the SMCCs and LGCCs used was 9.8% ± 0.8%. On day 1, specific siRNAs were transfected at a concentration of 50 nM using the transfection reagents following the manufacturer's protocol. The transfection medium was then replaced daily with regular culture medium containing serum for 72 hours prior to study. All studies were performed in quadruplicate unless otherwise specified.

SuperArray qPCR Assay and Real Time PCR Analysis

RNA was isolated from liver tissues or cell lysates using TRIzol (Invitrogen, Carlsbad, CA) or the miRVANA RNA Isolation Kit (Life Technologies, Carlsbad, CA), according to the manufacturer's protocol. Reverse transcription was done using 1 μg RNA with SABiosciences' RT^2 First Strand Kit (SABiosciences, Frederick, MD) according to the manufacturer's protocol. Mouse liver tissue or normal human hepatocytes cDNA was analyzed using SuperArray plates (Epigenetic Chromatin Modification Enzymes PCR Array**,** #PAMM-085Z or Mouse Fibrosis PCR Array, #PAMM-120Z, SABiosciences, Frederick, MD). To validate the translational significance of these gene expression findings, mice liver or human hepatocytes samples were analyzed using Real-time PCR.

SABiosciences's RT² qPCR Primer Assays or Taqman miRNA PCR assay were used. Real-time PCR was performed using SABiosciences' RT^2 SYBR Green/ROX qPCR Master Mix for a Stratagene Mx3005P Real-Time PCR System according to the manufacturer's protocol. ROX was used as an endogenous reference and data were analyzed using SABiosciences' PCR Array Data Analysis Template. The comparative C_T method ($\Delta\Delta C_T$) was used for quantification of gene expression. All samples were tested in triplicate, and average values used for quantification. For PCR Arrays, data analysis of gene expression was performed with online software provided by the manufacturer (Qiagen, Valencia, CA). The data were expressed as fold-changes with normalization of five housekeeping genes (β2 microglobulin, hypoxanthine phosphoribosyl-transferase 1, ribosomal protein L13a, GAPDH, and β-actin). The genes that showed more than two-fold higher changes in the PCR array were further analyzed using ingenuity pathway analysis (IPA) software (Ingenuity System, Qiagen, Redwood City, CA) for the functionally relevant pathway.

Western Blotting

Cells grown in 6-well dishes were washed twice with ice-cold PBS before lysis. Protein concentrations were measured and equivalent amounts of protein were mixed with gel electrophoresis sample buffer, separated in a 4%–20% linear gradient Tris-HCl-ready gel (Bio-Rad), and then transferred to nitrocellulose membranes. The membranes were blocked with milk and then incubated with primary antibodies and IRDye700- and IRDye800-labeled secondary antibodies (Rockland, Gilbertsville, PA) according to the

manufacturer's instructions. The protein of interest was visualized and quantitated using the LI-COR Odyssey Infrared Imaging System (LI-COR Bioscience, Lincoln, NE).

Senescence-Associated Galactosidase (SA-β-gal) Activity Assay and Cytochemical Staining for SA-β-Galactosidase

Liver tissues or cells were lysed in reporter lysis buffer (Promega, Madison, WI). Tissues or cell lysates containing equal amounts of total protein were diluted in equal volumes of 2× assay buffer containing 1.33 mg/ml *o*-nitrophenyl-d-galactopyranoside, 2 mm $MgCl_2$, and 100 μl of 2-mercaptoethanol in 200 mM phosphate buffer (pH 6.0), and incubated at 37 °C for 4 h. The absorbance at 420 nm was measured after addition of an equal volume of 1 M Na_2CO_3. Cytochemical staining for SA-β-galactosidase was performed using a Senescence β-Galactosidase Staining Kit (Cell Signaling Technology, Danvers, MA) at pH 6.0. All the experiments were repeated three times, and one of the representative results is shown.

Immunocytochemistry and Immunofluorescence

Cells were cultured to confluency on glass coverslips. Frozen cross sections (4-5 μm thick) were cut with a cryostat and mounted on glass slides. Monolayers or slides were washed twice and fixed in 4% ice-cold paraformaldehyde for 10 minutes, then blocked in 1x PBS containing 5% donkey serum for 1 hour at room temperature before incubation with primary antibodies overnight at 4°C, followed by secondary fluorescein isothiocyanate–conjugated anti-rabbit (1:200) or Texas Red–conjugated anti-mouse IgG

(1:200) for 2 hours at room temperature. After 3 washes, coverslips with monolayers were mounted on glass slides or slides with tissue sections were coverslipped with ProLong antifade mounting medium with DAPI (Molecular Probes). Images were viewed and captured using an Axiovert 200 Confocal Microscope Imaging System from Carl Zeiss MicroImaging Inc. (Thornwood, NY).

ELISA Assay

TGF-β (TGF-β ELISA KIT, BioSource^{TM} CA, USA) ELISA assays were performed according to the manufacturer's instructions. Negative and positive controls were included and a standard curve was determined for each assay. Sample size of the protein extract was 10 μL. Normalization was carried out by calculating relative protein concentration.

Cell Isolation, Labeling and Transplantation

Small and large cholangiocytes were isolated from healthy C57BL/6 mice, immortalized and cultured, as previously described (PMID: 19204666). Mouse liver stem cells were obtained from Celprogen (Torrance, CA) and cultured as recommended by the manufacturer. Cell viability was tested by trypan blue dye exclusion and was 80% or greater. For cell transplantation studies, bile duct ligation (BDL) surgery was performed on NOD/SCID mice and subsequently mice were injected intraperitoneally (IP) with 3×10^6 cells in MaxGel ECM (Sigma-Aldrich, St Louis, MO) (total volume = 0.1 ml) on

days 1 and 3 post BDL surgery. These animals were studied for reversal of biliary injury over 1 week versus vehicle-treated BDL mice.

To determine whether donor cells were distributed to various organs after transplantation, donor cells were labeled using the PKH26 Red Fluorescent Cell Linker Kit (Sigma-Aldrich, St Louis, MO) at room temperature according to the manufacturer's protocol. We then transplanted these cells into BDL NOD/SCID mice at 1 and 3 days post surgery via IP injection, followed by analysis of the presence of transplanted cells in the peritoneal cavity, liver, spleen, and lungs after 24 hours, 48 hours, and 7 days by detection of the presence of red fluorescence that transplanted cells were marked with by the PKH26 kit. Livers from these animals were analyzed for: (i) intrahepatic bile duct mass (IBDM) in paraffin-embedded liver sections (4-5 μm thick) by semiquantitative immunohistochemistry for CK-19, a specific marker of bile ducts (10 different fields analyzed from each sample obtained from 3 different animals); (ii) biliary apoptosis using the TUNEL kit (Promega) according to the manufacture's protocol; (iii) liver fibrosis by Sirius Red staining for identifying interstitial collagen with red color in paraffin-embedded liver sections (4–5 μm thick, 10 different fields analyzed from each sample obtained from 3 different animals); and (iv) the expression of Bax, FoxA2, Notch1, BMP1, Sox17, α-SMA and Col1A1 mRNA in total liver by real-time PCR [64].

Cholangiocyte Supernatants

After cholangiocytes were isolated, as described above, 1 x 10^6 cholangiocytes were placed in a solution of 1X Hanks Balanced Salt Solution (HBSS) + $CaCl_2$ and incubated

for 6 hours in a 37^{o}C water bath. The tubes were centrifuged at 1600 x g and the supernatant was collected and stored at -80^{o}C until analyzed.

Statistical Analysis

All data are expressed as mean ± SEM. The differences between groups were analyzed by Student's two tailed *t*-test when two groups were analyzed or ANOVA if more than two groups were analyzed. A *P* value <0.05 was used to indicate statistically significant differences.

2.4. Results

Characterization of Biliary Progenitor Phenotypes in Human and Murine Small and Large Cholangiocytes

To demonstrate potential progenitor phenotypes in small and large cholangiocytes in culture, we performed real-time PCR-based superarray analysis. The Stem Cell PCR Array was chosen because it contains 84 key genes related to the identification, growth and differentiation of stem/progenitor cells. Some of these markers are seen frequently in the definitive endoderm (DE) of the developing embryo, and these DE markers could be useful in the identification of progenitor cells located in small cholangiocytes. We found that 7 of the 84 genes were markedly upregulated in small cholangiocyte lines (SMCC) relative to large cholangiocyte lines (LGCC) used as controls; we also detected several down-regulated genes. The two most up-regulated genes were the *DE markers*, FoxA2 and Sox17 (Figure 1A). Up-regulation of these genes in mouse and human small and large cholangiocytes was also evaluated by real-time PCR, which confirmed the array data (Figure 1B). Expression of activated TGF-β-dependent Notch1 and Notch ligand, Jagged 1 (*JAG1*), was also found to be upregulated in SMCCs compared to LGCCs accompanied by a reduced level of E1A Binding Protein P300 (EP300). Interestingly, several other *markers* for *progenitor* cells of the adult epithelium, *such as BMP1 and ALDH1,* were also overexpressed in mouse and human SMCCs.

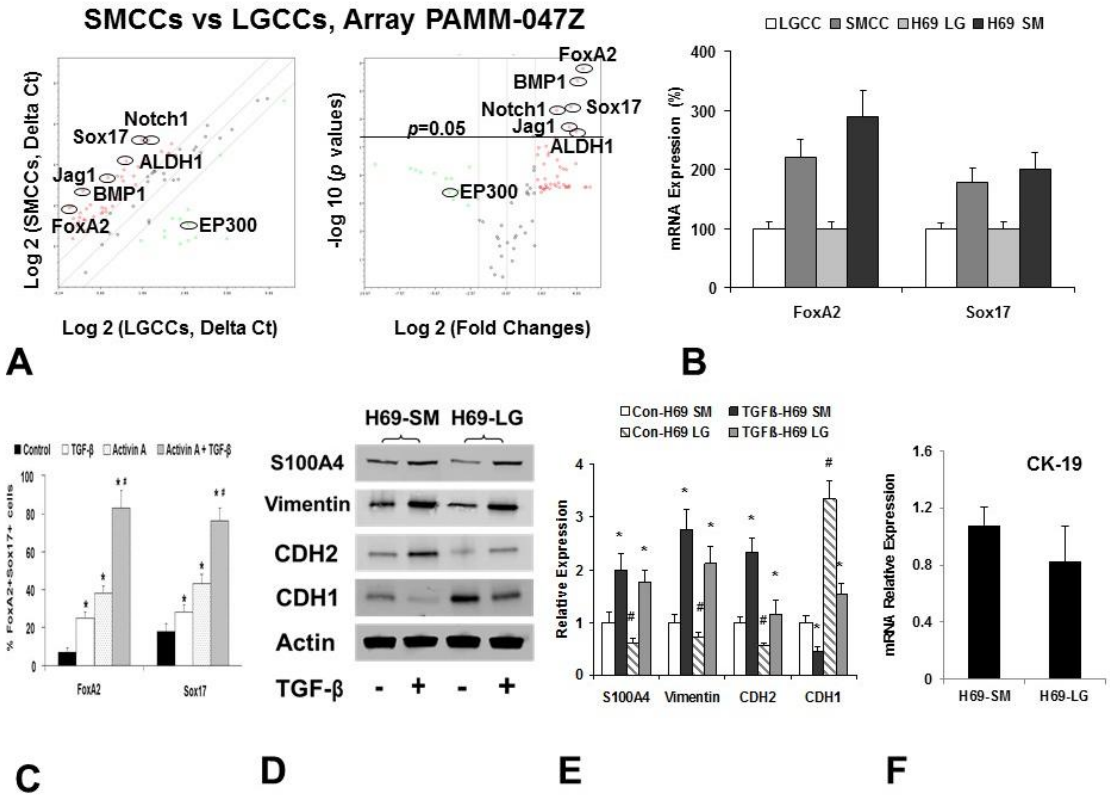

Figure 1. Functional analysis of FoxA2, Sox17, Notch1 and BMP1 in small cholangiocytes/biliary-committed progenitors. ***Panel A:*** Relative gene expression profile of small cholangiocytes (SMCCs) versus large cholangiocytes (LGCCs) is shown (n=3). The expression of a panel of diverse stemness-associated genes was evaluated by real-time PCR using the Mice Stem Cell PCR Array from SABioscience. FoxA2 and Sox17 are the most up-regulated genes among the six stem cell signaling pathways shown for biliary committed progenitors. ***Panel B:*** Total RNA was extracted from SMCC, LGCC, H69-SM and H69-LG cells, and FoxA2 and Sox17 expression was assessed by quantitative real-time PCR. The relative mRNA expression was normalized to expression of LGCC or H69-LG as % of control. *$p < 0.05$ when compared with mRNA expression of LGCC or H69-LG cells. ***Panel C:*** Immunocytochemistry for FoxA2 and Sox17 was performed in murine liver progenitor cells treated with TGF-β and/or activin A (both at 10 ng/ml) in William's E medium for 7 days. A significant increase in the percentage of FoxA2- and Sox17-positive cells was observed in LPC cell lines after TGF-β + activin A treatment. *$p < 0.05$, compared with expression in the TGF-β- or activin-only group. ***Panel D&E:*** *TGF-β regulated mesenchymal to epithelial transition (MET) process in human small and large cholangiocytes.* Proteins were isolated from human small and large cholangiocytes treated with TGF-β (10 ng/ml) or diluent control for 7 days. Western blot confirmed reduced MET process after TGF-β treatment**.** Western blots of H69 cell lysates (TGF-β-treated groups and controls) were performed and sequentially probed with antibodies against mesenchymal markers S100A4, vimentin, CDH2; epithelial markers CDH1, and β-actin as a loading control as indicated. Representative immunoblots are shown on the *Panel D* along with quantitative data that show the mean ± standard error (S.E.) from four separate blots of independent experiments on *Panel E*. * $p < 0.05$ relative to H69 controls, # $p < 0.05$ relative to isolated small H69 human cholangiocytes (SM). ***Panel F:*** H69 human cholangiocytes were separated by counterflow elutriation into small and large populations. RNA was extracted from these separate populations and cytokeratin-19 (CK-19) expression was analyzed with qPCR. No change was seen between the two groups.

TGF-β and Activin A Promote Human Liver Progenitor Cells to Acquire Small Biliary Phenotypes

DE has been successfully derived *in vitro* from mouse embryonic stem cells (ESCs) using culture conditions of low serum and high concentrations of activin A. Under these conditions, it has been shown that TGF-β improves the efficiency of activin A-induced DE differentiation from human ESCs [65]. We hypothesized that TGF-β improves the efficiency of activin A-induced biliary differentiation in human liver progenitor cells (LPCs). To test this hypothesis, we treated human LPCs with activin A in the presence or absence of TGF-β in William's E medium for 7 days on plates coated with Matrigel®, which has been shown to promote the differentiation of hepatic progenitor cells to cholangiocytes. After treatment in William's E medium for 7 days, cells were analyzed for the expression of FoxA2 and Sox17. Immunofluorescence staining (IF) revealed that approximately 80% of the cells treated with activin A and TGF-β expressed FoxA2 or Sox17, whereas only about 40% of the cells were FoxA2- or Sox17-positive when treated with activin A alone (Fig. 1C). TGF-β alone did not affect biliary differentiation. Real-time PCR confirmed that the expression of FoxA2 and Sox17 mRNA was significantly increased upon co-treatment with both activin A and TGF-β, whereas the addition of TGF-β alone did not induce biliary differentiation from human LPCs. Together, these preliminary data indicate that TGF-β augments human LPC-derived SMCC formation by acting synergistically with activin A.

Since TGF-β is a well-known mesenchymal to epithelial transition (MET) inhibitor, we aimed to demonstrate TGF-β activation of the mesenchymal markers, S100A4 and vimentin in small and large cholangiocytes *in vitro*. TGF-β (10 ng/ml) induced significant cell differentiation after 7 days of incubation, as measured by S100A4 and vimentin protein expression, as well as by the epithelial marker, E-cadherin (CDH2), to the mesenchymal marker, N-cadherin (CDH1), switch in human small and large cholangiocytes (Fig.1, D&E). Analysis of cytokeratin-19 (CK-19) levels by real-time PCR showed similar levels of CK-19 in H69 LGCCs compared to SMCCs (Fig. 1F).

FoxA2 and Sox17 Expression is Epigenetically Regulated

To evaluate the potential epigenetic mechanisms by which the expression of FoxA2 and Sox17 is deregulated in small cholangiocyte/biliary progenitors, we performed a Real-Time PCR-based Superarray analysis. The Epigenetic Chromatin Modification Enzymes PCR Array was chosen because it contains 84 key genes encoding enzymes known or predicted to modify genomic DNA and histones to regulate chromatin accessibility and gene expression. The two most down-regulated genes detected by PCR array in SMCCs relative to LGCCs were *DNMT3B* and *DNMT3A (Fig. 2A)*. Down-regulation of these genes was confirmed by real-time PCR (Fig. 2B). Additionally, analysis of the promoter regions of FoxA2 and Sox17 by the MethPrimer program [66] revealed the presence of several CpG islands ~2000 basepairs upstream of the 5'-coding regions, which are commonly modified by epigenetic regulation (Fig. 2C). To evaluate the direct relationship between methylation and FoxA2 or Sox17 expression in cholangiocytes, the

methylation inhibitor, 5-Aza-CdR, was used to treat SMCCs or LGCC *in vitro* before evaluating FoxA2 and Sox17 expression. The marked increases of FoxA2 and Sox17 expression were noted in LGCCs (but not SMCCs) compared to controls after 5-Aza-CdR treatment (Fig. 2D). These results suggest that the expression of FoxA2 and Sox17 may be potentially regulated by modulation of promoter methylation. Of note, histone acetylation has been shown to activate the expression of FoxA2 and Sox17 during the early stage of hepatocyte differentiation [67]. To evaluate the direct relationship between DNMT3A and cell size, DNMT3A was overexpressed in SMCCs. Overexpression of DNMT3A resulted in an increase in overall cell size (Fig. 2E) as well as increased levels of the LGCC markers, CFTR, secretin and secretin receptor [41] (Fig. 2F), indicating the ability of DNMT3A to influence cell size through possible downregulation of DE markers. Additionally, the direct relationship between FoxA2 and Sox17 expression was analyzed by real-time PCR. Overexpression of DNMT3A resulted in reduced levels of FoxA2, Sox17, Notch1 and BMP1 (Fig. 2G), indicating the relationship between DNMT3A and these endodermal markers.

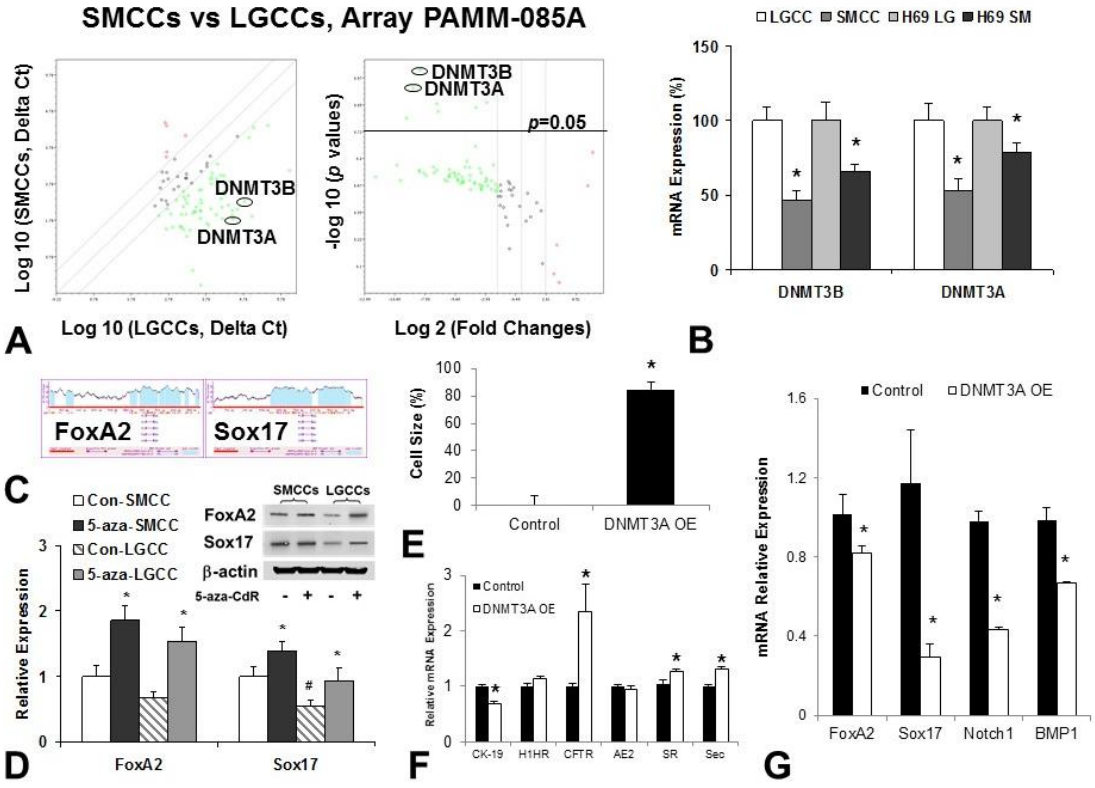

Figure 2. Epigenetic regulation of FoxA2 and Sox17 expression in biliary committed progenitor cells. ***Panel A:*** The expression of *DNMT3B* and *DNMT3A* is down-regulated in small cholangiocytes. Relative gene expression profile of SMCCs versus LGCCs is shown (n=3). The expression of a panel of diverse epigenetic-associated genes was evaluated by real-time PCR using the Mouse Epigenetic Chromatin Modification Enzymes PCR Array from SABioscience. Gene expression relative to GAPDH was plotted as volcano plots, depicting the relative expression levels (Log 2) for selected genes in SMCCs versus control LGCC panels (**Left**). The relative expression levels and p values for each gene in the related samples were also plotted against each other in the scatter plot (**Right**). *DNMT3B* and *DNMT3A* are the most down-regulated genes among the five epigenetic signaling pathways in cholangiocytes. ***Panel B:*** Real-Time PCR confirmed the reduced mRNA expression of DNMT3B and DNMT3A in cultured SMCCs, isolated SMCCs from BDL mice liver and small human cholangiocytes (H69-SM) compared to respective controls. The percentages shown represent the mean value (relative to control) normalized with GAPDH from four independent experiments. ***Panel C:*** Analysis of the promoter region using MethPrimer software revealed the presence of several CpG islands ~2000 basepairs upstream of the 5'-region of the FoxA2 and Sox17 sequences. ***Panel D:*** Small and large cholangiocytes were treated with 10 μM 5-aza-2'deoxy-cytidine (5-Aza-CdR) or diluent control for 72 hr. The expression of FoxA2, Sox17 and Notch1 was assessed by western blot analysis. 5-Aza-CdR increased FoxA2 and Sox17 expression in LGCCs but not SMCCs. Representative immunoblots are shown on the *top right* along with quantitative data that show the mean ± S.E. from four separate blots of independent experiments on the *bottom panel*. * $p < 0.05$ relative to controls, # $p < 0.05$ relative to SMCCs. ***Panel E:*** DNMT3A was overexpressed in SMCCs. Cells were harvested with trypsin, stained with trypan blue and cell size was measured compared to control as a percentage with the control set at 0. *p < 0.05 compared to control. ***Panel F:*** DNMT3A was overexpressed in SMCCs. RNA was extracted and markers of small and large cholangiocytes were measured with qPCR. *p < 0.05 compared to control. ***Panel G:*** DNMT3A was overexpressed in SMCCs. RNA was extracted and DE markers were measured with qPCR. *p < 0.05 compared to control.

Altered TGF-β-induced Signaling and Remodeling and Fibrosis in Experimental Models of Cholestatic Liver Injury In Vivo

Consistent with the role of TGF-β-induced cell differentiation *in vitro*, in rodent models of cholestasis, BDL or MDR2$^{-/-}$, secretion levels of soluble TGF-β were significantly up-regulated (Fig. 3A). To determine the mechanisms of TGF-β mRNA alterations and their effects on modulating target protein expression *in vivo*, we compared BMP1/FoxA2/Notch1/Sox17 expression in tissue homogenates and isolated cholangiocytes from mouse liver. The expression of BMP1/FoxA2/Notch1/Sox17 protein and mRNA was significantly decreased in BDL and MDR2$^{-/-}$ mouse liver and isolated cholangiocytes compared to normal controls (Fig. 3 B&C), which suggests alternate TGF-β-regulated miRNA/mRNA expression patterns in different liver cell types. To explore this further, we overexpressed TGF-β in SMCCs and analyzed levels of DE markers. Unlike in total liver or isolated pooled (that include both small and large) cholangiocytes, FoxA2 was increased in SMCCs (Fig. 3D) indicating that upregulation of TGF-β leads to upregulation of FoxA2, which may indicate activation of the progenitor cells contained in SMCCs. Activated DE differentiation markers, FoxA2 and Sox17, were observed in small bile ducts after cholestatic liver injury in BDL and MDR2$^{-/-}$ mice (Data not shown). To further assess the extent of fibrosis/cirrhosis in BDL/MDR2$^{-/-}$ mouse liver, Sirius Red staining was performed on liver sections from both animal models (Figure 3E&F). Control mice had a normal distribution of collagen, whereas those with BDL and MDR2$^{-/-}$ demonstrated obvious signs of fibrosis. Mice with

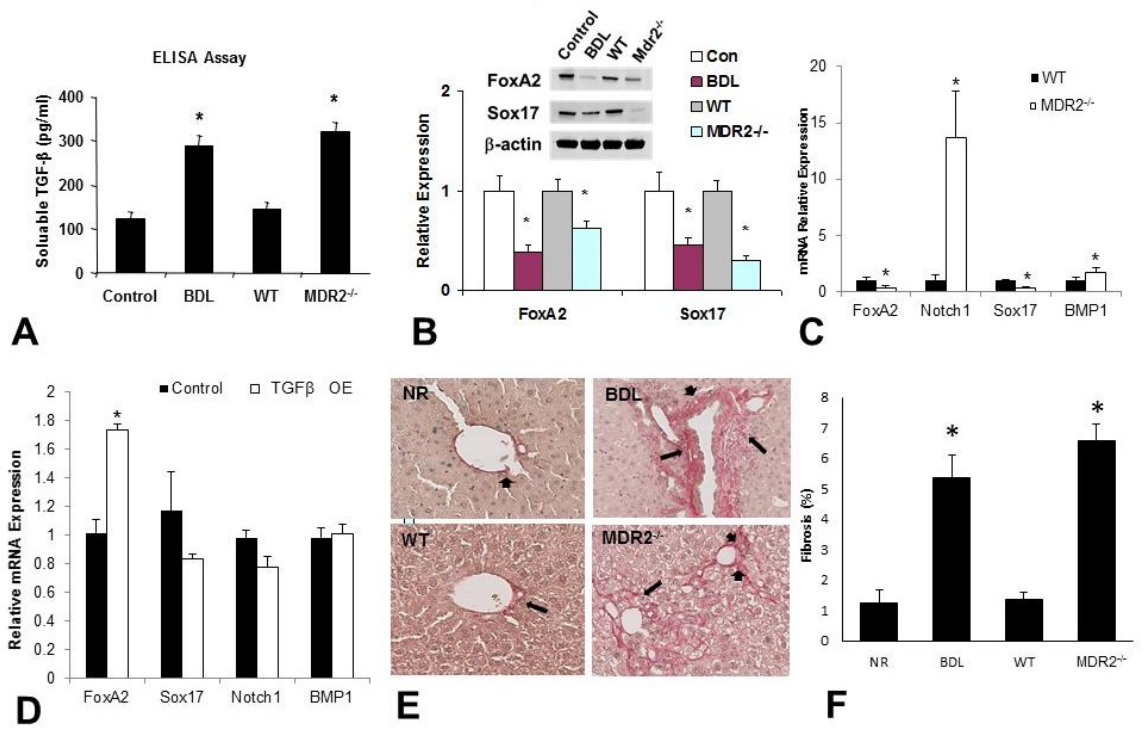

Figure 3. Altered cholangiocyte differentiation and remodeling process during cholestatic liver injury. ***Panel A:*** Supernatants from liver tissue homogenates obtained from a surgical (bile duct ligation [BDL]) or transgenic ($MDR2^{-/-}$) mouse model of cholestatic liver injury were harvested with respective controls (normal or wild type), and soluble TGF-β levels were measured by ELISA (n=4). There were significant increases in soluble TGF-β levels in liver of BDL or $MDR2^{-/-}$ mice. ***Panel B&C:*** Verification of specific protein and mRNA expression in BDL and $MDR2^{-/-}$ mice liver (n=4). Proteins and total RNA were isolated from BDL/$MDR2^{-/-}$ mice liver tissue homogenates, and expression of specific proteins and mRNAs were verified by western blot (*Panel B*) and Taqman real-time PCR analysis (*Panel C*). In *Panel B* representative immunoblots are shown on the *top panel* along with quantitative data that show the mean ± S.E. from four separate blots of independent experiments on the *bottom panel*. Reduced expression of FoxA2, BMP1, Sox17 and Notch1 after cholestatic liver injury was observed in both models. ***Panel D:*** TGF-β was overexpressed in SMCCs, RNA was extracted and levels of DE markers were measured with qPCR. *$p <$ 0.05 compared to control. ***Panel E-F:*** Percentages of positive cells stained with Sirius Red were counted in BDL and $MDR2^{-/-}$ mouse liver with the respective controls. Significantly increased intensity of liver fibrosis was confirmed in both models by enhanced Sirius Red expression ($n = 5$). *$p < 0.05$ *versus* normal or WT controls.

BDL injury demonstrated bridging fibrosis and those with MDR2$^{-/-}$ had diffuse collagen deposition, suggesting severe liver fibrosis in both models of cholestatic liver injury.

FoxA2 is Down-regulated in Human Cholestatic Livers

We have shown previously that TGF-β levels are elevated in patients with PSC and PBC as well as levels of fibrotic genes such as collagen 1A1, fibronectin and α-SMA [68]. Next, we aimed to determine whether the expression of DE and epigenetic markers is changed under cholestatic conditions in humans. FoxA2 mRNA levels were virtually undetectable in patients with PSC (Fig. 4A, left), as well as in those with PBC a reduction in expression was noted in 2 out of 3 livers examined (Fig. 4A, right). Meanwhile, the expression of Sox17 was significantly increased in PSC livers but reduced in PBC livers (Fig. 4B&C), suggesting different pathological mechanisms regulating this DE marker in human cholestatic liver disorders. In both PSC and PBC patients, Notch-1 and BMP-1 levels were increased compared to normal patients (Fig 4D&E). These results show that certain progenitor markers are indeed altered frequently in human PSC and PBC. To further verify the upstream mechanisms of FoxA2 regulation, we performed real-time PCR studies to detect the mRNA expression of the enzymes that catalyze the methyl-transfer reaction, the DNA methyltransferases. Both DNMT1 and DNMT3B were significantly up-regulated in PSC and PBC livers (Fig. 4B&C), which is consistent with our cell culture studies (Fig. 2D) and implies that there are potential epigenetic regulatory mechanisms of FoxA2 during the development and progression of human PSC and PBC. Thus, cholestatic liver injury of differing etiologies

causes downregulation of FoxA2 in humans, which may occur through the epigenetic regulation mechanisms and, together with our findings, suggests that low FoxA2 levels exacerbate fibrotic injury to the liver.

Role of Small Cholangiocyte Therapy in Ameliorating BDL-induced Biliary Damage and Liver Fibrosis

Because small cholangiocytes may possibly contain a compartment of progenitor cells for repairing the biliary epithelium, we performed studies to determine whether suitable biliary support exists by determining if using transplanted small cholangiocytes would permit hepatic repair and regrowth of the damaged liver. Because cholangiocytes can be transplanted in large numbers in the peritoneal cavity, readily equaling or exceeding those in the liver, we labeled cultured SMCCs and LGCCs with a red fluorescent marker (PKH26), suspended them in extracellular matrix (ECM) and injected them into BDL mice 1 and 3 days post-surgery. The translocation of engrafted biliary progenitors/cholangiocytes in the liver was detected in liver sections after cell therapy (Fig. 5A). Serum ALT and AST levels in NOD/SCID mice engrafted with SMCCs and liver stem cells ($3 \text{ X } 10^6$, i.p.) showed significant changes compared with vehicle-treated mice (Data not shown), along with significantly improved TGF-β levels in bile (Fig. 5B). The activated DE differentiation marker, FoxA2, was observed in BDL mice liver after cholestatic injury coupled with SMCC cell therapy (Fig. 5C). Furthermore, decreased Sirius Red staining (Fig. 5D&E), along with altered remodeling properties, such as activation of matrix metalloproteinase MMP-9/MMP-2 and silencing of tissue

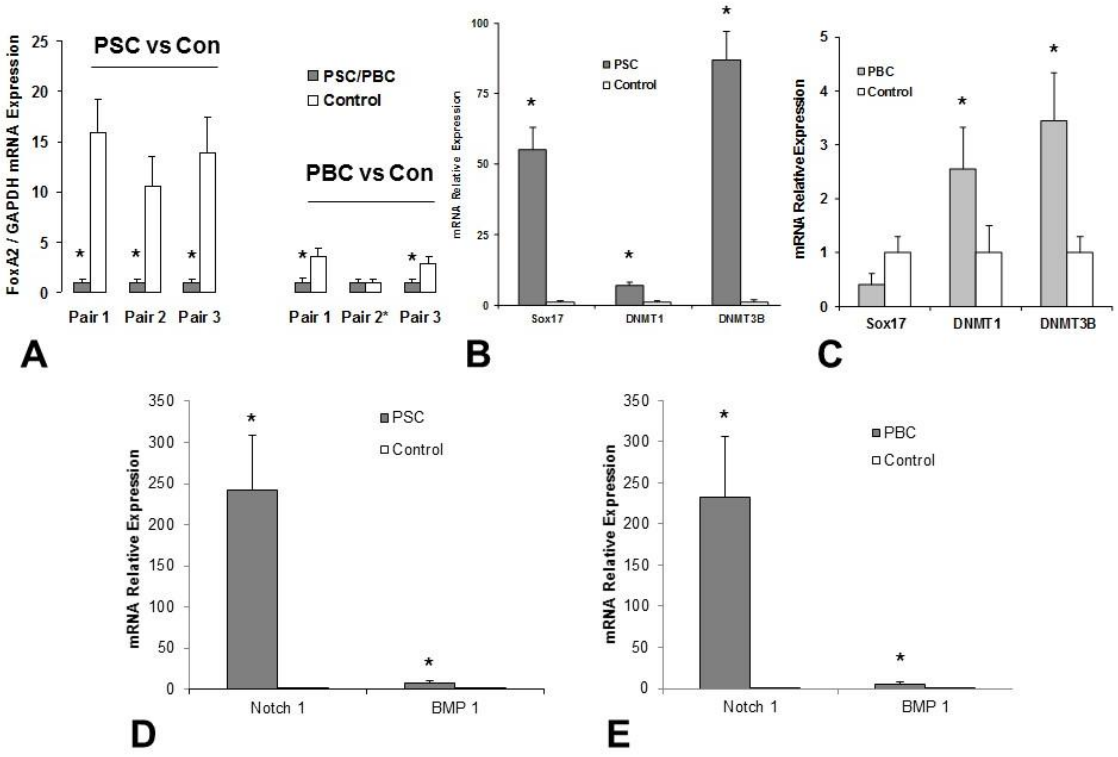

Figure 4. Enhanced fibrosis markers along with the reduced FoxA2 expression in human PSC/PBC liver. ***Panel A-E:*** Altered FoxA2, Sox17, Notch1 and BMP-1 expression along with enhanced DNA methyltransferase expression in human PSC and PBC liver tissues. Total RNA was isolated from human liver from normal controls or patients with PSC/PBC. Real-time PCR analysis was performed, and the ratio of specific mRNAs to GAPDH mRNA expression in human liver samples was determined. The PCR products were also verified by 1.8% agarose gel electrophoresis. FoxA2 was significantly reduced in 5 among 6 PSC/PBC livers relative to normal controls (Panel A). Meanwhile, the expression of Sox17 was only silenced in PBC liver tissues but increased in PSCs (Panel B&C). DNA methylation enzymes, DNMT1 and DNMT3B, were also increased in both PSC and PBC livers, suggesting the potential hypermethylation mechanisms of FoxA2 gene during PSC/PBC development. Additionally, both Notch-1 and BMP-1 were significantly reduced in PBC and PSC livers compared to controls (Panel D&E). Data represent mean ± S.E. from liver samples from three PSC or three PBC patients relative to three normal controls in three separate experiments. *$p < 0.05$ relative to normal controls.

inhibitor of metalloproteinase TIMP-3, as well as enhanced expression of remodeling protein α-SMA (Suppl. Fig. 1E), were observed in BDL mice liver recovered after SMCC engraft, suggesting that remodeling enzymes and proteins are important mediators for SMCC-mediated recovery of cholestatic liver injury and liver fibrosis. Additionally, we examined total liver tissue for markers of cholangiocytes and saw upregulation of the large cholangiocyte markers in BDL mice treated with either small or large cholangiocytes. BDL mice treated with LGCCs showed upregulation of secretin and secretin receptor (Fig. 5F), which isexpected due to the large influx of LGCCs. Additionally, we saw a decrease in the large cholangiocyte markers, AE2 and secretin receptor, in SMCC-treated cholangiocytes, most likely due to the large increase in small cholangiocytes.

Potential Molecular Mechanisms by which Biliary Cell Therapy Improves BDL-induced Biliary Damage and Liver Fibrosis

To examine the molecular mechanisms by which biliary cells reversed BDL-induced hepatobiliary damages, we used the Mouse Fibrosis PCR array (PAMM-120ZA, Qiagen) and combined it with PCR analysis of inflammation- and stem cell & development-related genes to evaluate mechanisms related to liver fibrosis, inflammation and stem cell signaling pathways. The α-SMA, MMP-8 and MMP-9 genes were the most down-regulated genes among the fibrotic signaling pathways in cholestatic liver (BDL) coupled with SMCC therapy compared to those treated with LGCC therapy (Fig. 6A). Ingenuity Pathway analysis (IPA) was performed to ascertain the cellular context of the

differentially expressed genes related to SMCC-mediated liver repair. Pathway analysis indicated that the hepatic cellular senescence pathway was the most inhibited through FoxA2-related signaling mechanisms (Fig. 6B). Further analysis with IPA uncovered several differentially regulated cellular senescence gene alterations following small cholangiocyte cell therapy. Several of these genes are regulated by FoxA2, including p16, PAI-1, CCL2 and EGR1. To evaluate overall cellular senescence in SMCC therapy animals, liver sections were stained with SA-β-Gal (Fig. 6C). SMCC therapy significantly reduced cellular senescence after BDL as quantified by SA-β-Gal staining (Fig. 6C) and fluorometric detection (Fig. 6E). Total liver isolates were used to evaluate levels of senescence markers, which revealed decreased levels of p16, PAI-1, EGR-1 and CCL2 in SMCC-treated BDL mice compared to BDL mice treated with vehicle (ECM) (Fig. 6G). To evaluate the direct relationship between senescence genes and FoxA2, the senescence gene, p16, was overexpressed in SMCCs, which led to a decrease in FoxA2 levels (Fig. 6D). This indicates a possible mechanism where damage leads to senescence and overexpression of senescence genes suppresses repair mechanisms. regulated genes among the fibrotic signaling pathways in cholestatic liver (BDL) coupled with SMCC therapy compared to those treated with LGCC therapy (Fig. 6A). Ingenuity Pathway analysis (IPA) was performed to ascertain the cellular context of the differentially expressed genes related to SMCC-mediated liver repair. Pathway analysis indicated that the hepatic cellular senescence pathway was the most inhibited through FoxA2-related signaling mechanisms (Fig. 6B). Further analysis with IPA uncovered several differentially regulated cellular senescence gene alterations following

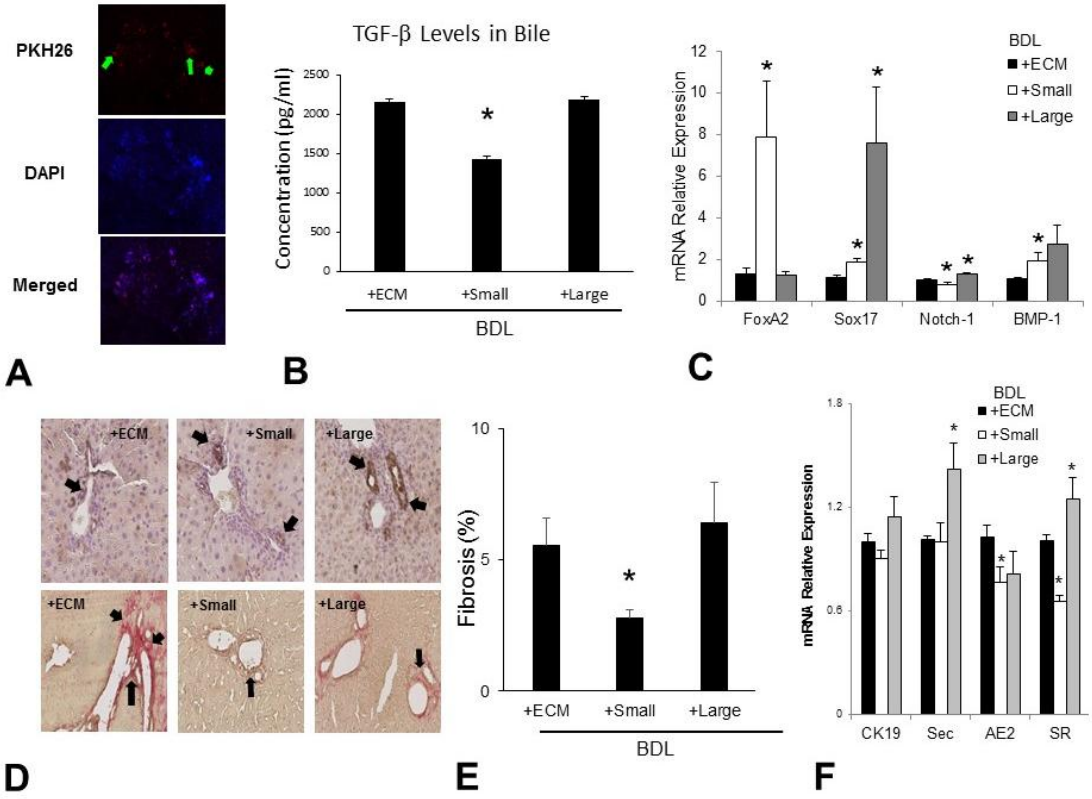

Figure 5. Effect of cell therapy on BDL-induced cholestatic liver injury. ***Panel A:*** Localization of transplanted small cholangiocytes inside mouse livers. An additional group of mice was used for detecting transplanted small cholangiocyte location. Locally transplanted small cholangiocytes were labeled using the PKH26 red fluorescent marker to detect small cholangiocytes that migrated to the liver in normal mice. A piece of mouse liver (~1 cm) was removed and fixed. The fluorescent signals from labeled small cholangiocytes (SMCCs) were predominantly detected in the mice liver 14 days after small cholangiocyte injection. ***Panel B:*** ELISA assay for TGF-β was carried out in the bile from small, large and large+FoxA2 overexpressed (OE) cholangiocytes transplanted in mice after BDL. The TGF-β secretion in bile was significantly reduced after small or large+FoxA2 OE cholangiocyte transplantation when compared to the large cholangiocyte transplantation and ECM control group after BDL. ***Panel C:*** Enhanced expression of FoxA2 was detected in SMCC-BDL mice liver relative to ECM control mice liver by *real-time PCR assay.* ***Panel D&E:*** Reduced staining of Sirius Red was seen in SMCC-BDL or LGCC+FoxA2 OE-BDL mouse livers when compared to the controls. Area of collagen present in liver sections stained with Sirius Red were quantified in BDL mice liver with small, large or large+FoxA2 OE cholangiocyte cell therapy relative to ECM control (*Panel E*). Significantly decreased intensity of liver fibrosis was detected in SMCC-BDL or LGCC+FoxA2 OE-BDL mouse liver relative to ECM controls by enhanced Sirius Red expression ($n = 5$). *Original magnifications ×200*. *$p < 0.05$ *versus* respective controls. ***Panel F:*** LGCC markers (AE2, Secretin (Sec), Secretin Receptor (SR)) and CK-19 were measured in cell therapy animals via qPCR (n=5) *p<0.05 vs ECM.

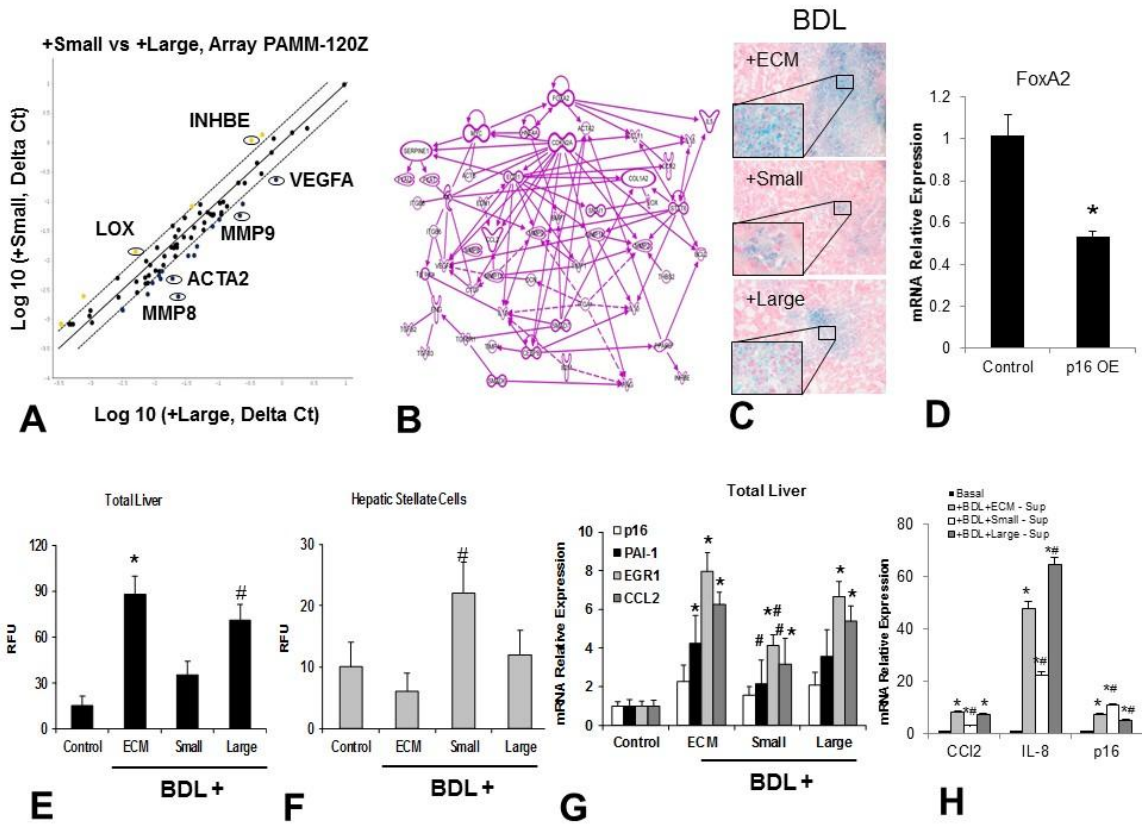

Figure 6. Effect of cell therapy on BDL-induced cellular senescence during cholestatic liver injury. ***Panel A:*** Relative gene expression profile of small cholangiocyte- versus large cholangiocyte-treated BDL liver is shown. The expression of a panel of diverse fibrosis-associated genes was evaluated by real-time PCR using the Mice Fibrosis PCR Array from SABioscience. Gene expression relative to GAPDH was plotted as volcano plots, depicting the relative expression levels (Log 10) for selected genes in BDL + Small versus BDL + Large control panels. α-SMA, MMP-2 and MMP-9 are the most down-regulated genes among the fibrotic signaling pathways in small cholangiocyte cell therapy after BDL injury. ***Panel B-C;E-G:*** **Altered cellular senescence after small cholangiocyte cell therapy.** Panel B presents Ingenuity Pathway analysis (IPA) of differentially regulated gene network after small cholangiocyte cell therapy. IPA was performed to understand the cellular context of the differentially expressed genes related to the recovery effects. Several genes implicated in cellular senescence are regulated by FoxA2, including p16 (CDKN2A), PAI-1 (SERPINE1), CCL2 and EGR1. Liver sections were stained with SA-β-Gal (Panel C), as described, to reveal cellular senescence in BDL mice +small relative to +ECM and +Large controls. Small cholangiocyte cell therapy significantly reduced cellular senescence after BDL as quantified by SA-β-Gal staining (Panel C) and flurometric detections (Panel E), whereas the enhanced cellular senescence in isolated hepatic stellate cells by LCM was observed (Panel F). The alterations of cellular senescence markers p16, PAI-1, CCL2 and EGR1 after small cholangiocyte therapy in BDL mice liver were also verified by qPCR (Panel G). *$p < 0.05$ *versus* normal controls. #$p < 0.05$ *versus* BDL+ECM controls. ***Panel D:*** p16 overexpression was performed in SMCCs, RNA was extracted and FoxA2 levels were measured with qPCR. *$p < 0.05$ *versus* control. ***Panel H:*** Cholangiocyte supernatants derived from BDL mice treated with ECM, SMCC or LGCC were used to treat cultured stellate cells and inflammatory markers (CCL2 and IL-8) and a senescence marker (p16) were measured with qPCR. *$p < 0.05$ *versus* basal. #$p < 0.05$ *versus* BDL+ECM ECM.

small cholangiocyte cell therapy. Several of these genes are regulated by FoxA2, including p16, PAI-1, CCL2 and EGR1. To evaluate overall cellular senescence in SMCC therapy animals, liver sections were stained with SA-β-Gal (Fig. 6C) as described. SMCC therapy significantly reduced cellular senescence after BDL as quantified by SA-β-Gal staining (Fig. 6C) and fluorometric detection (Fig. 6E). Total liver isolates were used to evaluate levels of senescence markers, which revealed decreased levels of p16, PAI-1, EGR-1 and CCL2 in SMCC-treated BDL mice compared to BDL mice treated with vehicle (ECM) (Fig. 6G). To evaluate the direct relationship between senescence genes and FoxA2, the senescence gene, p16, was overexpressed in SMCCs, which led to a decrease in FoxA2 levels (Fig. 6D). This indicates a possible mechanism where damage leads to senescence and overexpression of senescence genes suppresses repair mechanisms.

We then aimed to evaluate the mechanisms by which SMCCs were able to suppress fibrosis. Because stellate cells are implicated in liver fibrosis and cellular senescence is highly upregulated in total liver, we evaluated stellate cells from the livers of SMCC therapy mice for senescent markers. We found enhanced expression of the cellular senescence markers p16 and EGR1 in isolated mouse hepatic stellate cells by LCM (Fig. 7B), as well as upregulation of cellular senescence, as measured by fluorometric analysis (Fig. 5F), suggesting that senescence of activated stellate cells limits liver fibrosis during this FoxA2-mediated cell therapy process. We additionally isolated stellate cells from PSC patients with LCM and saw decreased levels of the senescence gene PAI-1 and

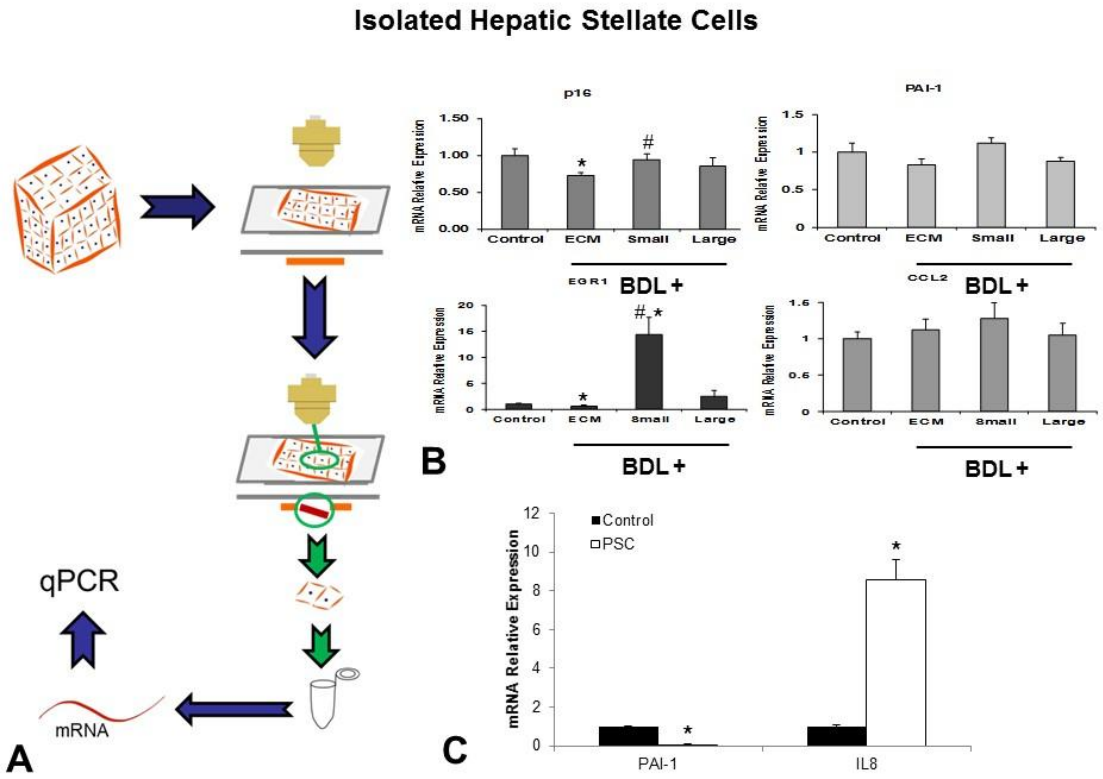

Figure 7. Alterations of cellular senescence markers in mouse hepatic stellate cells isolated by laser capture microdissection. Schematic representation of laser capture microdissection (LCM) procedures was displayed in ***Panel A***. Frozen liver sections from control, BDL, BDL-SMCC and BDL-LGCC mice were sectioned with a cryostat and affixed the membrane side of nuclease and human nucleic acid free 2.0mm PEN membrane slides. Sections were stained for desmin and a LCM system LMD7000 (Leica, Buffalo Grove, IL) was then used to capture desmin-positive hepatic stellate cells and collect them in a thin walled PCR tube. The collected cells were then used to isolate RNA with the Arcturus Pico Pure RNA Isolation Kit, and real-time PCR analysis for cellular senescence markers p16, PAI-1, EGR1 and CCL2 was carried out. Enhanced expression of p16 and EGR1 was discovered in isolated hepatic stellate cells from BDL-SMCC mouse liver when compared to control BDL groups (***Panel B)***, suggesting SMCC cell therapy inhibited liver fibrosis through the induction of cellular senescence in hepatic stellate cells. **p* < 0.05 *versus* normal or WT controls; #*p* < 0.05 *versus* Control-BDL mice liver. ***Panel C:*** Formalin fixed-paraffin embedded liver sections from PSC patients were sectioned at 6μm and affixed to the membrane side of PEN membrane slides. Sections were stained for desmin and a LCM system LMD7000 was used to capture desmin-positive cells. The collected cells were used to extract RNA as described above and the senescence marker PAI-1 and the inflammation marker IL-8 were quantified with qPCR. *p < 0.05 versus normal.

increased levels of the inflammatory gene IL-8 (Fig. 7C), indicating that the stellate cells are active in this disease model. To evaluate the interactions between cholangiocytes and stellate cells, we used isolated cholangiocytes from our BDL cell therapy-treated animals to extract supernatants that contain the cytokines, extracellular vesicles and other molecules that are secreted by cholangiocytes and treated cultured stellate cells in these supernatants. After a 48-hour incubation, the stellate cells treated with SMCC-BDL cholangiocyte supernatants showed decreased levels of the inflammatory markers CCL2 and IL-8 and increased levels of p16 (Fig. 6H), indicating that molecules or vesicles secreted by cholangiocytes are able to influence inflammation and senescence in stellate cells. This ability to influence these cells most likely influences the activity of stellate cells and thus influences the fibrosis seen in SMCC-treated BDL mice.

2.5. Discussion

The maintenance of homeostasis of the biliary epithelium is critical for the prevention and recovery from hepatobiliary damage that occurs during the pathogenesis of chronic cholestatic liver diseases such as PBC and PSC. Although the functional role for biliary progenitor cells in liver regeneration has been proposed, the molecular mechanisms by which transcriptional factors such as FoxA2 modulate hepatobiliary regrowth and hepatic repair are unknown. We identified DE markers, including FoxA2, Sox17 as well as BMP1, that are upregulated in SMCCs compared to control LGCCs by PCR array analysis. FoxA2 was also more enhanced in murine liver progenitor cells compared to SMCCs and LGCCs, and reduced in the liver tissues from human PSC/PBC patients. As in PBC and PSC, reduced FoxA2 expression was observed in murine small bile ducts in BDL and MDR2$^{-/-}$ mouse liver, suggesting that it is an important mediator of biliary injury and recovery. The translocation of engrafted biliary progenitors/cholangiocytes into the liver after IP injection was confirmed by PKH26 red fluorescence labeling detected within the liver following cell therapy. Serum ALT and AST levels in NOD/SCID mice engrafted with SMCCs were significantly decreased compared to vehicle-treated mice, along with significantly improved liver fibrosis. Enhanced expression of the DE differentiation marker FoxA2 was observed in BDL mouse liver after SMCC cell therapy, along with the reduced hepatic/enhanced hepatic stellate cellular senescence. Overexpression of FoxA2 in LGCCs and subsequent IP injection into BDL mice showed similar reductions in biliary injury to that seen with SMCC cell therapy. The identification of FoxA2 as an important transcriptional regulator of

recovering events *in vivo* emphasizes an essential role of this DE marker in mediating biliary regeneration and repair. This discovery also provides insight into the contribution of altered remodeling, epigenetic regulation and senescence in recovery of severe liver injury.

Cholangiopathies cause morbidity and mortality and are the principal reason for liver transplantation. They are characterized by spotty rather than diffuse proliferation and loss of cholangiocytes lining different sized bile ducts. The elucidation of the intracellular mechanisms regulating the differential regenerative responses of small and large cholangiocytes to cholestasis and liver injury/toxins will play a pivotal role in the development of therapeutic strategies for the treatment of liver diseases (e.g., PBC, PSC and cholangiocarcinoma). These cholangiopathies represent a serious public health concern due to the lack of novel therapeutic approaches and this subsequently results in higher liver transplantation or mortality [40, 69]. During chronic hepatobiliary injury, a population of bipotent liver progenitor cells (LPCs) becomes activated to regenerate both cholangiocytes and hepatocytes [70-72]. Cholangiocytes and hepatocytes share embryologic origins and this common heritage contributes to traits carried into adulthood [73, 74]. If small cholangiocytes with multipotential capacity exist within human and rodent bile ducts, these cells should also possess the ability to differentiate into either large cholangiocytes or hepatocytes during liver damage, such as diseased conditions in which large cholangiocytes or hepatocytes are lost or regenerative mechanisms are hampered. Due to the plasticity of intrahepatic cholangiocytes and hepatocytes, it has been postulated that terminally differentiated cells of one lineage may directly

differentiate into another lineage or undergo trans-differentiation [75]. However, the data are interpretable also as expansion and differentiation of a progenitor population [76]. Recent studies have demonstrated that meticulously isolated and rigorously characterized gallbladder epithelial cells cultured under defined *in vitro* conditions acquire hepatocyte-like properties, such as the ability to synthesize bile acids and take up low-density lipoprotein, without expression of markers of oval cells or hematopoietic progenitor cells [73]. The recent discovery of biliary pluripotent cell populations provides for an alternative mechanism for the expansion and differentiation of certain subpopulations of cholangiocytes as opposed to transdifferentiation [39]. Therefore, specific subpopulations of cells, such as small cholangiocytes that express known biliary progenitor cell markers, can be hypothesized to contain a multipotent cell population when exposed to certain pathological conditions. Our studies have suggested that such cells could attain functional *pluripotent* characteristics under the condition that large cholangiocytes are damaged or lost, and subsequently they could be used to repopulate damaged bile ducts and livers [48, 77].

DNA methylation is an important epigenetic modification that can regulate gene expression and is tightly regulated by at least three DNA methyltransferases (DNMT1, DNMT3A and DNMT3B). Aberrant DNA methylation has been implicated in many human diseases, including primary biliary disorders [78, 79]. Intrahepatic accumulation of toxic bile acids and excretion products causes cellular injury. Recent developments indicate that accumulation of toxic bile acids induces epigenetic alterations, particularly acetylation, methylation of histones, and hypo- and hypermethylation of DNA [80]. This

has created a renewed interest in biliary pathogenesis and is providing novel insight into actions of bile acids at the nucleosomal level in relation to gene expression and pathophysiological consequences. Although DNA methylation has been tightly linked to liver injuries and poor disease outcome in many hepatic disorders, including human PBC, its application to progenitor phenotype-related mRNA expression is novel. A better understanding of how specific DNA methyltransferases contribute to aberrant mRNA expression will clearly advance the field and increase the knowledge of the mechanisms regulating the pathogenesis of cholestasis.

DNA methylation regulated by TGF-β activation has been demonstrated during chronic liver injury and malignant transformation. There is ample evidence for increased TGF-β activation in cholestatic liver injury [52, 81, 82]. Analysis of the transcriptional changes that accompany the process of biliary differentiation has identified several interrelated signaling pathways that are critical during bile duct differentiation *in vitro* [83]. The molecule at the apex of these signaling pathways is BMP1, an astacin metalloprotease. BMP1 cleaves procollagen and allows the triple helix of collagen to form in the extracellular matrix. Therefore, BMP1 may play a prominent role in the remodeling of the extracellular matrix surrounding the developing bile ducts [84]. Interestingly, BMP1 is down regulated when biliary progenitor cells are cued to differentiate towards mature cholangiocytes [85]. Transient inhibition of the constitutive BMP pathway, either alone or in combination with TGF-β inhibition, is critical to the downstream effector FoxA2 signaling in stem cell cultures [86]. The observation that a number of BMP and TGF-β

responsive genes (such as FoxA2) are activated during bile duct differentiation *in vitro* suggests their essential roles in the formation of biliary structures.

Hepatobiliary regeneration is critical for the recovery of cholestatic liver diseases such as PSC and PBC. Accumulation of senescent hepatobiliary cells, which are insensitive to mitotic stimuli, may impair the reserve for hepatobiliary regeneration. In addition, the association between increased hepatobiliary nuclear area and hepatobiliary dysfunction suggests that senescent cholangiocytes/hepatocytes may not function as normal mature cholangiocytes/hepatocytes. There is also an association between senescence measured as increased expression of senescence markers in cholangiocytes and hepatocytes and impaired liver synthetic function (increasing prothrombin time and decreasing serum albumin level) [87]. Thus, accumulation of senescent cholangiocytes/hepatocytes may contribute to loss of functional hepatobiliary mass with sufficient accumulation of such cells eventually leading to hepatobiliary decompensation and liver-related death, accounting for the strong link between cholangiocyte/hepatocyte senescence markers and adverse liver-related outcome. During clinical and biochemical dysfunction with progressive cholestatic liver disease, up to 87% of hepatobiliary cells in cholestatic liver diseases (CLDs) expressed senescence markers and may have impaired function. However, senescence of activated stellate cells limits liver fibrosis through reduced secretion of extracellular matrix components, enhanced secretion of extracellular matrix-degrading enzymes, and enhanced immune surveillance. The discovery of an association between reduced hepatic/enhanced hepatic stellate cellular senescence and FoxA2, a DE

maker of liver development and recovery in CLD in particular, suggests an important translational mechanism in CLD development, progression and recovery.

In conclusion, we have demonstrated the epigenetic regulation of FoxA2 expression during cholestatic liver injury. Additionally, we have shown that the expression of downstream anti-cellular senescence/fibrosis signaling of biliary regrowth/repair could be modulated by FoxA2. This indicates that therapeutic strategies to increase FoxA2 may be potentially useful to rebuild the hepatobiliary system after liver injury. Further work is warranted to evaluate the functional role of FoxA2 and the identified downstream targets and to develop therapeutic strategies by taking advantage of FoxA2 overexpression *in vivo*. The ability to therapeutically manipulate mRNA expression is also feasible, and recent proof-of-concept studies have shown that mRNA agonists targeted to the liver can modulate expression of downstream genes. Moreover, aberrantly expressed mRNAs of FoxA2 and other DE markers may be useful to establish a diagnosis and for assessing prognosis in liver injury. Knowledge of specific processes, such as biliary proliferation, senescence, remodeling and mesenchymal transition that are regulated by FoxA2, and the identification of critical targets for such DE markers, provides novel insights into the mechanisms in the development and recovery of the intrahepatic biliary epithelium and hepatic function after chronic liver injury.

3. AMELIORATION OF FIBROSIS AND INFLAMMATION BY STEM CELL DERIVED EXTRACELLULAR VESICLES IN A MOUSE MODEL OF PSC

3.1. Overview

Background: Primary Sclerosing Cholangitis (PSC) is a progressive liver disease characterized by chronic biliary inflammation leading to biliary strictures and fibrosis. Activation of stellate cells (HSCs) by inflammatory cytokines leads to widespread fibrosis, whereas senescence appears to be able to deactivate HSCs, halting fibrosis progression. Stem cells in the liver could communicate with HSCs or Kupffer cells through release of extracellular vesicles (EVs) that contain cytokines, microRNAs and various other signaling molecules. Aim: to evaluate the effects of EVs on fibrosis and inflammation in MDR2$^{-/-}$ mice that exhibit biliary inflammation and fibrosis as seen in human PSC. **Methods**: EVs were isolated from cell culture medium of cultured liver stem cells (LSCs) or mesenchymal stem cells (MSCs) by differential centrifugation. Stellate cells were treated with LSC-derived EVs +/- lipopolysaccharide (LPS) or TGF-β treatment and fibrosis levels were measured with qPCR. Isolated stem cell derived EVs (resuspended in sterile PBS) were injected weekly for 2 weeks via the lateral tail vein into MDR2$^{-/-}$ mice. Mice were euthanized and livers were harvested 1 week after the last injection. Immunohistochemistry (IHC) was performed for collagen deposition, biliary mass and Kupffer cell proliferation. H69 human cholangiocytes were treated with stem cell derived EVs, after a medium change, the H69 medium was placed on stellate cells and fibrosis, inflammation and senescence were measured with qPCR.

Results: Stellate cells +/- LPS or TGF-β treated with LSC-derived EVs showed decreased expression of fibrosis markers. *In vivo*, Kupffer cells were reduced in stem cell-derived EV-treated MDR2$^{-/-}$ mice. Sirius Red staining for collagen deposition was significantly reduced along with decreased biliary mass in stem cell-derived EV-treated mice compared to controls. In stellate cells treated with medium from H69-EV treated cholangiocytes, fibrosis and inflammation expression was decreased and senescence expression was increased. **Conclusion**: Stem cell-derived EVs have the ability to decrease liver fibrosis and inflammation in a mouse model of PSC by modulation of cholangiocytes which, in turn, induces senescence in HSCs. These results show promise for a potential treatment in PSC patients to reduce inflammation and subsequent fibrosis.

3.2. Introduction

Cholangiopathies are diseases of the biliary tract and comprise many forms of liver disease that primarily affect the cells of the bile ducts, cholangiocytes. Cholangiopathies are typically characterized by destruction and/or damage of the bile ducts, which leads to a ductular reaction as a compensation mechanism [6, 88]. Primary sclerosing cholangitis (PSC) is a form of cholangiopathy that primarily affects men aged 30-40 [89]. PSC is thought to be an inflammatory autoimmune disease that attacks cholangiocytes. The chronic inflammation leads to destruction of the bile ducts, causing blockage of the bile ducts that eventually leads to cirrhosis and liver failure [89].

The $MDR2^{-/-}$ mouse is a commonly used mouse model of PSC. The $MDR2^{-/-}$ mouse has a mutation in the ABCB4 gene, the gene for multidrug resistance protein 2 (MDR2), which prevents the mice from secreting phospholipid into the bile [90]. This causes the bile to become corrosive and destroy the cholangiocytes, leading to a histological appearance very similar to PSC patients.

The liver is the only organ in the body that can regenerate itself. This makes the liver an organ with remarkable capacity for repair. When liver repair does not work correctly, fibrosis occurs. Hepatic stellate cells (HSCs) have been implicated as the main cell type responsible for fibrotic scarring in the liver and regulation of these cells is important to prevent fibrosis [23]. The cells responsible for the regulation of liver repair is debatable. It has been claimed that stem cells are resident in the liver, while some claim that

mesenchymal stem cells repair the liver and others claim that hepatocytes and/or cholangiocytes repair themselves by their own progenitor cell populations [20, 91, 92]. Extracellular vesicles (EVs) are secreted by cells in order to communicate with other cells at local or distant locations. EVs comprise exosomes, microvesicles and apoptotic bodies [93]. They are typically 30-800nm in size and have been shown to be important in many disease states [94]. Mesenchymal stem cell-derived EVs (MSCEVs) have been shown to be efficacious in reducing the immune response in type 1 diabetes and uveoretinitis as well as kidney repair [95, 96]. Additionally, EVs in bile have been shown to be useful as biomarkers of malignant biliary stenosis with 100% accuracy [97]. This study aimed to evaluate stem cell-derived EVs in a mouse model of PSC.

3.3. Materials and Methods

Extraction of Extracellular Vesicles (EVs)

Eight 75mm^2 flasks of cultured human liver stem cells (Celprogen, Torrance, CA) or human mesenchymal stem cells (Sciencell, Carlsbad, CA) were grown to confluency and cultured for 24 hours in serum-free medium. The medium was removed from the cells and centrifuged at 300 x g for 10 minutes. The supernatant was removed and centrifuged for 1200 x g for 10 minutes. The supernatant was removed and centrifuged for 2 hours at 425,000 rpm. The pellet was resuspended in phosphate buffered saline (PBS) (Sigma-Aldrich, St. Louis, MO) and analyzed with a Nanosight LM10 (Malvern, Salisbury, UK).

Electron microscopy

Human mesenchymal stem cells and human liver stem cells were fixed in 25% electron microscopy-grade glutaraldehyde (Electron Microscopy Sciences, Hatfield, PA) and fixed samples were sent to the Molecular Microbiology Imaging Facility at Washington University (St. Louis, MO) for transmission electron microscopy analysis.

Evaluation of miR-181 and fibrosis marker expression levels in hepatic stellate cells after EV treatment

Human hepatic stellate cells (Sciencell, Carlsbad, CA) were cultured to 80% confluency and treated with 10ng/mL TGF-β (R&D Systems, Minneapolis, MN) or 2ng/mL

lipopolysaccharide (LPS, Sigma-Aldrich, St Louis, MO) and then treated with human liver stem cell-derived EVs (LSCEV) at 4 x 10^7 particles/well for 48 hours. Cells were harvested with a cell scraper and RNA was extracted with the miRVana RNA isolation kit (Invitrogen, Carlsbad, CA) according to manufacturer instructions. For qPCR for the fibrotic markers, ACTA2 and Col1A1, cDNA was made using the iScript cDNA synthesis kit using the manufacturer's instructions. The qPCR was run using primers obtained from Qiagen (Germantown, MD) and iTaq Universal SYBR Green Supermix, as directed by the manufacturer. For microRNA (miRNA) studies, cDNA was made using the Taqman miRNA Reverse Transcription Kit (Applied Biosystems, Foster City, CA) and miRNA primers from ThermoFisher (Waltham, MA). The qPCR was performed using miRNA primers from ThermoFisher and Taqman Fast Universal PCR Master Mix (Applied Biosystems, Foster City, CA). All qPCR experiments were run on an Applied Biosystems ViiA7 Real-Time PCR System (ThermoFisher, Waltham, MA). The comparative CT method ($\Delta\Delta$CT) was used for quantification of gene expression. All samples were tested in triplicate, and average values used for quantification.

Animal studies

The Animal Care and Use Committee of Baylor Scott & White approved all the animal protocols used in this study. Male and female MDR2$^{-/-}$ (FVB.129P2-Abcb4^{tm1Bor}/J) mice and wild type (FVB/NJ) controls (27 wks of age) were originally obtained from Jackson Laboratories (Bar Harbor, ME) and subsequently bred in-house. Liver stem cell-derived EVs were injected intravenously at 4.6x10^7 particles per injection and

mesenchymal stem cell-derived EVs were injected intravenously at 1.28 x 10^8 particles per injection via the lateral tail vein once per week for 2 weeks. Mice were sacrificed and livers were collected at 29 weeks. RNA was extracted using the miRVANA kit, cDNA was prepared and qPCR was performed as described above. Portions of liver were also fixed in 10% neutral buffered formalin (Sigma-Aldrich, St Louis, MO) and embedded in paraffin for histological analysis. Cholangiocytes were isolated by counterflow elutriation followed by immunoaffinity separation [8] with a monoclonal antibody (a gift of Dr. R Faris, Brown University, Providence, RI) against an unidentified antigen expressed by all non-malignant intrahepatic human (H69) (Meng and Alpini, unpublished observations, 2014) and murine cholangiocytes.

Evaluation of biliary mass

To evaluate biliary mass, formalin-fixed paraffin-embedded (FFPE) livers were sectioned at 6μm using a microtome and affixed to glass slides. After rehydration, antigens were unmasked with antigen unmasking solution (Vector Labs, Burlingame, CA) and blocked using the VECTASTAIN Elite ABC HRP Kit (Vector Labs). Liver sections were incubated overnight at 4°C with specific antibody to CK-19 (AbCam, San Francisco, CA) (1:50), washed in PBS, incubated for 1 hr at room temperature with a secondary biotinylated antibody using the VECTASTAIN Elite ABC HRP Kit (Vector Labs), and further incubated with the ABC reagent for 30 min and developed with 3–3′ diaminobenzidine (Vector Labs). For all immunoreactions, negative controls were included. Immunohistochemical observations were taken by BX-51 light microscopy

(Olympus, Tokyo, Japan) with a Videocam (Spot Insight; Diagnostic Instrument, Sterling Heights, MI) and processed with Adobe Photoshop (San Jose, CA). Images were subjectively graded by 3 blinded observers.

Analysis of fibrosis

To evaluate fibrosis, FFPE liver sections were rehydrated and stained using the NovusUltra Sirius Red Stain Kit (IHC World, Ellicott City, MD). Briefly, slides were incubated in Weigert's Iron Hematoxylin for 10 minutes. After rinsing in water for 10 minutes, slides were stained with Pico Sirius Red for 1 hr. Slides were rinsed and then incubated in 1% acetic acid for 1 min, then dehydrated and coverslipped. Images were subjectively graded by 3 blinded observers.

The qPCR analysis for the fibrotic marker, Col1A1, was performed using isolated cholangiocytes or samples of total liver. RNA was extracted, cDNA was made and qPCR was performed as stated above.

Analysis of inflammation

Kupffer cell numbers were used to evaluate inflammation in liver sections. FFPE liver sections were immunohistochemically stained as with CK-19 described above using an antibody for F4/80 (Santa Cruz Biotechnology, Dallas, TX). Images were subjectively graded by 3 blinded observers.

Evaluation of crosstalk between stem cells, cholangiocytes and stellate cells

In order to evaluate the ability of stem cell EVs to modulate stellate activation through crosstalk with cholangiocytes, human non-malignant H69 cholangiocytes (H69 cells) were treated with LSC-derived EVs (LSCEVs) or MSCEVs for 48 hours. The medium was changed to serum-free medium after 48 hours and incubated for 24 hours. The medium from the H69 cells was then placed on human hepatic stellate cells for 48 hours. Stellate cells were harvested, RNA was extracted and qPCR was performed as described above for fibrosis, inflammation and senescence.

Statistics

Data are expressed as the mean ± standard error (S.E.) from at least three separate experiments performed in triplicate unless otherwise noted. The differences between groups were analyzed using a two-tailed Student t test when only two groups were present and ANOVA when there were more than two groups. The null hypothesis was rejected at the 0.05 level unless otherwise specified.

3.4. Results

Extracellular vesicles are secreted by stem cells

To determine if human liver stem cells (LSCs) and human mesenchymal stem cells (MSCs) secrete extracellular vesicles (EVs). LSCs and MSCs were plated to 60% confluence, fixed with glutaraldehyde and imaged with transmission electron microscopy. Upon examination, it was found that both LSCs and MSCs released EVs (Figure 8A, 8B). The release of EVs by both cell types confirmed that EV collection was possible from both cell types.

EVs were then extracted with centrifugation and characterized with a Nanosight instrument. LSCs secreted vesicles that were most abundant between 180 to 250nm (Figure 8C). We gathered EVs from LSCs at a concentration of 12.09 particles per frame, which equated to a concentration of $1.39x10^8$ particles/ml. From MSCs, we extracted vesicles that were most abundant between 100-220nm (Figure 8D). MSC EVs were at a concentration of 33.64 particles per frame, which was a concentration of $3.85x10^8$ particles/ml. Because EVs have been shown to contain numerous miRNAs and proteins that are able to regulate gene expression, EVs may possibly be able to regulate fibrosis and therefore be used as a treatment.

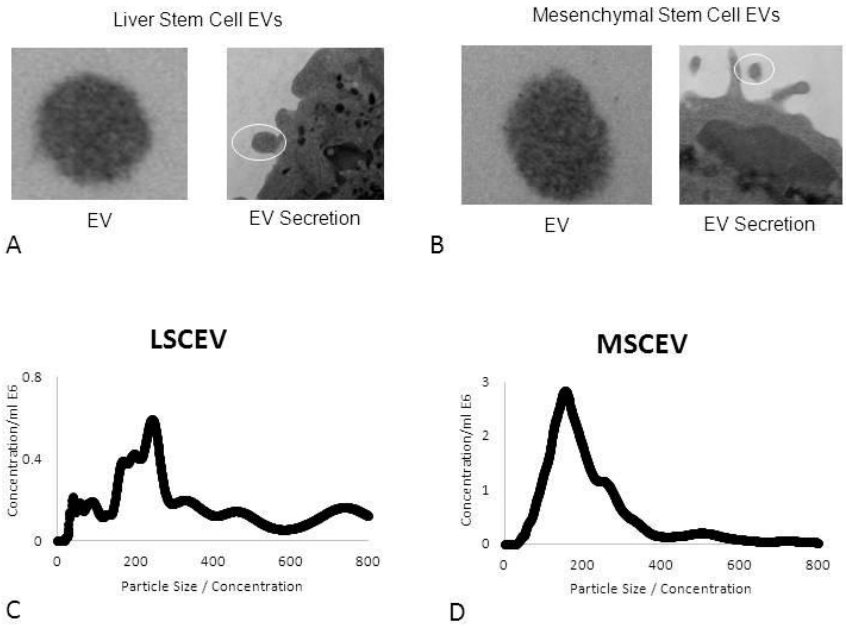

Figure 8. Stem cells secrete EVs that can be collected and quantified. Transmission electron microscopy images of liver stem cells (A) and mesenchymal stem cells (B) show secretion of EVs. After collection, Nanosight analysis shows the largest abundance of liver stem cell EVs in the range of 180 to 250nm (C) and mesenchymal stem cell EVs in the range of 100-220nm (D).

Liver stem cell derived EVs reduce fibrosis markers in stellate cells

In order to determine whether stem cell derived EVs had an effect on cells responsible for fibrosis, human hepatic stellate cells (HSCs) were cultured to 70% confluency. HSCs were treated with transforming growth factor beta (TGF-β) or LPS to simulate liver injury. The TGF-β- or LPS-treated cells were then treated with LSCEVs for 48 hours. Treatment of stellate cells with LPS or TGF-β induces increases in the expression of ACTA2, the gene for alpha-smooth muscle actin (α-SMA), and Col1A1, the gene for Collagen Type 1 Alpha 1 Chain (Figure 9A-B). This effect was ameliorated when LPS or TGF-β treated stellate cells were treated with LSCEVs, indicating that stellate cells could possibly be deactivated by LSCEVs.

Liver stem cell derived EVs reduce fibrosis and inflammation and increase FoxA2 in MDR2$^{-/-}$ mice

After ensuring that LSCEVs were effective *in vitro*, stem cell-derived EVs were tested *in vivo*. LSCEVs were injected via the lateral tail vein into MDR2$^{-/-}$ mice at a concentration of 46 million particles per injection per mouse weekly for 2 weeks. Control mice were injected with vehicle (saline) weekly for 2 weeks. Livers were collected and analyzed for fibrosis, inflammation and FoxA2 expression.

Sirius Red staining of livers for collagen deposition showed a large increase in staining in MDR2$^{-/-}$ mice compared to their wild type counterparts, indicating a large increase in collagen deposition and fibrotic scarring in the MDR2$^{-/-}$ mice (Figure 9C). Two

treatments of intravenous LSCEVs reduced collagen deposition, indicating less fibrosis and improved liver function. Additionally, collagen expression was decreased in cholangiocytes isolated from LSCEV-treated MDR2$^{-/-}$ mice compared to control-treated MDR2$^{-/-}$ mice (Figure 9D). Taken together, this indicates that LSCEVs were able to reduced fibrosis in MDR2$^{-/-}$ most likely by halting further progression of the disease but possibly repairing the damage that had already occurred.

FoxA2 was previously shown to be important in the regulation of liver repair during small cholangiocyte cell therapy [98]. FoxA2 was therefore measured with IHC in liver sections. FoxA2 expression was shown to be decreased in the

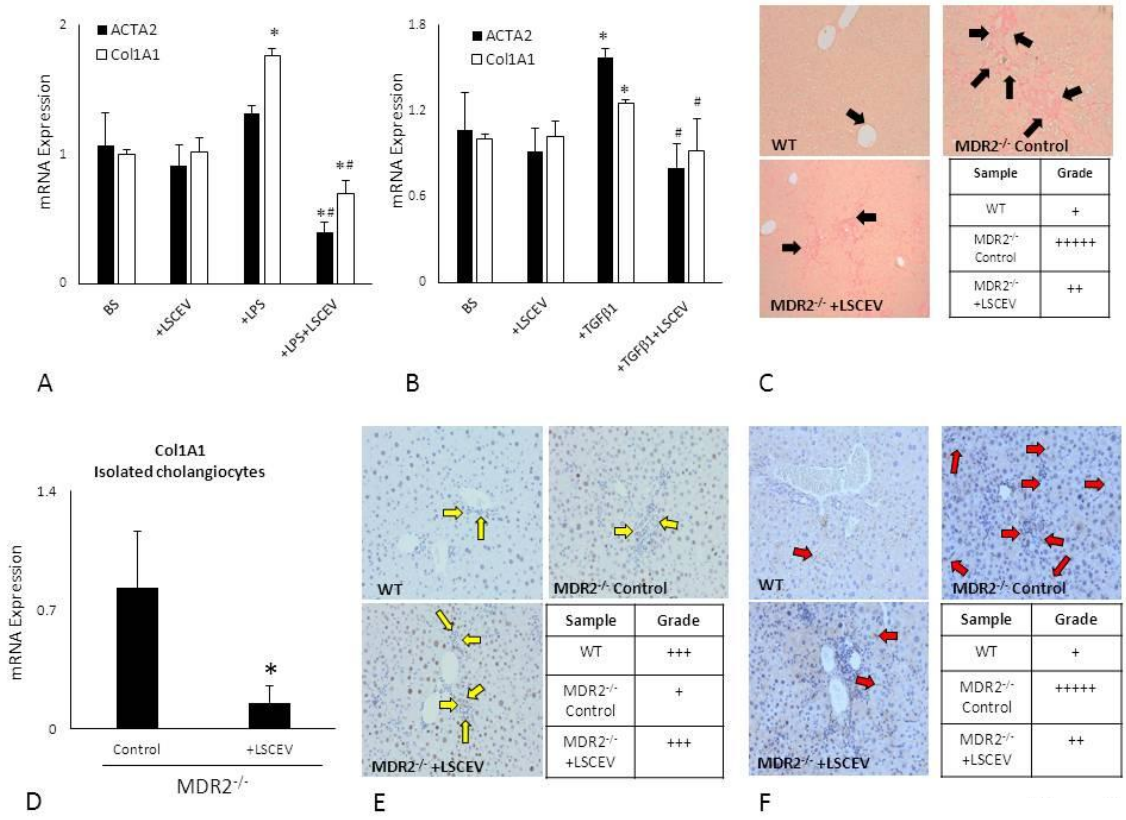

Figure 9. Liver stem cell-derived EVs (LSCEVs) reduce fibrosis and inflammation and increase FoxA2 in MDR2$^{-/-}$ mice. Hepatic stellate cells (HSCs) treated with TGF-β (B) or LPS (A) showed increased fibrosis markers, but treatment with LSCEVs reduced expression of these markers to normal levels. Sirius Red staining of liver sections showed increased fibrosis in MDR2$^{-/-}$ mice that was decreased with LSCEV treatment (C). The qPCR analysis of isolated cholangiocytes showed decreased levels of Col1A1 in LSCEV-treated MDR2$^{-/-}$ mice compared to controls. *p<0.05 vs. Control (D). FoxA2 immunohistochemistry showed reduced staining in cholangiocytes in MDR2$^{-/-}$ mice compared to wild type, which is restored with LSCEV treatment (E). F4/80 staining for Kupffer cells shows increased numbers of Kupffer cells in MDR2-/- mice (F). This increase was reduced with LSCEV treatment.

cholangiocytes of MDR2$^{-/-}$ control mice, however, treatment with LSCEVs restored FoxA2 expression in cholangiocytes (Figure 9E). This indicates that the cholangiocytes are possibly better able to repair damaged cholangiocytes without allowing progression of fibrosis.

Because inflammation is a precursor to fibrosis, liver sections were stained with a maker for liver-resident macrophages, Kupffer cells. Predictably, control-treated MDR2-/- liver sections showed an increased number of Kupffer cells, indicating that there was more inflammation present in these mice compared to wild type mice (Figure 9F). LSCEV-treated mice showed a reduction in the number of Kupffer cells, indicating a reduction in inflammation in these animals.

Mesenchymal stem cell derived EVs reduce biliary mass, fibrosis and inflammation in MDR2$^{-/-}$ mice.

Because mesenchymal stem cells are precursors of liver cells and it has been proposed that mesenchymal stem cell therapy may be a good prospect for cell therapy to treat liver fibrosis [99], MSCEVs were injected at 46 million particles per injection per mouse weekly for 2 weeks. In order to determine if liver function was restored with stem cell-derived EV therapy, serum liver enzyme levels were measured. Alanine Aminotransferase (ALT), Aspartate Aminotransferase (AST) and Alkaline Phosphatase (ALP) were elevated in control MDR2$^{-/-}$ mice compared to wild type mice (Figure 10A).

Treatment with MSCEVs reduced the elevation of these enzymes, signifying that the liver is most likely functioning better after treatment with MSCEVs.

The ductular reaction is a vital component of cholangiopathies and is thought to be a compensating mechanism for the destruction of bile ducts [5]. CK-19 staining for cholangiocytes shows increased biliary mass in MDR2 control mice correlating with an increased ductular reaction but this was decreased in MDR2 knockout mice treated with MSCEVs (Figure 10B).

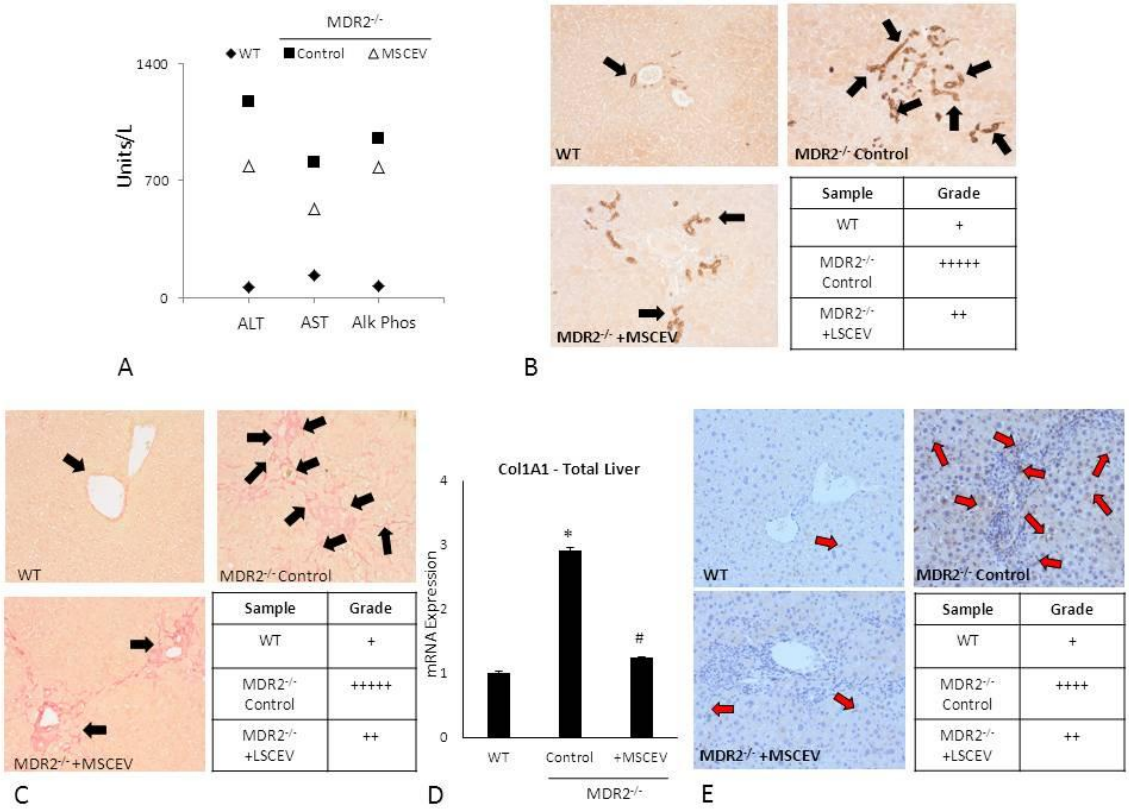

<u>Figure 10</u>. Mesenchymal stem cell-derived EVs (MSCEVs) reduce serum liver enzymes, biliary mass, fibrosis and inflammation. Concentrations of circulating liver enzymes in serum were increased in MDR2$^{-/-}$ mice and this increase was attenuated in MDR2$^{-/-}$ mice treated with MSCEVs (A). CK-19 staining for cholangiocytes showed increased biliary mass in MDR2$^{-/-}$ mice that was decreased in MDR2-$^{-/-}$ mice treated with MSCEVs (B). Sirius Red staining of liver sections showed increased fibrosis in MDR2$^{-/-}$ mice that was decreased with MSCEV treatment (C). The qPCR analysis of total liver isolates showed decreased levels of Col1A1 in MSCEV-treated MDR2$^{-/-}$ mice compared to controls. *p<0.05 vs. WT, #p<0.05 vs. Control (D). F4/80 staining for Kupffer cells showed increased numbers of Kupffer cells in MDR2-/- mice that was reduced with MSCEV treatment (E).

Collagen deposition staining with Sirius Red once again showed an increase in collagen deposition in MDR2$^{-/-}$ mice compared to wild type mice (Figure 10C). MSCEV treatment decreased Sirius Red staining, indicating less fibrosis. Additionally, total liver homogenates were analyzed for collagen expression with qPCR. Collagen levels were elevated in MDR2$^{-/-}$ control mice compared to wild type (Figure 10D). This elevation of collagen expression was reduced to normal levels when MDR2$^{-/-}$ mice were treated with MSCEVs. Taken together, these measurements indicate that MSCEVs reduce fibrosis in MDR2$^{-/-}$ mice.

Evaluation of inflammation via IHC staining for Kupffer cells showed increased staining in MDR2$^{-/-}$ control mice, but this was reduced when MDR2$^{-/-}$ mice were treated with MSCEVs.

Stem cells communicate through cholangiocytes to deactivate stellate cells

In order to ascertain the communication between stem cells, cholangiocytes and HSCs in order to regulate fibrosis, stem cell-derived EVs were used to treat H69 cells (nonmalignant cholangiocytes) for 48 hours. The medium on the H69 cells was changed to serum-free medium and allowed to incubate for 48 hours before being transferred to HSCs for 48 hours. HSCs were then analyzed for fibrosis, inflammation and senescence.

HSCs have been shown to undergo a transformation from a quiescent state to a mesenchymal state upon activation [23]. This activation is what causes HSCs to move to the area of injury and secrete extracellular matrix for dividing cells [100]. HSCs treated with medium from H69 cells previously treated with LSCEVs or MSCEVs showed a decrease in ACTA2 levels (Figure 11A, D). This indicates that the cells are less fibrotic and may in fact be deactivated. Because inflammation is often involved in fibrosis, the expression of the inflammatory marker interleukin-8 (IL-8) was measured in HSCs treated with medium from H69 cells treated with LSCEVs. There was a slight trend of reduction in the IL-8 levels secreted by HSCs treated with medium from H69 cells treated with LSCEVs compared to controls, but it was not a significant decrease (Figure 11B).

Senescence has been previously shown to be important in the deactivation of HSCs during liver injury [98]. When HSCs were treated with medium from H69 cells treated with LSCEVs, there was a significant increase in senescence as measured with p16 (Figure 11C). Medium from H69 cells treated with MSCEVs showed an upward trend that was not significant (Figure 11E). The increase in senescence coupled with a decrease in fibrotic markers and a downward trend in inflammation suggests that LSCEVs and MSCEVs are able to control fibrosis by communication with cholangiocytes which in turn communicate with HSCs and cause them to deactivate.

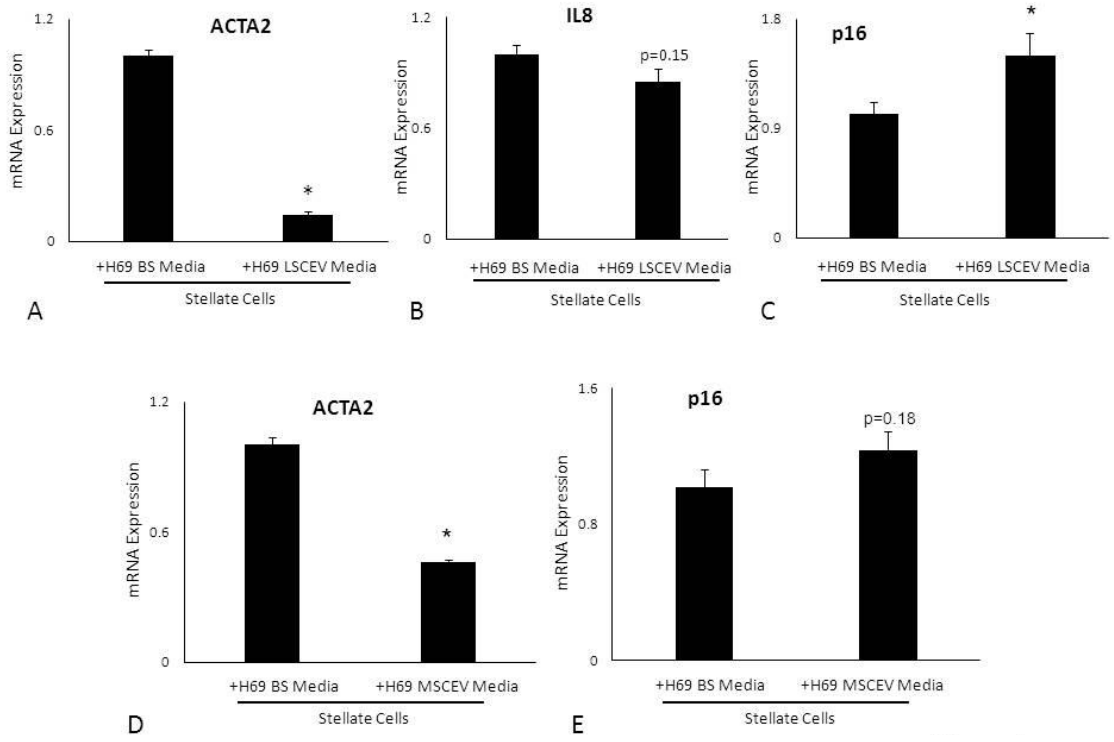

Figure 11. HSCs treated with medium from stem cell-derived EV-treated H69 cholangiocytes show reduced fibrosis and inflammation and increased senescence. Medium from H69 cholangiocytes treated with LSCEVs used to treat HSCs reduced expression of fibrosis markers (A) and inflammatory markers (B) and increased expression of senescence markers (C). HSCs treated with medium from H69 cholangiocytes treated with MSCEVs reduced fibrosis markers (D) and increased senescence markers (E). *$p<0.05$ vs. HSCs+H69 basal (BS) medium

3.5. Discussion

The ability of the liver to coordinate repair after injury is vital to maintenance of a functional organ, especially in the case of diseases such as PSC which obliterates large portions of the biliary tract and leading to cholestasis. It is unclear whether stem cells, hepatocytes or cholangiocytes are the main cellular regulators of repair after liver injury. We have shown that LSCs and MSCs secrete EVs and these EVs are able to modulate stellate cell fibrotic markers. *In vivo,* stem cell-derived EVs were able to reduce liver enzyme levels, biliary mass, fibrosis and inflammation but increased FoxA2 expression in cholangiocytes. We further investigated the interplay of signals by treating cholangiocytes with stem cell-derived EVs and then treated HSCs with the medium from these cells. This showed that stem cell-derived EVs altered signaling in cholangiocytes, which altered their secretion of cytokines or EVs that reduced fibrosis and inflammation but increased senescence in HSCs, essentially deactivating these cells.

Because HSCs are the main cell responsible for liver fibrosis, HSC deactivation is key to preventing fibrosis in the liver after injury and/or inflammation. It has been shown that HSCs can be deactivated by blocking TGF-β/SMAD signaling [101]. This is interesting in terms of stem cell-derived EV therapy considering that we showed that fibrotic markers were decreased in cultured HSCs treated with TGF-β and stem cell-derived EVs. Blockage of the TGF-β/SMAD pathway could be a mechanism by which stem cells induce decreases in fibrosis. Additionally, it has been speculated that fibrosis can

indeed be bidirectional, meaning that fibrosis can increase and decrease, depending on the molecular pathways that are active [24]. This could be a mechanism by which stem cells are able to improve fibrosis in the late stage MDR2$^{-/-}$ mice. If indeed, the improvement in fibrosis that we see is attributed to this, it would be very beneficial to PSC patients since most do not seek medical attention until later stages of their disease.

EVs are vital to allowing cells to communicate with one another. Several groups have manipulated EV contents to deliver therapeutics or used them as biomarkers for specific diseases [102]. The contents of EVs have not been analyzed in detail and this could be the next step to understanding how stem cells communicate with cholangiocytes and other cell types to reduce fibrosis. In a microRNA array that analyzed RNA from EVs, we saw that there was upregulation of the miR-181 family members (which include let-7) in LSCEVs and MSCEVs compared to hepatocyte derived EVs (unpublished data). This could be an indication of the mechanisms by which stem cells communicate with cholangiocytes and the contents of EVs, including microRNA components, should be investigated further.

PSC is a cholangiocyte disease and therefore secretion of markers of damage and/or inflammation from cholangiocytes is most likely the impetus for activation of stellate cells, increases of Kupffer cells and most likely any infiltration of other immune cells. Therefore, it is reasonable to think of the cholangiocyte as the central regulator of the degree of injury and fibrosis in the liver. We have shown in both BDL and MDR2$^{-/-}$ mice that FoxA2 is reduced after injury and correlates with increased fibrosis and

inflammation. Additionally, we have shown that FoxA2 is reduced in PSC patient liver tissue [98]. Treatment of BDL mice with small cholangiocytes and treatment of $MDR2^{-/-}$ mice with LSCEVs both restored FoxA2 levels in cholangiocytes and resulted in reduced inflammation. FoxA2 could be a signal to surrounding cells that the cholangiocytes are healthy and could help to explain why this correlates with decreased fibrosis and HSC senescence.

In conclusion, we have shown that stem cell-derived EVs are able to reduce fibrosis and inflammation and increase FoxA2 expression in cholangiocytes. We additionally showed that stem cell-derived EVs can induce cholangiocytes to deactivate HSCs. Taken together with past data, these data indicate that therapeutic strategies aimed at increasing FoxA2 in cholangiocytes could lessen the inflammation and fibrosis seen in PSC patients. Although therapy using cell-derived EVs is in its infancy, manipulation of the contents of EVs shows a strong therapeutic potential in many diseases. More research needs to be done to characterize the contents of EVs and evaluate the mechanisms by which stem cell-derived EVs modulate cholangiocytes. This insight could lead to therapies that are targeted and specific to the cholangiopathies.

4. THE LET-7/LIN28 AXIS REGULATES ACTIVATION OF HEPATIC STELLATE CELLS IN ALCOHOLIC LIVER INJURY*

4.1. Overview

The let-7/Lin28 axis is associated with the regulation of key cellular regulatory genes known as microRNAs (miRNAs) in various human disorders and cancer development. This study evaluated the role of the let-7/Lin28 axis in regulating a mesenchymal phenotype of hepatic stellate cells in alcoholic liver injury. We identified that ethanol feeding significantly downregulated several members of the let-7 family in mouse liver, including let-7a and let-7b. Similarly, the treatment of human hepatic stellate cells (hHSCs) with lipopolysaccharide (LPS) and transforming growth factor-β (TGF-β) significantly decreased the expression of let-7a and let-7b. Conversely, overexpression of let-7a and let-7b suppressed the myofibroblastic activation of cultured hHSCs induced by LPS and TGF-β, as evidenced by repressed expression of ACTA2, COL1A1, TIMP1, and FN1; this supports the notion that HSC activation is controlled by let-7. A combination of bioinformatics, dual-luciferase reporter assay, and western blot analysis revealed that Lin28B and high-mobility group AT-hook 2 (HMGA2) were the direct targets of let-7a and let-7b. Furthermore, Lin28B deficiency increased the expression of

let-7a/let-7b as well as reduced HSC activation and liver fibrosis in mice with alcoholic liver injury. This feedback regulation of let-7 by Lin28B is verified in hepatic stellate cells isolated by laser capture microdissection from the model. The identification of the let-7/Lin28 axis as an important regulator of HSC activation, as well as its upstream modulators and downstream targets, will provide insights into the involvement of altered miRNA expression in contributing to the pathogenesis of alcoholic liver fibrosis and development of novel therapeutic approaches for human alcoholic liver diseases.

4.2. Introduction

Alcoholic steatohepatitis with steatosis (fatty liver) and peri-sinusoidal fibrosis, represent a crucial step in progression of alcoholic liver disease (ALD) [103, 104]. Despite the importance of liver fibrosis in the disease process, the causes of fibrosis and diminished regeneration, especially in liver cirrhosis, remain poorly understood. Enhanced mesenchymal reactions are associated with liver fibrosis [105] and are characterized as generation of myofibroblasts [106, 107].

Repair of the liver occurs after injury through a coordinated interplay of resident and infiltrating cells. However, if the injury is too great to repair at a similar or greater rate than the injury, scarring ensues in the form of fibrosis [108]. The main cell types that are involved in liver fibrosis are hepatic stellate cell (HSCs) [109]. HSCs are liver-specific mesenchymal cells that play a critical role in liver injury and fibrosis. HSCs are typically quiescent, vitamin A storing pericytes [110]. However, when the liver is injured, HSCs are activated to become myofibroblastic cells [111]. Activated HSCs travel to the site of an injury to secrete extracellular matrix (ECM) for dividing cells to attach [100]. If the liver is unable to replace the damaged cells, HSCs deposit an excessive amount of ECM causing a fibrotic scar. The mechanisms by which the liver reacts to alcohol are being studied extensively. One such mechanism is the activity of the small regulatory non-coding RNAs, microRNAs (miRNAs). These small non-coding RNAs can regulate genes by direct binding to DNA or mRNA [112]. We have

previously shown that let-7 is important in alcoholic and chronic liver injury; we have also shown that the reduction of let-7 increases the severity of fibrosis and other injuries [63, 113, 114]. Several variants of let-7, let-7a, let-7b and let-7g, are down-regulated in the serum of ethanol-fed mice [115]. The potential target genes of the let-7 family include Lin28, a key promoter of mesenchymal reaction, cell migration, and generation of induced pluripotent stem cells [116]. Recent studies have shown that miR-200c, another miRNA that is regulated by Lin28, may regulate the mesenchymal reaction in cancer. Overexpression of miR-200c inhibits mesenchymal reaction and supports termination of cancer progression [117, 118]. It has been hypothesized that the mesenchymal phenotypes regulate the ability to either recover from injury or progress to a cirrhotic condition. More mesenchymal reactions promote liver fibrosis, whereas inhibiting them triggers liver healing and regeneration [119].

The let-7/Lin28 axis regulates hepatocellular carcinoma development [115, 120] and is associated with an increased risk of type 2 diabetes mellitus [121]. However, the functional role of let-7/Lin28 in alcoholic liver injury remains unclear. Thus, we assessed the role of aberrant expression of the let-7/Lin28 axis in HSCs in ALD by posing four questions: i) Is let-7/Lin28 expression altered in ethanol-exposed mice and ALD human liver tissues? ii) Does modulation of let-7/Lin28 alter activation of HSCs *in vitro* and in animals with ALD? iii) What is the upstream regulator of let-7/Lin28 in HSCs in ALD? iv) What are the downstream targets of let-7/Lin28 involved in HSC activation in ALD?

4.3. Methods and Materials

Evaluation of the role of the let-7/Lin28 axis in the mesenchymal reaction in (hHSCs)

Primary hHSCs were purchased from Sciencell (Carlsbad, CA). Cells were cultured as recommended by the manufacturer. Cells were treated with 86mM ethanol (EtOH; Sigma-Aldrich, Saint Louis, MO) for 72 hours. Cells were harvested with a cell scraper, and RNA was extracted with the mirVana isolation kit (ThermoFisher, Waltham, MA). The cDNA was made with the iScript reverse transcriptase kit (BioRad, Hercules, CA). Real-time PCR was performed using the SYBR Green Supermix (BioRad, Hercules, CA) and premade PCR primers (Qiagen, Germantown, MD) on an Applied Biosystems ViiA 7 PCR machine. For miRNA real-time PCR, cDNA was made with the RT2 reverse transcriptase kit (ThermoFisher, Waltham, MA) with premade primers (ThermoFisher, Waltham, MA) and Taqman reagents (ThermoFisher, Waltham, MA). The HSCs were also treated with 2.5ng/mL transforming growth factor beta (TGF-β; R&D Biosystems, Minneapolis, MN) or 1ng/mL lipopolysaccharide (LPS, Sigma-Aldrich, Saint Louis, MO). Cells were harvested, RNA was extracted, and real-time PCR was performed as above.

Transfections

Transfections were performed by nuclear electroporation or with lipofectamine 3000 (ThermoFisher Scientific, Waltham, MA) using the Nucleofector system (Amaxa Biosystems, Koln, Germany). For electroporation, fifty µl of 100 nM miRNA precursor,

antisense inhibitor, or controls (Ambion, Austin, TX) were added to 1 x 10^6 cells suspended in 50 µl of Nucleofector solution at room temperature. The sequences of the miRNA precursors and inhibitors used can be obtained from Ambion. After electroporation, transfected cells were resuspended in culture medium containing 10% fetal bovine serum for 48–72 hours prior to study. Lipofectamine transfections were performed according to manufacturer's instructions using siRNA obtained from Thermofisher (Waltham, MA). All studies were performed in quadruplicate unless otherwise specified.

Real-time PCR for mature miRNA

The expression of mature miRNAs in human hepatic cell lines was analyzed by TaqMan miRNA Assay (Applied Biosystems, Foster City, CA). Briefly, single-stranded cDNA was synthesized from 10 ng of total RNA in 15-µl reaction volume by using the TaqMan MiRNA Reverse Transcription Kit (Applied Biosystems). The reactions were initially incubated at 16°C for 30 min and then at 42°C for 30 min. The reactions were inactivated by incubation at 85°C for 5 min. Each cDNA generated was amplified by quantitative PCR via sequence-specific primers from the TaqMan miRNA Assays on a MX 3000P PCR Instrument (Stratagene, San Diego, CA). The 20-µl PCR included 10 µl of 2 × Universal PCR Master Mix (No AmpErase UNG), 2 µl of each 10× TaqMan MiRNA Assay Mix, and 1.5 µl of reverse transcription (RT) product. The reactions were incubated in a 96-well plate at 95°C for 10 min, followed by 40 cycles of 95°C for 15 s and 60°C for 1 min. The threshold cycle (CT) is defined as the fractional cycle

number at which the fluorescence passes the fixed threshold. SuperArray real-time PCR array and real-time PCR analysis: The RNA was isolated from liver tissues or cell lysates using TRIzol (Invitrogen, Carlsbad, CA) according to the manufacturer's protocol; after isolation, the RNA was subsequently cleaned using Qiagen's RNeasy Kit (Qiagen, Valencia, CA), again according to the manufacturer's protocol. The optional on-column DNase treatment was performed. Reverse transcription was done using 1 µg RNA with SABiosciences RT2 First Strand Kit (SABiosciences, Frederick, MD) according to the manufacturer's protocol. Mouse liver tissue or normal cDNA from hHSCs was analyzed using SuperArray plates Mouse Fibrosis PCR array (#PAMM-120A), SABiosciences, Frederick, MD). To validate the translational significance of these gene expression findings, mice liver and human HSC samples were analyzed using real-time PCR. SABiosciences's RT² Real-Time PCR Primer Assays or Taqman miRNA PCR assay were used. Real-time PCR was performed using SABiosciences' RT2 SYBR Green/ROX Real-Time PCR Master Mix for a Stratagene Mx3005P Real-Time PCR System according to the manufacturer's protocol. 6-carboxyfluorescein was used as an endogenous reference, and data were analyzed using SABiosciences' PCR Array Data Analysis Template. The comparative CT method was used for quantification of gene expression. All samples were tested in triplicate, and average values were used for quantification.

Animal studies

All animal studies were reviewed and approved by the Animal Care and Use Committees of Baylor Scott & White and the University of Southern California according to the National Research Council's Guide for the Care and Use of Laboratory Animals. Lin28atm1.2Gqda/J (Lin28B KO) and C57BL/6J (wild type) mice were purchased from Jackson Labs (Bar Harbor, ME). Animals were treated with the intragastric EtOH infusion model as previously described (23). After euthanasia, livers were harvested, part of the liver was fixed with formalin and embossed in paraffin, and the remaining liver was flash frozen and stored at -80°C. Evaluation of Lin28A/B and let-7 levels was performed by extracting RNA with the miRVana kit and real-time PCR was performed as above.

Western blotting

Cells grown in 100-mm dishes were lysed, and protein content was quantitated using the Bradford protein assay. Equivalent amounts of protein were resolved by sodium dodecyl sulfate polyacrylamide gel electrophoresis and transferred to nitrocellulose membranes. Membranes were blocked and incubated with the specific primary antibody (rabbit anti-Lin28B and goat anti-high-mobility group AT-hook (HMGA2), Santa Cruz Biotechnology, Dallas, TX) overnight at 4°C, washed and incubated with the appropriate IRDye700- and IRDye800-labeled secondary antibodies (Rockland, Gilbertsville, PA) (1:1000) for 1 hr. Blots were stripped and re-probed with mouse monoclonal antibodies for β-actin (Sigma, St Louis, MO) (1:1000), or total glyceraldehyde-3-phosphate

dehydrogenase antibody (1:1000), which was used for normalization. Protein expression was visualized and quantified using the LI-COR Odyssey Infrared Imaging System (LI-COR Bioscience, Lincoln, NE).

Luciferase reporter assay

Intact putative let-7a and let-7b recognition sequence from the 3'-UTR of Lin28B and HMGA2 (pMIR-Lin28B/HMGA2-wt-3'-UTR) or with random mutations (pMIR-Lin28B/HMGA2-mut-3'-UTR) were cloned downstream of the firefly luciferase reporter gene. Cells were co-transfected with 1 μg pMIR- Lin28B/HMGA2-wt or mut-3'-UTR construct and 1 μg pRL-TK Renilla luciferase expression construct with or without precursor miR-34a using TransIT-siQUEST transfection reagent (Mirus, Madison, WI, USA). Luciferase assays were performed 72 hours after transfection using the Dual Luciferase Reporter Assay system (Promega, Madison, WI).

Cell migration assays

Cell migration was assessed by using the Oris Cell Migration assay kit (Platypus Technologies, Madison, WI). Briefly, cells were stained with calcein AM (Calbiochem, Gibbstown, NJ) and plated (10,000 cells/well) in a 96-well plate provided with an insert that prevented the cells from attaching in a central analytic zone. After overnight incubation at 37°C, medium was changed to serum-free medium containing the compounds, and the insert was removed to allow cells to migrate into the central zone. The cells that had migrated into the central zone were labeled by calcein AM and

quantified fluorometrically by using the SpectraMax M5 Plate Reader from Molecular Devices (Sunnyvale, CA).

Immunohistochemistry analysis

Lobular necrosis was evaluated in liver sections stained with hematoxylin-eosin. Liver sections were incubated overnight at 4°C with specific antibody (1:50), washed in phosphate buffer saline (PBS), incubated for 20 min at room temperature with a secondary biotinylated antibody (Dako Cytomation LSAB Plus System-HRP, Glostrup, Denmark), and further incubated with Dako ABC for 20 min and developed with 3–3′ diaminobenzidine (Dako Cytomation Liquid DAB Plus Substrate Chromogen System). For all immunoreactions, negative controls were included. Immunohistochemical observations were taken by BX-51 light microscopy (Olympus, Tokyo, Japan) with a Videocam (Spot Insight; Diagnostic Instrument, Sterling Heights, MI) and processed with an image analysis system.

Evaluation of liver steatosis and fat deposition

Formalin-fixed paraffin-embedded (FFPE) sections were sectioned at 6μm and affixed to charged glass slides. Slides were re-hydrated in xylenes followed by decreasing percentages of ethanol. Hematoxylin and eosin (H&E) staining was performed by immersing slides in gill's hematoxylin (Vector Laboratories, Burlingame, CA) and subsequently eosin before dehydrating slides through elevating alcohol washes and xylenes. The Oil Red O kit (IHC World, Woodstock, MD) was used to stain slides for

fat deposition following directions from the manufacturer and dehydrated as above. Evaluation of Liver Fibrosis: The FFPE sections were sectioned at 6μm and affixed to charged glass slides. Slides were re-hydrated in xylenes followed by decreasing percentages of ethanol. The Sirius Red kit (IHC World, Woodstock, MD) was used to stain slides for collagen deposition following directions from the manufacturer and dehydrated as above. Sirius Red staining was quantified with Image J software (24). Immunofluorescence was performed on FFPE liver sections using antibodies from ABCam (San Francisco, CA). Real-time PCR was performed on total liver RNA isolates as described above.

Isolation of HSCs and evaluation of mesenchymal and fibrotic markers

Frozen liver tissue was sectioned at 10 μm and stained with fluorescent antibodies specific for desmin (Abcam, San Francisco, CA). Desmin-positive cells were isolated with laser capture microdissection (LCM) using a Leica LMD7 microscope. The RNA was isolated from desmin-positive cells using the PicoPure RNA Isolation Kit (ThermoFisher, Waltham, MA), cDNA was made, and real-time PCR was performed as above.

Human Tissues

Human liver tissue from normal and ALD patients was purchased from XenoTech, Kansas City, KS (Table 2). The RNA was isolated, cDNA was made, and real-time PCR was performed as above.

Statistical Analysis

Data are expressed as the mean ± standard error from at least three separate experiments performed in triplicate unless otherwise noted. The differences between groups were analyzed using a two-tailed Student t test when only two groups were present and ANOVA when there were more than two groups. The null hypothesis was rejected at the 0.05 level unless otherwise specified.

Table 2. Characteristics of liver donors from control and alcoholic liver disease patients.

	Age	Gender	Pathological Diagnosis	Alcohol Frequency
ALD Patient 1	48	Male	Steatohepatitis, ballooned hepatocytes, lobular inflammation, moderate portal inflammation (40% Fat)	Heavy
ALD Patient 2	43	Male	Steatohepatitis (80% Fat)	Heavy
ALD Patient 3	64	Male	Steatohepatitis, scattered ballooned hepatocytes (20% Fat)	Heavy
ALD Patient 4	51	Female	Steatohepatitis (70% Fat)	Heavy
Control 1	67	Female	None	Occasional
Control 2	68	Male	None	N/A
Control 3	51	Male	None	Occasional
Control 4	63	Female	None	Occasional

4.4. Results

Presence of enhanced mesenchymal phenotypes due to long-term ethanol exposure in mice liver

Recent studies from the chronic-plus-binge ethanol feeding model suggest that binge drinking induces significant activation of HSCs, leading to liver fibrosis in chronic ethanol-fed mice [122]. To test the impact of chronic alcohol drinking on hepatic mesenchymal phenotypes and liver injury, we analyzed the role of the mesenchymal markers vimentin, S100A4, and fibronectin in mouse livers with chronic alcoholic liver injury. Eight weeks of intragastric feeding of ethanol (~27 g/kg/day) induced significant liver damage (Fig. 12A) and increases in serum alanine aminotransferase level compared with control mice (Fig. 12B), along with significantly enhanced expression of fibrosis markers such as *Vim, Fn1 Acta2, Col1a1* and *Timp1* (Fig. 12D and E). These results, along with liver histologic findings (Fig. 12C), indicate that long-term ethanol feeding induced liver fibrotic responses.

Altered let-7/Lin28 axis in ethanol-exposed mice liver tissues

We have demonstrated the aberrant expression of selected miRNAs after alcoholic liver injury, including the significant reduction of let-7 family members [104, 113, 123]. To further extend these observations in alcoholic liver injury, we analyzed the expression of let-7 family members in five pairs of ethanol-treated mouse and control liver tissues using the Taqman real-time PCR assay. The expressions of several let-7 miRNAs

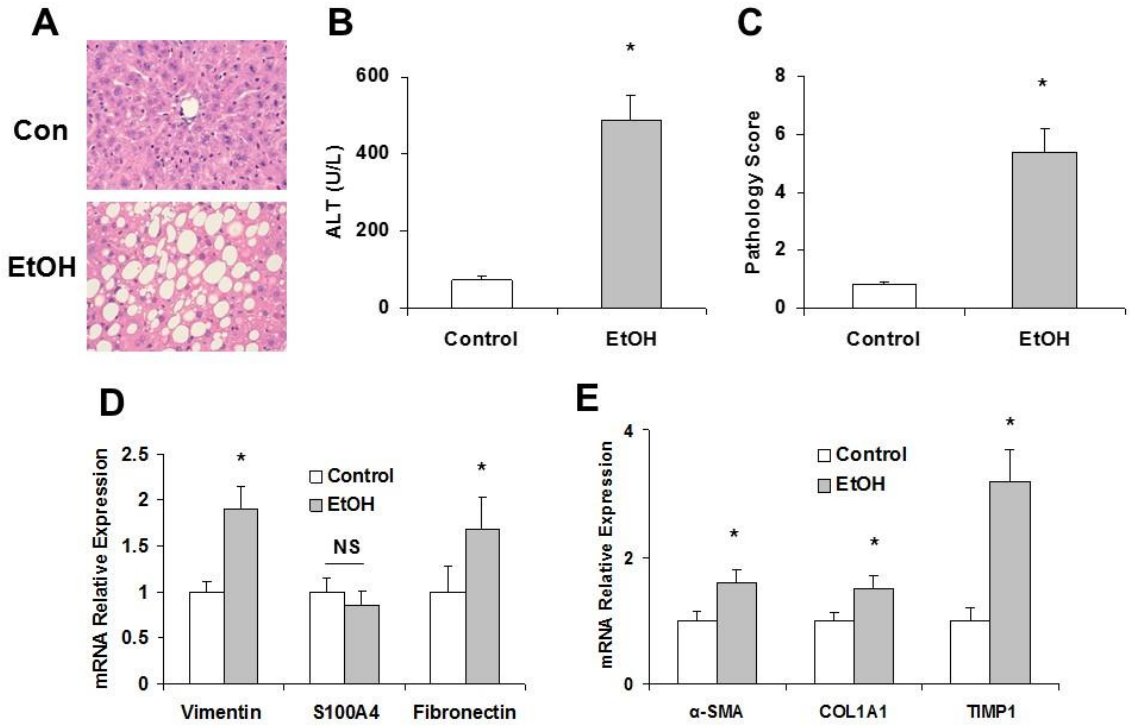

Figure 12. ***Intragastric ethanol feeding induces liver injury and increases expression of mesenchymal and fibrotic markers.*** (A) C57Bl/6J mice were fed either a control or ethanol diet for eight weeks (n=5). Livers were harvested, fixed in formalin, and embedded in paraffin. A number of 6mm sliced liver sections were affixed to glass slides, rehydrated and stained with hematoxylin and eosin (H&E) to evaluate gross histology. The H&E histology of control (upper) and ethanol-fed mice (lower) showed increased steatosis and liver injury in ethanol-fed mice. (B) Serum was extracted from both control-fed and ethanol-fed mice, and alanine aminotransferase (ALT) levels were measured. The ALT levels were shown to be increased in ethanol-fed mice, correlating the increased steatosis seen in panel A. (C) The H&E histology was scored by three separate observers from one (no damage) to 10 (severe damage) to quantify the level of liver damage based on the levels of steatosis, hepatic ballooning, loss of liver structure, etc. It was found after combining the scores from the three observers, that the histopathology scores were significantly higher in the ethanol-fed mice. (D) The mRNA levels of the mesenchymal markers (vimentin, S100A4 and fibronectin) in total liver samples were measured with real-time PCR in control and ethanol-fed mice. Mesenchymal markers were shown to be elevated in ethanol-fed mice compared to control. (E) The fibrosis markers (α-SMA, Col1A1, and TIMP1) were evaluated in total liver samples derived from control and ethanol-fed mice. Ethanol-fed mice were shown to have significantly increased mRNA levels of these markers compared to control-fed mouse livers. Data is presented as +/- SEM (n=5). *p<0.05 relative to controls.

(including let-7a, let-7b and let-7g) were markedly decreased (more than half) in ethanol-exposed liver tissues compared with control liver tissues (Fig. 13A). The expression of let-7a and let-7b was also decreased in LPS- and TGF-ß-treated hHSCs with a higher migration rate compared with controls (Fig. 13 B&C). Inhibition of let-7a and let-7b in hHSCs also significantly increased cell migration rate (Fig. 13D). To further verify the expression of let-7 in human alcoholic liver disease (ALD), real-time PCR analysis was performed for total RNA from patient ALD and normal human liver tissues obtained from XenoTech (Kansas City, KS). The expression of let-7a and let-7b was decreased by 50% or more in three of the four ALD samples compared with the control liver tissues (Fig. 13 E&F). These results indicate that reduced expression of let-7 is a common event in clinical and experimental ALD.

A main target gene of let-7 is an RNA-binding protein and stem cell marker, Lin28. Elevation of Lin28 and decrease of let-7 are linked with highly aggressive diseases in other organs, and their importance in liver diseases is also suggested [115]. Significantly increased expression of Lin28B (but not Lin28A) was observed in ethanol-fed mouse livers relative to controls, along with the enhanced expression of another let-7 target gene, HMGA2 [124] (Fig. 14A). Additionally, both Lin28B and HMGA2 are significantly increased in LPS- and TGFß-treated hHSCs (Fig. 14B) as well as in human ALD samples, suggesting the potential role of the let-7/Lin28B axis in human ALD and liver fibrosis (Fig. 14 C-E).

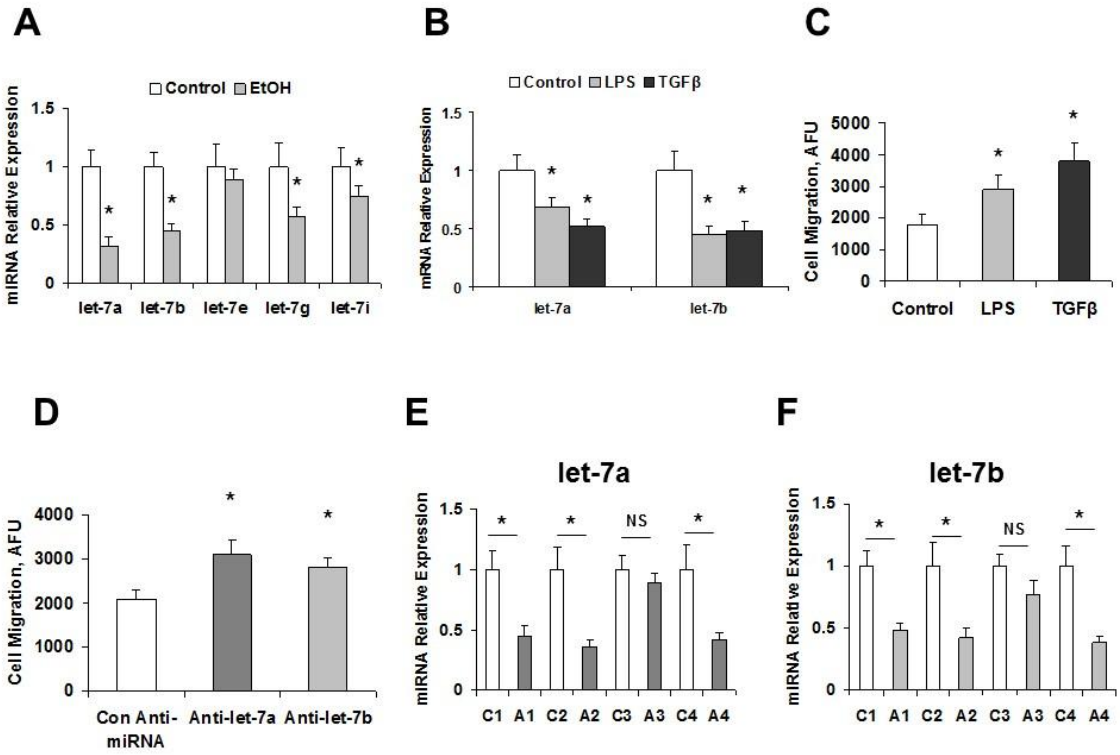

Figure 13. ***let-7 levels affect migration and levels are decreased upon exposure to LPS, TGFβ or EtOH.*** These hHSCs were cultured as recommended by the manufacturer on poly-L-lysine-coated plates. All hHSCs at 70-80% confluency were treated with 10 mM ethanol, 1 ng/ml TGF-β or LPS (1 μg/ml) for 72 hours. Cells were collected and total RNA was extracted. Real-time PCR was performed to evaluate the levels of let-7 family miRNA after treatment with ethanol (A), LPS, or TGF-β (B). Cellular migration was analyzed in hHSCs with the Oris Cell Migration assay kit after LPS or TGF-β treatment (C) or let-7 knockdown (D). Migrating cells were positively stained by calcein AM, and levels of migrating cells were quantified with a spectrophotometer. The presence of LPS, TGF-β, and let-7 inhibition increased the migration ability of hHSCs. (E-F) Total liver samples from human alcoholic liver disease or control patients were analyzed for let-7 levels with real-time PCR (E-F). Alcoholic patient liver samples showed significant reductions in both let-7a and let-7b. Data is presented as +/- SEM (n=5). *$p<0.05$ relative to specific control group. *NS*: No significant difference.

Regulation of Lin28B and HMGA2 by let-7 in hHSCs

To verify that *Lin28B* and *HMGA2* are bona fide targets of translational regulation by let-7 in hHSCs, we performed studies using luciferase reporter constructs containing the let-7a/let-7b recognition sequence from the 3′-UTR of *Lin28B* and *HMGA2* inserted downstream of the luciferase gene (Fig. 15 A-B). Transfection with let-7a/let-7b precursor in hHSCs decreased reporter activity of both L*in28B* and *HMGA2* in normal hHSCs. However, when these studies were repeated with reporter constructs that contained random mutations in the recognition sequence, the effects of reporter deactivation by let-7a/let-7b precursor were abolished (Fig. 15 C&D). Moreover, reductions in *Lin28B* and *HMGA2* expression occurred in hHSCs incubated with pre-let-7a/let-7b for three days (Fig. 15E). Western blot analysis also demonstrated significant reduction of Lin28B: 0.40±0.08 (Pre-let-7a, p=0.01), 0.62 ± 0.10 (Pre-let-7b, p=0.03); and HMGA2: 0.55±0.09 (Pre-let-7a, p=0.03), 0.44 ± 0.07 (Pre-let-7b, p=0.02) relative to Pre-miRNA controls respectively (n=6). Concomitant with reduced HMGA2 expression, there was significant repression of the snail family transcriptional repressor (Snail) and the twist family bHLH transcription factor (Twist), which are the known downstream mediators of HMGA2 mesenchymal signaling (Fig. 15E). In contrast, transfection with a precursor to miR-21 (which can also modulate mesenchymal phenotypes in normal hHSCs) did not alter the expression of *Lin28B* and *HMGA2* with a relative expression of 1.2 ± 0.2-fold and 0.9 ± 0.4-fold of controls, respectively. Taken together, these findings confirm that *Lin28B* and *HMGA2* are the biologically relevant targets of let-7a/let-7b in hHSCs.

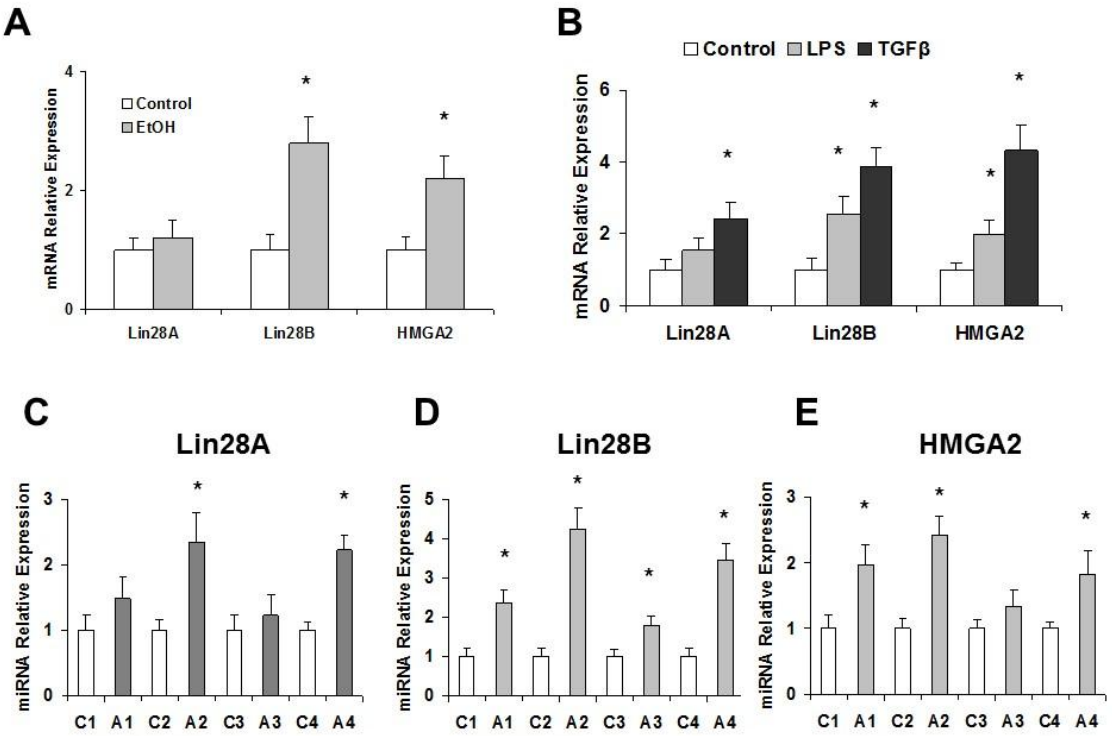

Figure 14. ***Ethanol, LPS or TGF-β exposure increases Lin28 and HMGA2 levels.*** These hHSCs were cultured as recommended by the manufacturer on poly-L-lysine-coated plates. The HSCs at 70-80% confluency were treated with 10 mM ethanol as well as 1 ng/ml TGF-β or 1 μg/ml LPS for 72 hours. Cells were collected and total RNA was extracted. The Lin28A/B and HMGA2 levels were measured by real-time PCR in hHSCs treated with ethanol (A), LPS or TGF-β (B). The Lin28A/B and HMGA2 levels were all elevated in hHSCs treated with LPS, TGF-β, and ethanol. (C-E) Total liver samples from human alcoholic liver disease or control patients were analyzed for Lin28A/B and HMGA2 levels with real-time PCR. Data is presented as +/- standard error (n=5). *p<0.05 relative to specific control group.

Regulation of let-7/Lin28 associated mesenchymal phenotypes in hHSCs

We have previously demonstrated a role for miR-34a in alcoholic liver injury. However, the role of let-7 in ALD remains unknown. Thus, we performed studies aimed to explore the possible biological significance of aberrant let-7 by using an anti-sense oligo inhibitor specific to let-7a and let-7b. First, we verified the efficacy of transfection and target effects by assessing the expression of mature let-7a and let-7b by real-time PCR in hHSCs transfected with anti-let-7a and let-7b inhibitors (Fig. 16A). Significant upregulation of vimentin and fibronectin was seen after anti-let-7a and anti-let-7b treatment (Fig. 16B). We also quantified let-7a/let-7b expression in let-7a/let-7b transfected cells before and after alcohol exposure and demonstrated that alcohol significantly decreased let-7a and let-7b by 0.6-fold and 0.5-fold in hHSCs, respectively. A prolonged ethanol treatment (1 wk) without let-7a/let-7b transfection also reduced let-7a/let-7b expression by 0.4-fold and 0.3-fold, respectively. In these cells, the expression of vimentin and fibronectin was upregulated. These observations indicate a role for let7 in the regulation of mesenchymal phenotypes of hHSCs after alcoholic exposure.

The ability to migrate into injured areas of tissues is a phenotypic characteristic of HSC activation and a key determinant of the hepatic fibrogenetic process. To assess the effect of Lin28B on cell motility, hHSCs were transfected with either control, Lin28B or HMGA2 siRNAs, and vertical cell migration was assessed. Silencing Lin28B or

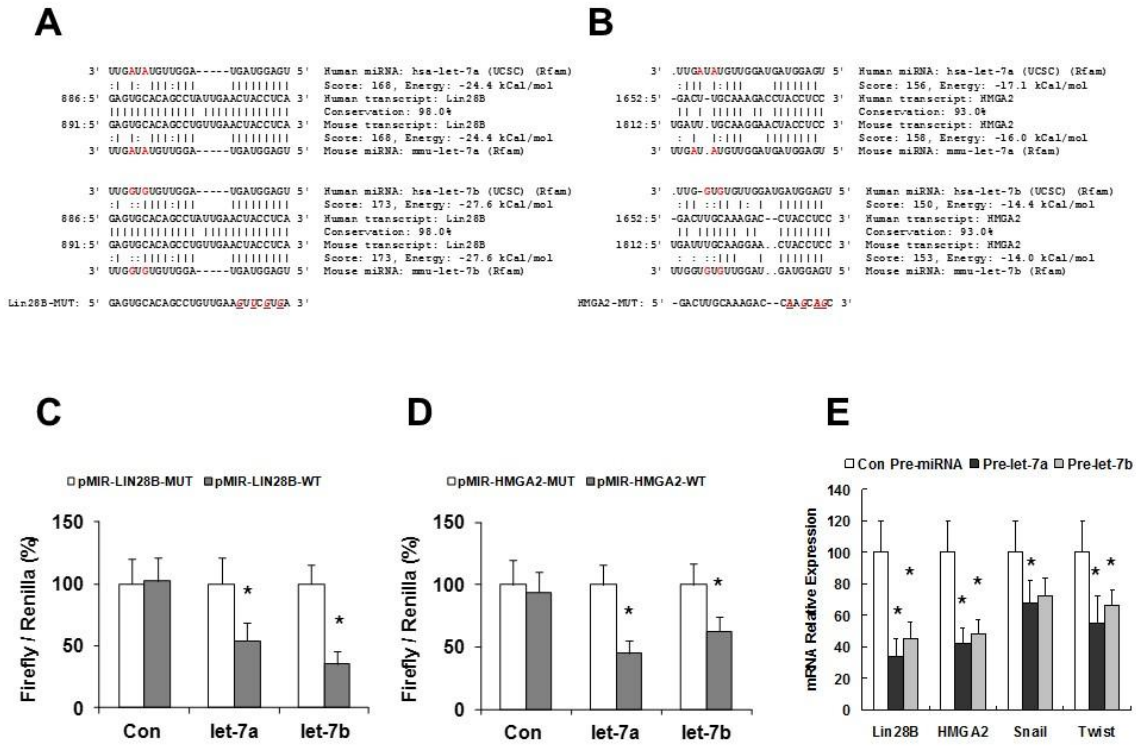

Figure 15. ***let-7 is increased upon blockage of Lin28B or HMAG2 and blockage of let-7 can alter mesenchymal mediators.*** The intact let-7a and let-7b recognition sequences from the 3'-UTR of Lin28B and HMGA2 or with random mutations were cloned downstream of the firefly luciferase reporter gene (A-B). Luciferase assays were performed 72 hours after transfection of pre-let-7a, pre-let-7b and control pre-miRNA. The let-7 levels were analyzed with real-time PCR after these constructs were used to block Lin28B (C) and HMGA2 (D). The let-7 levels were increased after knockdown of either Lin28B or HMGA2. (E) Plasmids for let-7a/b were transfected into hHSCs by electrophoresis, cells were harvested after 48 hours, total RNA was extracted, and Lin28 and HMGA2 (as well as the mesenchymal mediators Snail and Twist) were evaluated with real-time PCR. Overexpression of let-7 induced decreases in both isoforms of Lin28 as well as HMGA2, Snail, and Twist. Data is presented as +/- SEM (n=5). *p<0.05 relative to specific control group.

HMAG2 decreased the cell migration index (Fig. 16C, G). In addition, silencing of Lin28B significantly decreased the fibrogenic markers *ACTA2* and *TIMP3* (Fig. 16D). Furthermore, cell motility was significantly increased after ethanol treatment (Fig. 16E). This effect was accompanied by increased Lin28B, decreased let-7a/let-7b, and upregulated vimentin and fibronectin (Fig. 16F). Silencing of HMGA2 in stellate cells did not alter let-7a levels but decreased TIMP1 expression in HSCs (Fig. 16H). Collectively, these results support a functional role for ethanol-induced Lin28B/let-7 axis in activating hHSC and stimulating their migration.

Reduced mesenchymal phenotypes and liver fibrosis in Lin28B deficient mice

To extend our study on Lin28B to *in vivo*, we carried out intragastric ethanol feeding for eight weeks in Lin28B-deficient and WT control mice. Intragastric ethanol feeding induced severe steatosis and changes in liver structure. In contrast, Lin28B-deficient mice fed an intragastric ethanol diet showed a reduction in the degree of steatosis and liver structure alterations, suggesting that Lin28B promotes recovery during alcoholic liver injury (Fig. 17 A&B). Plasma levels of the liver enzyme alanine aminotransferase and total liver pathology scores were decreased in Lin28B-deficient mice with EtOH compared with WT mice with EtOH (Fig. 17C). Significant reductions in type I collagen and ACTA2 were noted in Lin28B deficient-EtOH mice compared with WT-ETOH mice (Fig. 18A). Further, significant reductions in vimentin and fibronectin mRNA were noted in Lin28B-deficient EtOH-treated mice (Fig. 18B). A fibrosis PCR

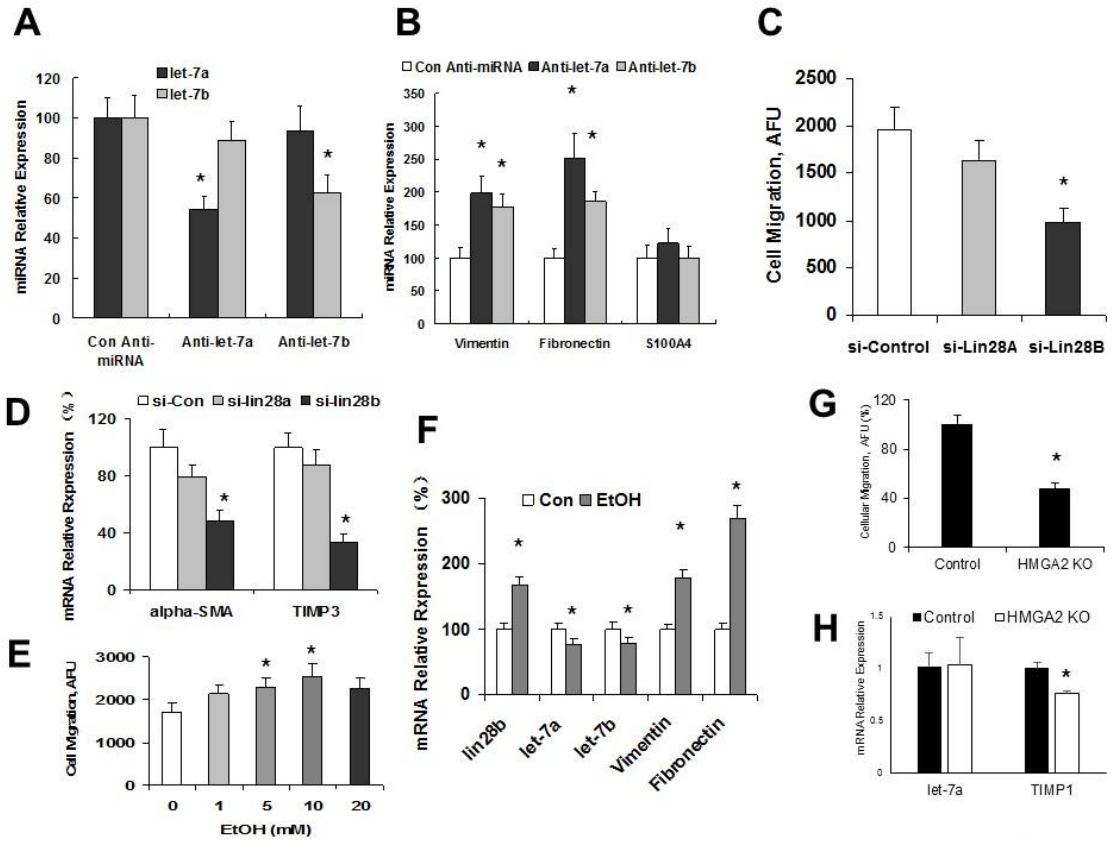

Figure 16. ***The Lin28/let-7 axis controls cellular migration and mesenchymal marker expression.*** The hHSCs were transiently transfected for inhibitors of let-7 via electrophoresis. Cells were harvested 48 hours after transfection, RNA was extracted and real-time PCR was performed for levels of let-7 (A) and mesenchymal markers (B). Knockdown of let-7 was confirmed in panel A. The silencing of let-7 induced these cells to increase levels of the mesenchymal markers, Vimentin, S100A4, and fibronectin. (C) The hHSCs were transiently transfected for siRNAs to Lin28A or Lin28B via electrophoresis. Cellular migration was analyzed in Lin28A/B repressed hHSCs with the Oris Cell Migration assay kit. (D) The Lin28A/B repressed cells were harvested 48 hours after transfection, RNA was extracted, and real-time PCR was performed for the fibrosis markers α-SMA and TIMP3. Silencing of Lin28B reduced the levels of fibrotic markers. (E) The hHSCs were treated with 10 mM ethanol for 72 hours and cellular migration was measured as above. Treatment with ethanol increased cellular migration in a dose dependent manner. (F) The hHSCs treated with ethanol were harvested after 72 hours, RNA was extracted, and real-time PCR was performed for Lin28, let-7, and the mesenchymal markers Vimentin and fibronectin. Lin28B levels were elevated, let-7 levels were decreased, and Vimentin and fibronectin levels were increased after treatment with ethanol. (G) HSCs were transfected with siRNA against HMGA2 and cellular migration was measured as above. Migration is presented as a percentage of si-control migration. (H) mRNA was extracted from HSCs transfected for si-HMGA2 and let-7a and TIMP1 levels were measured by qPCR. Data is presented as +/- SEM (n=5). *p<0.05 relative to specific control groups.

array also identified obvious reduction of liver fibrosis-related genes such as α-SMA (ACTA2), TIMP-4, MMP-1, integrin-B6 and caveolin (Fig. 18C). Ingenuity Pathway Analysis (IPA) was performed to ascertain the cellular context of the differentially expressed genes related to Lin28B deficiency-mediated liver repair. Pathway analysis indicated that the hepatic mesenchymal/fibrotic pathway was the most inhibited through let-7/Lin28-related signaling mechanisms (Fig. 18D). Further analysis with IPA uncovered several differentially regulated mesenchymal/fibrotic gene alterations following Lin28B silencing in ethanol-fed mouse liver. Several of these genes are regulated by the let-7/Lin28 axis, including vimentin, fibronectin, HMGA2, Twist, Snail, TIMP-1, TIMP-4, MMP-3 and MMP-9. These studies indicate that the loss of Lin28B ameliorates alcoholic liver injury and fibrosis through the inhibition of mesenchymal signaling pathways.

Since activation of HSCs is central in the development of liver fibrosis, we analyzed HSC activation *in vivo* by staining liver sections for desmin (HSC marker) or *α*-SMA (marker of activated HSCs) and quantified the percentage of positive cells. Ethanol feeding increased the number of desmin-positive and *α*-SMA-positive cells in WT mice; these findings were accompanied by increased Sirius Red staining and collagen deposition (Fig. 19 A-C). In Lin28B-deficient mice, EtOH inductions of desmin-positive or *α*-SMA-positive cells were suppressed compared with WT mice with EtOH; these findings were also accompanied by decreased Sirius Red staining and collagen

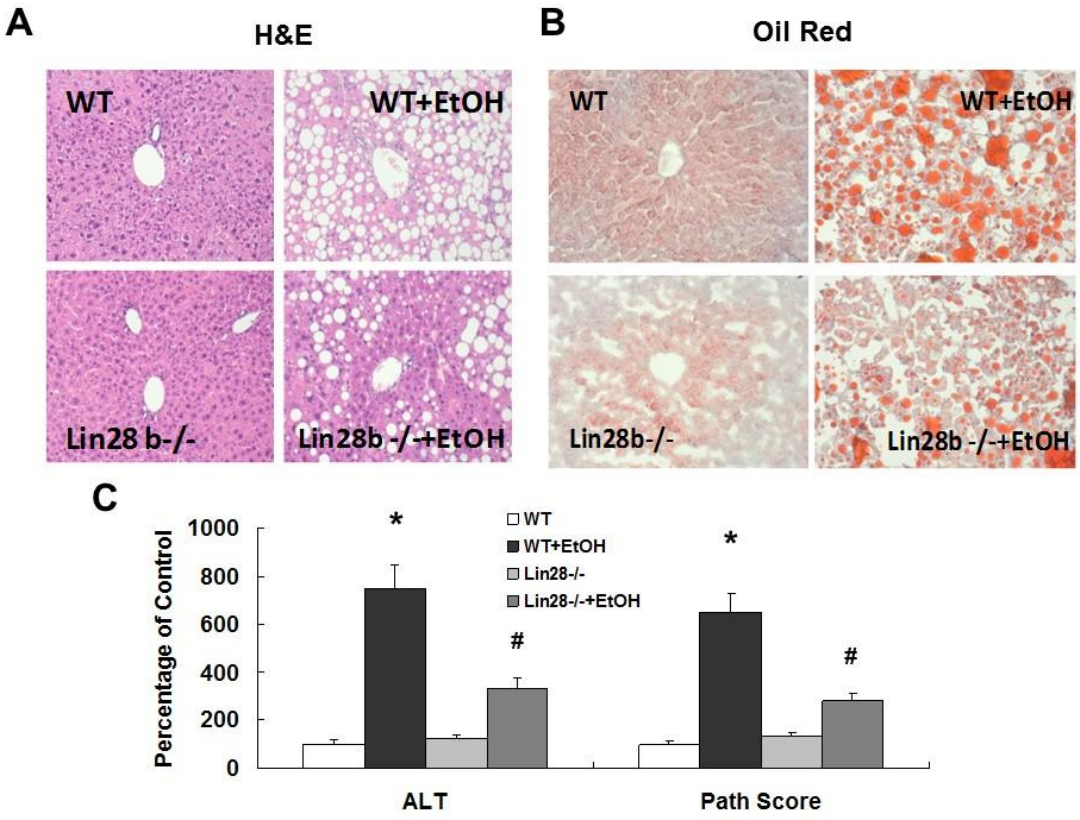

Figure 17. ***The recovery effects of Lin28B deficiency in ethanol feeding mice.*** The H&E (A) and Oil Red O (B) staining were performed in FFPE and frozen sections, respectively, in wild type and Lin28B-deficient mice with or without ethanol feeding. Red staining in Oil Red O sections is positive for lipid. The H&E staining showed reduced steatosis and other liver damage in Lin28B deficient mice. Additionally, Oil Red O staining showed reduced fat deposition in Lin28B-deficient mice. Serum ALT levels and histopathological scores were evaluated in wild type and Lin28B-deficient mice with or without ethanol feeding (C). The ALT levels and overall histopathology scores were reduced in Lin28B-deficient mice. Data is presented as +/- SEM (n=5). *p<0.05 relative to WT control group; #p<0.05 relative to WT+EtOH group.

deposition (Fig. 19 A-C). In HSCs that were isolated from WT-EtOH mice by laser capture microdissection (LCM) (Fig. 19D), we detected increased mRNA expression of *Col1a1*, *MMP-13* (mouse MMP-1 is MMP-13), *Timp-1*, and *Timp-4* when compared with WT without EtOH (Fig. 19 E-F). In contrast, HSCs that were isolated from Lin28B-deficient mice with EtOH had reduced inductions of these parameters compared with WT mice with EtOH (Fig. 19 E&F). No significant differences of fibrosis markers were noted between HSCs isolated from WT controls and Lin28B-deficient controls. These data further support our notion that increased Lin28B contributes to HSC activation and alcoholic liver fibrosis.

Identification of feedback loop in HSCs isolated from Lin28B deficient mice

The miRNA, let-7 can activate TRIM71, which targets Lin28 for ubiquitin-mediated proteasomal degradation, thus inhibiting Lin28 expression at both posttranscriptional and posttranslational levels [125]. The Lin28B-let-7 positive feedback loop was discovered in human cancer development and progression and established that Lin28 (which is targeted by let-7) inhibits the biogenesis of let-7 family miRNAs to support Lin28 expression [126, 127]. To confirm the feedback loop in HSC in alcoholic liver injury, total liver tissues and LCM-isolated HSCs from WT and Lin28B-deficient mice (with or without EtOH treatment) were analyzed for the expression of let-7 family members by Taqman real-time PCR assay. Indeed, the expression of let-7a and let-7b was significantly upregulated in the total liver from Lin28B-deficient mice when compared to WT mice (with or without EtOH respectively) (Fig. 20A). However, only

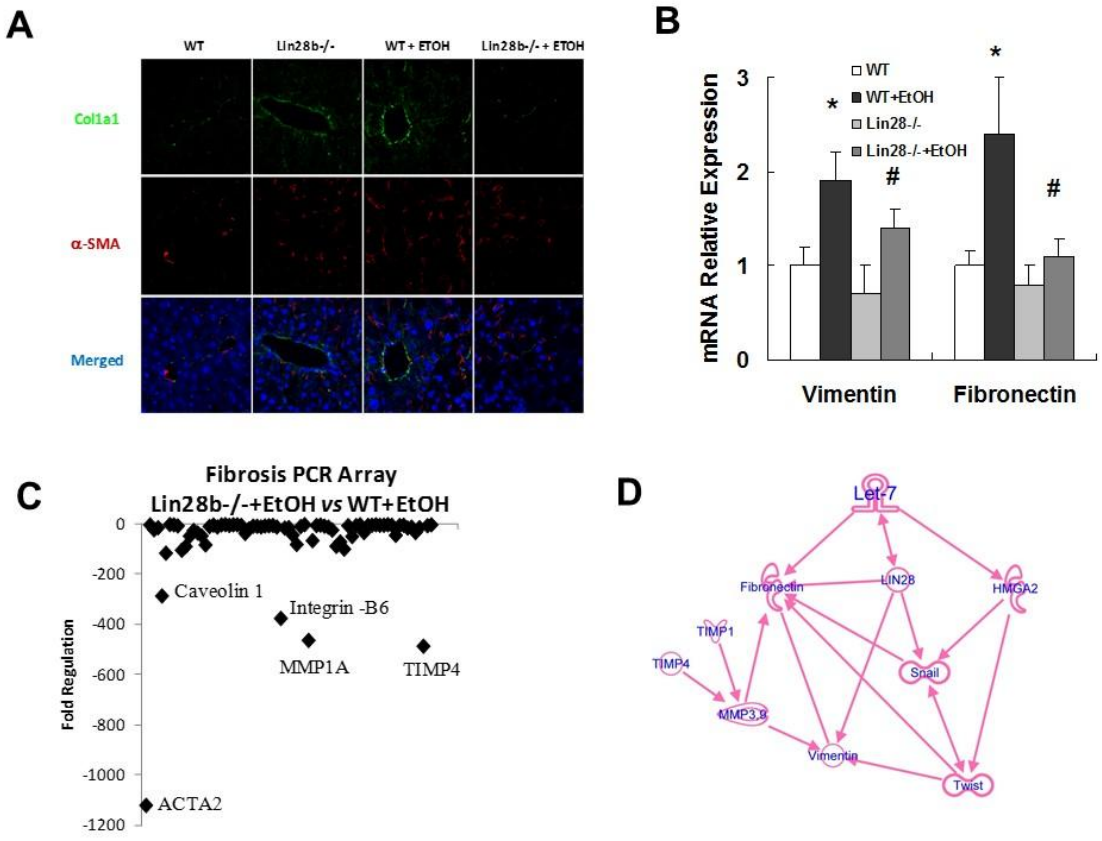

Figure 18. ***Liver fibrosis and mesenchymal markers are decreased in Lin28B-deficient mice with alcoholic liver injury.*** Immunofluorescence was used to identify the location of Collagen 1A1 (green) and α-SMA (red) in liver sections (A). Real-time PCR was performed in total liver probed for the mesenchymal markers vimentin and fibronectin (B). These mesenchymal markers were reduced in Lin28B-deficient mice. A fibrosis PCR array (SABioscience, Frederick, MD) was used to evaluate levels of fibrotic markers in Lin28B-deficient ethanol-fed mice compared to wild type ethanol-fed mice (C). Lower levels of markers indicate that these markers were decreased in Lin28B-deficient ethanol-fed mice compared to wild type ethanol-fed mice. The markers most downregulated in Lin28B-deficient mice were ACTA2 (α-SMA), TIMP-4, and MMP-1. *Panel D* presents Ingenuity Pathway Analysis (IPA) of differentially regulated gene network after Lin28B deficiency in ethanol-fed mice. IPA was performed to understand the cellular context of the differentially expressed genes related to the recovery effects of Lin28B silencing during alcoholic liver injury. Several mesenchymal and fibrotic genes implicated in HSC activations are regulated by Lin28B deficiency in vivo, including Vimentin, fibronectin, HMGA2, Twist, Snail, TIMP-1, TIMP-4, MMP-3 and MMP-9. Data is presented as +/- SEM (n=5). *p<0.05 relative to WT control group; #p<0.05 relative to WT+EtOH group.

let-7a was significantly upregulated in LCM-isolated HSCs from Lin28B-deficient mice when compared to WT mice (with or without EtOH, respectively), suggesting the pathologic role of the Lin28B-let-7a positive feedback in HSC activation and liver fibrosis (Fig. 20B). Furthermore, the expression of the let-7 target gene HMGA2, along with its downstream mediators of mesenchymal transition, Snail and Twist, were all significantly downregulated in Lin28B-deficient mice with EtOH when compared with WT mice with EtOH, further supporting a critical role of a Lin28-let-7a-HMGA2 feedback loop in activation of HSCs in alcoholic liver fibrogenesis (Fig. 20 C-D).

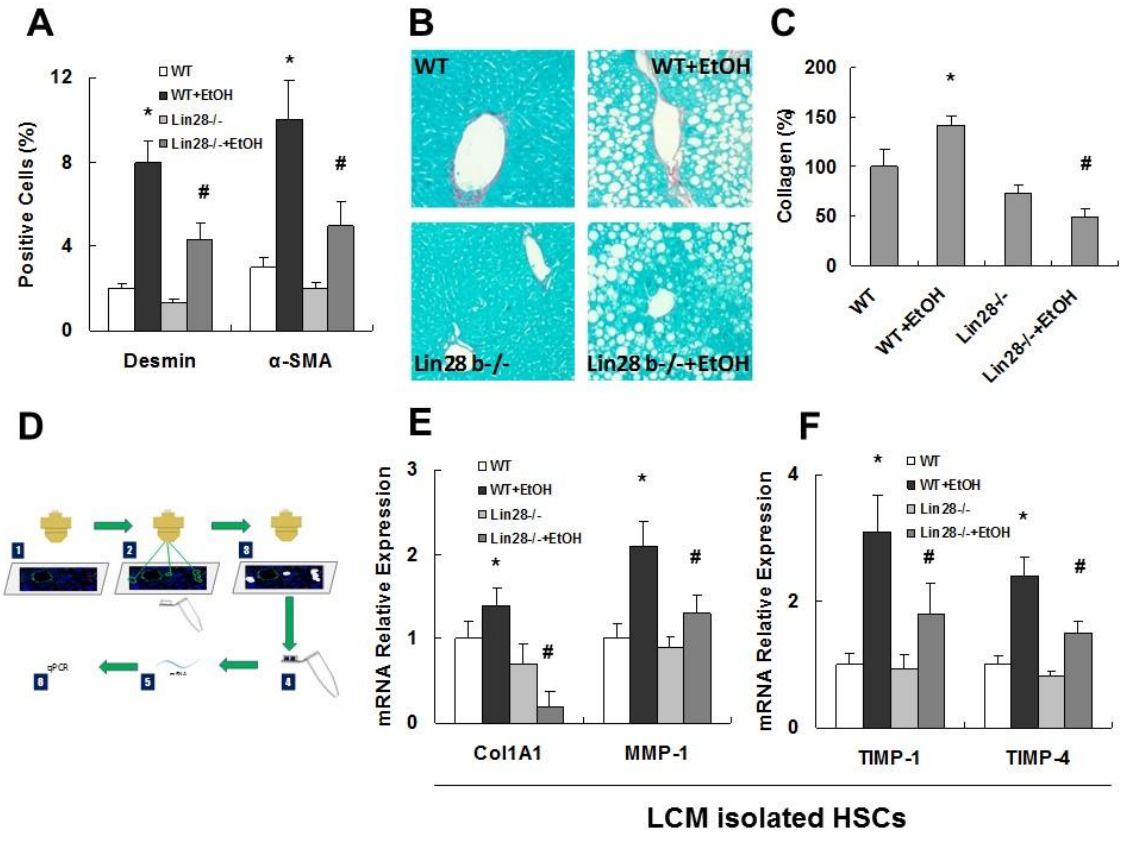

Figure 19. ***Reduced hepatic stellate cell activation in Lin28B deficient mice with alcoholic liver injury.*** Frozen liver sections were stained for desmin with immunofluorescence (A). Quantitative analysis of desmin and α-SMA staining for hepatic stellate cells in wild type and Lin28B-deficient mice with and without ethanol feeding are displayed. Desmin-positive cells were reduced in Lin28B-deficient mice with or without ethanol feeding compared to their respective controls. Sirius Red staining for collagen deposition was performed in liver sections (B) and quantified with Image J software (C). Collagen deposition was shown to be significantly reduced in Lin28B-deficient ethanol-fed mice compared to wild type ethanol-fed mice. The LCM procedure was used to isolate desmin-positive hepatic stellate cells. RNA was extracted from hepatic stellate cells and real-time PCR was performed (D). The fibrosis markers, collagen 1A1, MMP1 (E) TIMP1 and TIMP4 (F) were evaluated with real-time PCR after LCM of desmin-positive cells in liver sections. Collagen 1A1, MMP1, TIMP1 and TIMP4 that were elevated in wild type ethanol-fed mice was reduced in Lin28B-deficient ethanol-fed mice. Data is presented as +/- SEM (n=6). *p<0.05 relative to WT control group; #p<0.05 relative to WT+EtOH group.

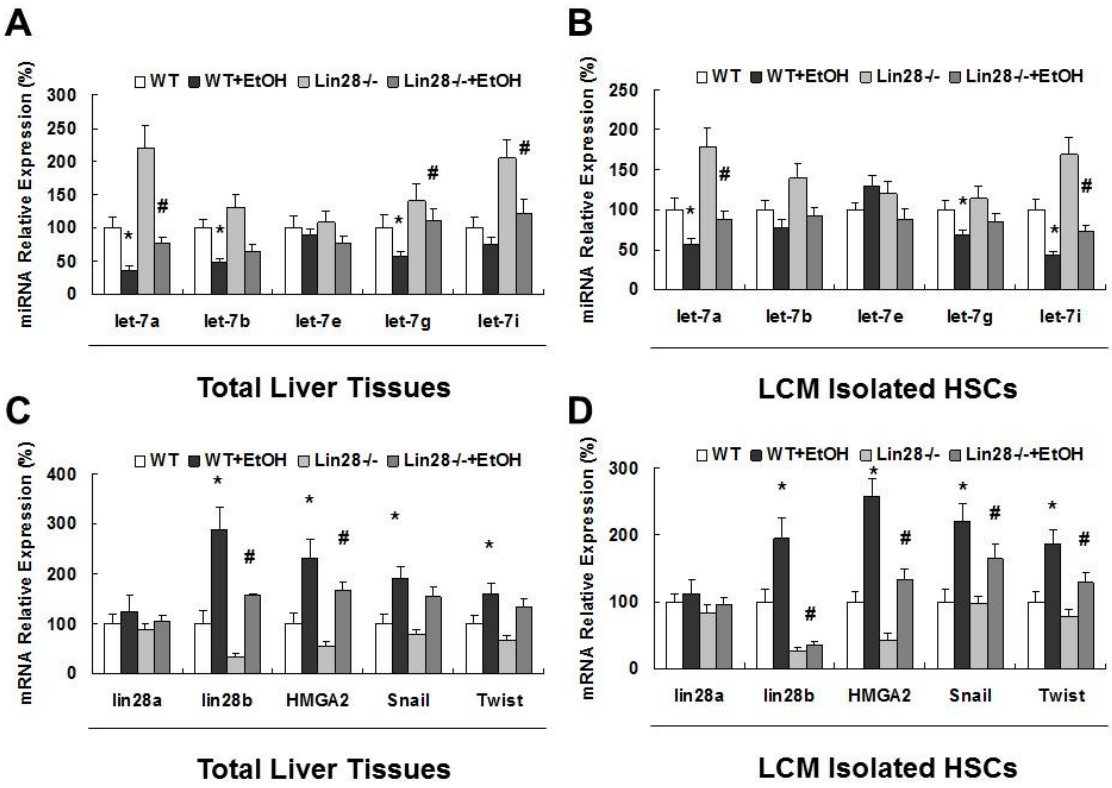

Figure 20. ***Lin28B-deficient mice showed increased let-7 levels, decreased HMGA2 levels and decreased levels of mesenchymal mediators in total liver and isolated hepatic stellate cells.*** The levels of let-7 (A-B), Lin28, HMGA2 and the mesenchymal mediators Snail and Twist (C-D) were evaluated with real-time PCR in total liver (A,C) and after laser capture microdissection of desmin-positive cells in liver sections (B,D). Data are presented as +/- SEM (n=6). **p*<0.05 relative to WT control group; #*p*<0.05 relative to WT+EtOH group.

4.5. Discussion

In this study, we described the role of altered expression of the let-7/Lin28 axis by ethanol and its contribution to mesenchymal phenotypic changes that are associated with ALD progression. The results suggest that decreased let-7a and let-7b is associated with HSC activation in ALD mouse livers and in LPS/TGFβ-treated HSCs compared with controls. We propose that let-7 contributes to anti-alcoholic liver injury and tissue reparation through modulating HSC activation by inhibition of HSC activation markers. Some of these effects are mediated through let-7 targets, Lin28B, and HMGA2, which are all known to be involved in mesenchymal reactions and ALD. Altered expression of let-7/Lin28 was shown by *in situ* hybridization during HCC development and a similar role for let-7/Lin28 has been postulated in the development of type 2 diabetes mellitus. The silencing of Lin28 in Lin28B-deficient mice can inhibit activation of HSCs and subsequently facilitate tissue recovery in ethanol-fed mouse liver. These findings taken together support a functional role for let-7/anti-Lin28 modulation in promoting liver tissue repair and against liver fibrosis during the development of ALD.

The miRNA, let-7, is a vital mediator of liver damage in many liver diseases. It has been shown to be decreased in several forms of acute and chronic liver diseases, but it has not yet been analyzed in ALD. We have shown that administration of ethanol, both *in vitro* and *in vivo,* decreases let-7 levels and increases fibrosis markers and the stem cell marker, Lin28B. *In vitro,* HSCs treated with the inflammatory proteins LPS or TGF-

β exhibited decreased levels of let-7 as well as increased levels of migration, Lin28A/B, HMGA2, and mesenchymal markers. Knockout of let-7 in HSCs led to increased migration, indicating that lack of let-7 allows HSCs to become more activated. In human ALD tissues, let-7 levels were decreased while Lin28A/B levels and HMAG2 levels were increased, which indicates that these factors are involved in the severe injury to the liver induced by alcohol consumption. Knockout of Lin28B or HMGA2 in HSCs decreased cell migration and fibrosis levels. Lin28B-deficient mice showed decreased levels of fibrosis and mesenchymal markers in addition to decreased histopathology scores and decreased alanine aminotransferase levels compared to wild type ethanol-fed mice. Isolated HSCs from these mice showed decreased levels of fibrosis markers and mesenchymal mediators as well as increased levels of let-7.

It has been noted that ALD is characterized by a typical disease progression that begins as alcoholic fatty liver and eventually progresses to cirrhosis and possible hepatocellular carcinoma (HCC). It is unclear what controls the progression of the disease, but it may be tied to the livers of certain patients that have the inability to repair the damage caused by alcohol in a timely manner. The let-7/Lin28 axis is vitally important in the differentiation of cells during development. Cells that have more Lin28 activation have more of a stem cell or mesenchymal phenotype, whereas cells with high levels of let-7 are well-differentiated cells. This is well displayed in HCC. Lin28B has been shown to be upregulated in HCC samples while let-7 is downregulated [128]. This reactivation of

Lin28B in HCC samples indicates an attempt by the liver to repair the extensive damage caused by cirrhosis that continued uncontrolled.

The let-7/Lin28 axis appears to be an important tool that is utilized by the liver in order to repair injury and control the transformation of cells from the epithelial to mesenchymal (EMT) phenotype. Because HSCs need to undergo a mesenchymal transition in order to become activated and move to the area of injury where they lay down ECM for dividing cells, the let-7/Lin28 axis could be an important key to this activation. As we have shown, downregulation of Lin28B may decrease overall liver damage such as steatosis and fibrosis. This fibrosis reduction appears to be a result of blockage of HSC activation through modulation of the mesenchymal mediators Snail and Twist. Therefore, inhibition of Lin28B in patients could be an important therapeutic target for halting the progression of ALD and saving the lives of these patients as well as reducing the cost of care for these patients and the cost of liver transplantation.

Our findings identify a previously unrecognized mechanism for direct regulation of Lin28 and HMGA2 and mesenchymal reactions in HSCs; this mechanism involves non-coding RNA (ncRNA) in ALD. Aberrant mesenchymal reactions have been implicated in many human diseases including ALDs. The abusive consumption of alcohol can cause serious cellular injuries that often lead to activation of mesenchymal transition. Although let-7/Lin28 signaling has been tightly linked to liver injuries and disease outcome in many hepatic disorders, including human ALDs, its application to ethanol-

dependent ncRNA expression is novel. A better understanding of how ethanol interacts with specific cytokines to contribute to aberrant ncRNA expression in HSCs will clearly advance the field and increase our understanding of the mechanisms involved in the development of ALDs. Employing LCM and single cell analysis approaches to identify transcriptional and translational factors and their modified targets in HSCs during ALD development and progression are lacking, but such strategies could identify other novel targets that could be genetically or epigenetically modified in ALD.

With chronic alcohol abuse, the early and reversible liver damage occurs in HSCs and other hepatic cell types long before the onset of clinically symptomatic and irreversible forms of hepatitis, fibrosis, and cirrhosis. Currently, the mechanisms and regulation of ALDs at single cell levels are poorly understood, and the ALD-associated putative biomarkers and regulatory molecules in HSCs remain tenuous and unproven. In this study, we characterized the role of dysregulated let-7/Lin28 axis in ethanol-induced altered *mesenchymal signaling in HSCs* and Lin28 deficiency to ALD progression. The data presented here may have direct application to the future translational research targeting HSC activation and mesenchymal reactions for an improved diagnosis and treatment of ALD patients.

5. CONCLUSIONS

The studies presented here show that small cholangiocyte cell therapy in BDL mice is able to ameliorate liver fibrosis through de-activation of HSCs and activation of FoxA2. Small cholangiocyte cell therapy may reduce activity of DNMTs, which allows for demethylation of modulation of epigenetic methylation markers on FoxA2.

Additionally, we have shown that stem cell-derived EVs are able to reduce liver fibrosis by restoring FoxA2 in cholangiocytes that, in turn, deactivate HSCs in a mouse model of PSC. Furthermore, we have shown that a component of stem cell-derived EVs, let-7, modulates fibrosis in ALD mice by alteration of HSC mesenchymal markers.

FoxA2 has been shown to be important in liver repair. The activation or deactivation of FoxA2 by methylation could be important in the regulation of repair and subsequent reduction of fibrosis. Although not in liver, it was shown that silencing of FoxA2 by hypermethylation, contributed to hypersecretion of mucus during COPD [129]. FoxA2 suppression has also been linked to cancer growth and tumorigenesis and treatment with FoxA2 inhibits this cellular transformation [130]. It has also been theorized that FoxA2 may have a tumor suppressor role in endometrial cancer [131]. We have shown that FoxA2 is reduced in cholangiocytes during cholestatic liver injury. The repression of FoxA2 in damaged cholangiocytes could be a signal to the other cells in the liver and to resident or peripheral stem cells that the cholangiocytes have been injured. The

reduction of FoxA2 in the cholangiocytes could be the trigger not only to Kupffer cells to induce inflammation, but also to stellate cells to become activated. The lack of FoxA2 expression could be the lynchpin that maintains normal repair of the liver.

It is most likely that FoxA2 suppression alone is not sufficient to induce stem cells and/or progenitor cells to secrete EVs to help repair the liver. This is apparent in BDL or MDR2$^{-/-}$ mice where FoxA2 is decreased, but the liver continues to degenerate over time. It is unclear if stem cells are activated in these types of liver injury and the injury is so severe that it overwhelms any attempts at repair, or if they remain quiescent and do not react to help repair the liver injury. It also may be the case that in a dysfunctional liver, the amounts of EVs that are secreted by stem cells are not sufficient to affect the liver. It is clear that large amounts of stem cell-derived vesicles are enough to raise FoxA2 levels, which correlates with decreased fibrosis, biliary mass and inflammation.

EVs have been shown to be useful in various ways in medicine. Detection of circulating vesicles during disease, for example, is important. It has been reported that there are elevated EVs in the serum of patients with cardiovascular disease and in the synovial fluid of osteoarthritis patients [132, 133]. Treatment with EVs is a novel concept and a few groups have attempted it. In one study, EVs were shown to reduce inflammation in both diabetes and uveoretinits [95]. Other groups are using EVs as drug delivery systems and loading them with specific therapeutic contents [134]. Any of these methods for the use of EVs could be beneficial for liver disease patients. One way in which this has been

utilized is in adenocarcinoma patients where they showed elevated levels of Helicobacter pylori-derived extracellular vesicles in the gastric juices of these patients [135].

One known component of stem-cell-derived EVs is the miRNA, let-7, which has been shown to be decreased during liver injury [115]. The miRNA let-7 has been shown to inhibit IL-6, a primary component of the inflammatory response [136]. Overexpression of let-7 in ALD mice by inhibition of Lin28 reduced fibrosis and steatosis. This is consistent with the idea that stem-cell-derived EVs, which contain let-7, can reduce fibrosis and inflammation in liver disease. There is no direct link between let-7 and FoxA2. However, levels of let-7 are typically higher in differentiated cells and FoxA2 has been suggested to be a tumor suppressor, so they may possibly be in parallel pathways that are upregulated when cells are in a differentiated state.

One of the most important aspects of fibrosis is HSC activation. Because stellate cells undergo a transformation from a quiescent cell to a myofibroblast, an epithelial to mesenchymal transition must take place. We have shown that mesenchymal markers in HSCs are reduced in Lin28 knockout (let-7 overexpression) mice, indicating a reduction in EMT. Because let-7 is correlated with a more differentiated state, it is more than likely that HSCs are unable to undergo EMT, forcing them to remain in a quiescent state. An important characteristic of successful anti-fibrotic treatments appears to be induction of senescence in HSCs. We have seen in all three of these studies that reduction of fibrosis correlates with increases in stellate cell senescence, whereas increased fibrosis

correlated with decreased senescence. In the case of HSCs, senescence may indicate a deactivation of HSCs or possibly a mesenchymal to epithelial transition (MET). This form of deactivation could be especially important in cholangiopathies and ALD because these diseases typically progress to cirrhosis and end stage liver disease. The ability to deactivate stellate cells in cholestatic or ALD patients could possibly halt the progression of these diseases into end stage disease.

In conclusion, we have shown that liver fibrosis can be improved in cholestatic and alcoholic liver disease by treatment with progenitor cells, stem cell-derived EVs or let-7, a component of EVs. Successful treatment with these agents has a few common themes: 1. Increased expression of Fox2; 2. Reduced expression of inflammatory and fibrosis markers and 3. Deactivation of HSCs through reduction of mesenchymal markers and increased senescence. More studies are necessary to refine any of these treatments for the clinic, but there are promising data to indicate that these treatments could be modified to help treat cholestatic and/or ALD patients.

REFERENCES

1. Siegel, R.L., K.D. Miller, and A. Jemal, *Cancer statistics, 2015.* CA Cancer J Clin, 2015. **65**(1): p. 5-29.

2. Rahib, L., et al., *Projecting cancer incidence and deaths to 2030: the unexpected burden of thyroid, liver, and pancreas cancers in the United States.* Cancer Res, 2014. **74**(11): p. 2913-21.

3. Hale, A.J., *The minute structure of the liver: a review.* Glasgow Med J, 1951. **32**(10): p. 283-301.

4. Dawson, A.M., *Bile salts and fat absorption.* Gut, 1967. **8**(1): p. 1-3.
5. Falkowski, O., et al., *Regeneration of hepatocyte 'buds' in cirrhosis from intrabiliary stem cells.* J Hepatol, 2003. **39**(3): p. 357-64.

6. Lazaridis, K.N. and N.F. LaRusso, *The Cholangiopathies.* Mayo Clin Proc, 2015. **90**(6): p. 791-800.

7. Yoo, K.S., W.T. Lim, and H.S. Choi, *Biology of Cholangiocytes: From Bench to Bedside.* Gut Liver, 2016. **10**(5): p. 687-98.

8. Alpini, G., et al., *Molecular and functional heterogeneity of cholangiocytes from rat liver after bile duct ligation.* Am J Physiol, 1997. **272**(2 Pt 1): p. G289-97.

9. Tanimizu, N. and T. Mitaka, *Re-evaluation of liver stem/progenitor cells.* Organogenesis, 2014. **10**(2): p. 208-15.

10. Oikawa, T., et al., *Model of fibrolamellar hepatocellular carcinomas reveals striking enrichment in cancer stem cells.* Nat Commun, 2015. **6**: p. 8070.

11. Itoh, T. and A. Miyajima, *Liver regeneration by stem/progenitor cells.* Hepatology, 2014. **59**(4): p. 1617-26.

12. Zhang, L., et al., *The stem cell niche of human livers: symmetry between development and regeneration.* Hepatology, 2008. **48**(5): p. 1598-607.

13. Greenbaum, L.E. and R.G. Wells, *The role of stem cells in liver repair and fibrosis.* Int J Biochem Cell Biol, 2011. **43**(2): p. 222-9.

14. Zong, Y. and B.Z. Stanger, *Molecular mechanisms of bile duct development.* Int J Biochem Cell Biol, 2011. **43**(2): p. 257-64.

15. Fischer, U.M., et al., *Pulmonary passage is a major obstacle for intravenous stem cell delivery: the pulmonary first-pass effect.* Stem Cells Dev, 2009. **18**(5): p. 683-92.

16. Figueroa, F.E., et al., *Mesenchymal stem cell treatment for autoimmune diseases: a critical review.* Biol Res, 2012. **45**(3): p. 269-77.

17. Sharma, R.R., et al., *Mesenchymal stem or stromal cells: a review of clinical applications and manufacturing practices.* Transfusion, 2014. **54**(5): p. 1418-37.

18. Wakitani, S., et al., *Repair of articular cartilage defects in the patello-femoral joint with autologous bone marrow mesenchymal cell transplantation: three case reports involving nine defects in five knees.* J Tissue Eng Regen Med, 2007. **1**(1): p. 74-9.

19. Fiore, E., et al., *[Mesenchymal stem cells and regenerative medicine in liver cirrhosis]*. Medicina (B Aires), 2017. **77**(2): p. 135-142.

20. Van Haele, M. and T. Roskams, *Hepatic Progenitor Cells: An Update.* Gastroenterol Clin North Am, 2017. **46**(2): p. 409-420.

21. Gao, B. and R. Bataller, *Alcoholic liver disease: pathogenesis and new therapeutic targets.* Gastroenterology, 2011. **141**(5): p. 1572-85.

22. Higashi, T., S.L. Friedman, and Y. Hoshida, *Hepatic stellate cells as key target in liver fibrosis.* Adv Drug Deliv Rev, 2017.

23. Tsuchida, T. and S.L. Friedman, *Mechanisms of hepatic stellate cell activation.* Nat Rev Gastroenterol Hepatol, 2017.

24. Iredale, J.P., A. Pellicoro, and J.A. Fallowfield, *Liver Fibrosis: Understanding the Dynamics of Bidirectional Wound Repair to Inform the Design of Markers and Therapies.* Dig Dis, 2017. **35**(4): p. 310-313.

25. Arrese, M., A. Eguchi, and A.E. Feldstein, *Circulating microRNAs: emerging biomarkers of liver disease.* Semin Liver Dis, 2015. **35**(1): p. 43-54.

26. Jiang, J., et al., *Association of MicroRNA expression in hepatocellular carcinomas with hepatitis infection, cirrhosis, and patient survival.* Clin Cancer Res, 2008. **14**(2): p. 419-27.

27. Moss, E.G., R.C. Lee, and V. Ambros, *The cold shock domain protein LIN-28 controls developmental timing in C. elegans and is regulated by the lin-4 RNA.* Cell, 1997. **88**(5): p. 637-46.

28. Moss, E.G. and L. Tang, *Conservation of the heterochronic regulator Lin-28, its developmental expression and microRNA complementary sites.* Dev Biol, 2003. **258**(2): p. 432-42.

29. Yu, F., et al., *let-7 regulates self renewal and tumorigenicity of breast cancer cells.* Cell, 2007. **131**(6): p. 1109-23.

30. Nam, Y., et al., *Molecular basis for interaction of let-7 microRNAs with Lin28.* Cell, 2011. **147**(5): p. 1080-91.

31. Rybak, A., et al., *A feedback loop comprising lin-28 and let-7 controls pre-let-7 maturation during neural stem-cell commitment.* Nat Cell Biol, 2008. **10**(8): p. 987-93.

32. Le, M.T., et al., *MicroRNA-125b is a novel negative regulator of p53.* Genes Dev, 2009. **23**(7): p. 862-76.

33. Le, M.T., et al., *MicroRNA-125b promotes neuronal differentiation in human cells by repressing multiple targets.* Mol Cell Biol, 2009. **29**(19): p. 5290-305.

34. Bousquet, M., et al., *MicroRNA miR-125b causes leukemia.* Proc Natl Acad Sci U S A, 2010. **107**(50): p. 21558-63.

35. O'Connell, R.M., et al., *MicroRNAs enriched in hematopoietic stem cells differentially regulate long-term hematopoietic output.* Proc Natl Acad Sci U S A, 2010. **107**(32): p. 14235-40.

36. Ooi, A.G., et al., *MicroRNA-125b expands hematopoietic stem cells and enriches for the lymphoid-balanced and lymphoid-biased subsets.* Proc Natl Acad Sci U S A, 2010. **107**(50): p. 21505-10.

37. Ge, Y., Y. Sun, and J. Chen, *IGF-II is regulated by microRNA-125b in skeletal myogenesis.* J Cell Biol, 2011. **192**(1): p. 69-81.

38. Guo, S., et al., *MicroRNA miR-125a controls hematopoietic stem cell number.* Proc Natl Acad Sci U S A, 2010. **107**(32): p. 14229-34.

39. Cardinale, V., et al., *The biliary tree--a reservoir of multipotent stem cells.* Nat Rev Gastroenterol Hepatol, 2012. **9**(4): p. 231-40.

40. Alpini, G., et al., *Morphological, molecular, and functional heterogeneity of cholangiocytes from normal rat liver.* Gastroenterology, 1996. **110**(5): p. 1636-43.

41. Alpini, G., et al., *Molecular and functional heterogeneity of cholangiocytes from rat liver after bile duct ligation.* Am J Physiol Gastrointest Liver Physiol, 1997. **272**(2 Pt 1): p. G289-97.

42. Alpini, G., et al., *Heterogeneity of the proliferative capacity of rat cholangiocytes after bile duct ligation.* Am J Physiol Gastrointest Liver Physiol, 1998. **274**(4 Pt 1): p. G767-75.

43. Roskams, T.A., et al., *Nomenclature of the finer branches of the biliary tree: canals, ductules, and ductular reactions in human livers.* Hepatology, 2004. **39**(6): p. 1739-45.

44. Alvaro, D., et al., *Proliferating cholangiocytes: a neuroendocrine compartment in the diseased liver.* Gastroenterology, 2007. **132**(1): p. 415-31.

45. Glaser, S., et al., *Morphological and functional heterogeneity of the mouse intrahepatic biliary epithelium.* Lab Invest, 2009. **89**(4): p. 456-69.

46. Han, Y., et al., *Recent advances in the morphological and functional heterogeneity of the biliary epithelium.* Exp Biol Med (Maywood), 2013. **238**(5): p. 549-65.

47. Martinez-Anso, E., et al., *Immunohistochemical detection of chloride/bicarbonate anion exchangers in human liver.* Hepatology, 1994. **19**(6): p. 1400-6.

48. Glaser, S., et al., *Differential transcriptional characteristics of small and large biliary epithelial cells derived from small and large bile ducts.* Am J Physiol Gastrointest Liver Physiol, 2010. **299**(3): p. G769-77.

49. Yao, S., et al., *Long-term self-renewal and directed differentiation of human embryonic stem cells in chemically defined conditions.* Proc Natl Acad Sci U S A, 2006. **103**(18): p. 6907-12.

50. Christodoulou, C., et al., *Mouse ES and iPS cells can form similar definitive endoderm despite differences in imprinted genes.* J Clin Invest, 2011. **121**(6): p. 2313-25.

51. Bochkis, I.M., et al., *Hepatocyte-specific ablation of Foxa2 alters bile acid homeostasis and results in endoplasmic reticulum stress.* Nat Med, 2008. **14**(8): p. 828-36.

52. Long, X.B., et al., *Let-7a microRNA functions as a potential tumor suppressor in human laryngeal cancer.* Oncol Rep, 2009. **22**(5): p. 1189-95.

53. Boulter, L., et al., *Macrophage-derived Wnt opposes Notch signaling to specify hepatic progenitor cell fate in chronic liver disease.* Nat Med, 2012. **18**(4): p. 572-9.

54. Liu, M., et al., *IKKalpha activation of NOTCH links tumorigenesis via FOXA2 suppression.* Mol Cell, 2012. **45**(2): p. 171-84.

55. Kikuchi, Y., et al., *Notch signaling can regulate endoderm formation in zebrafish.* Dev Dyn, 2004. **229**(4): p. 756-62.

56. Maeda, Y., V. Dave, and J.A. Whitsett, *Transcriptional control of lung morphogenesis.* Physiol Rev, 2007. **87**(1): p. 219-44.

57. Chatzipantelis, P., et al., *CD56 as a useful marker in the regenerative process of the histological progression of primary biliary cirrhosis.* Eur J Gastroenterol Hepatol, 2008. **20**(9): p. 837-42.

58. Nagy, P., H.C. Bisgaard, and S.S. Thorgeirsson, *Expression of hepatic transcription factors during liver development and oval cell differentiation.* J Cell Biol, 1994. **126**(1): p. 223-33.

59. Kuver, R., et al., *Murine gallbladder epithelial cells can differentiate into hepatocyte-like cells in vitro.* Am J Physiol Gastrointest Liver Physiol, 2007. **293**(5): p. G944-55.

60. Strack, I., et al., *beta-Adrenoceptor blockade in sclerosing cholangitis of Mdr2 knockout mice: antifibrotic effects in a model of nonsinusoidal fibrosis.* Lab Invest, 2011. **91**(2): p. 252-61.

61. Ludwig, J., E.R. Dickson, and G.S. McDonald, *Staging of chronic nonsuppurative destructive cholangitis (syndrome of primary biliary cirrhosis).* Virchows Arch A Pathol Anat Histol, 1978. **379**(2): p. 103-12.

62. Alpini, G., et al., *Biliary physiology in rats with bile ductular cell hyperplasia. Evidence for a secretory function of proliferated bile ductules.* J Clin Invest, 1988. **81**(2): p. 569-78.

63. Glaser, S., et al., *Secretin stimulates biliary cell proliferation by regulating expression of microRNA 125b and microRNA let7a in mice.* Gastroenterology, 2014. **146**(7): p. 1795-808 e12.

64. Francis, H., et al., *Small mouse cholangiocytes proliferate in response to H1 histamine receptor stimulation by activation of the IP3/CaMK I/CREB pathway.* Am J Physiol Cell Physiol, 2008. **295**(2): p. C499-513.

65. Hay, D.C., et al., *Highly efficient differentiation of hESCs to functional hepatic endoderm requires ActivinA and Wnt3a signaling.* Proc Natl Acad Sci U S A, 2008. **105**(34): p. 12301-6.

66. Li, L.C., *Designing PCR primer for DNA methylation mapping.* Methods Mol Biol, 2007. **402**: p. 371-84.

67. Fu, S., et al., *Involvement of histone acetylation of Sox17 and Foxa2 promoters during mouse definitive endoderm differentiation revealed by microRNA profiling.* PLoS One, 2011. **6**(11): p. e27965.

68. Wu, N., et al., *The secretin/secretin receptor axis modulates liver fibrosis through changes in transforming growth factor-beta1 biliary secretion in mice.* Hepatology, 2016. **64**(3): p. 865-79.

69. Marzioni, M., et al., *Taurocholate prevents the loss of intrahepatic bile ducts due to vagotomy in bile duct-ligated rats.* Am J Physiol Gastrointest Liver Physiol, 2003. **284**(5): p. G837-52.

70. Hu, M., et al., *Wnt/beta-catenin signaling in murine hepatic transit amplifying progenitor cells.* Gastroenterology, 2007. **133**(5): p. 1579-91.

71. Sekiya, S. and A. Suzuki, *Direct conversion of mouse fibroblasts to hepatocyte-like cells by defined factors.* Nature, 2011. **475**(7356): p. 390-3.

72. Weiss, T.S., et al., *Hepatic progenitor cells from adult human livers for cell transplantation.* Gut, 2008. **57**(8): p. 1129-38.

73. Lee, S.P., C.E. Savard, and R. Kuver, *Gallbladder epithelial cells that engraft in mouse liver can differentiate into hepatocyte-like cells.* Am J Pathol, 2009. **174**(3): p. 842-53.

74. Yovchev, M.I., et al., *Identification of adult hepatic progenitor cells capable of repopulating injured rat liver.* Hepatology, 2008. **47**(2): p. 636-47.

75. Song, L. and R.S. Tuan, *Transdifferentiation potential of human mesenchymal stem cells derived from bone marrow.* FASEB J, 2004. **18**(9): p. 980-2.

76. Turner, R., et al., *Human hepatic stem cell and maturational liver lineage biology.* Hepatology, 2011. **53**(3): p. 1035-45.

77. Glaser, S.S., et al., *Morphological and functional heterogeneity of the mouse intrahepatic biliary epithelium.* Lab Invest, 2009. **89**(4): p. 456-69.

78. Lleo, A., et al., *Immunoglobulin M levels inversely correlate with CD40 ligand promoter methylation in patients with primary biliary cirrhosis.* Hepatology, 2012. **55**(1): p. 153-60.

79. Mitchell, M.M., et al., *Epigenetic investigation of variably X chromosome inactivated genes in monozygotic female twins discordant for primary biliary cirrhosis.* Epigenetics, 2011. **6**(1): p. 95-102.

80. Chiang, J.Y., *Bile acids: regulation of synthesis.* J Lipid Res, 2009. **50**(10): p. 1955-66.

81. Jensen, K., et al., *Autocrine regulation of biliary pathology by activated cholangiocytes.* Am J Physiol Gastrointest Liver Physiol, 2012. **302**(5): p. G473-83.

82. Li, T. and J.Y. Chiang, *A novel role of transforming growth factor beta1 in transcriptional repression of human cholesterol 7alpha-hydroxylase gene.* Gastroenterology, 2007. **133**(5): p. 1660-9.

83. Ader, T., et al., *Transcriptional profiling implicates TGFbeta/BMP and Notch signaling pathways in ductular differentiation of fetal murine hepatoblasts.* Mech Dev, 2006. **123**(2): p. 177-94.

84. Pappano, W.N., et al., *Coding sequence and expression patterns of mouse chordin and mapping of the cognate mouse chrd and human CHRD genes.* Genomics, 1998. **52**(2): p. 236-9.

85. Spee, B., et al., *Characterisation of the liver progenitor cell niche in liver diseases: potential involvement of Wnt and Notch signalling.* Gut, 2010. **59**(2): p. 247-57.

86. Cai, J., et al., *BMP and TGF-beta pathway mediators are critical upstream regulators of Wnt signaling during midbrain dopamine differentiation in human pluripotent stem cells.* Dev Biol, 2013. **376**(1): p. 62-73.

87. Aravinthan, A., et al., *Hepatocyte expression of the senescence marker p21 is linked to fibrosis and an adverse liver-related outcome in alcohol-related liver disease.* PLoS One, 2013. **8**(9): p. e72904.

88. Williams, M.J., A.D. Clouston, and S.J. Forbes, *Links between hepatic fibrosis, ductular reaction, and progenitor cell expansion.* Gastroenterology, 2014. **146**(2): p. 349-56.

89. Eaton, J.E., et al., *Pathogenesis of primary sclerosing cholangitis and advances in diagnosis and management.* Gastroenterology, 2013. **145**(3): p. 521-36.

90. Smit, J.J., et al., *Homozygous disruption of the murine mdr2 P-glycoprotein gene leads to a complete absence of phospholipid from bile and to liver disease.* Cell, 1993. **75**(3): p. 451-62.

91. Gilsanz, C., et al., *Adipose-derived mesenchymal stem cells slow disease progression of acute-on-chronic liver failure.* Biomed Pharmacother, 2017. **91**: p. 776-787.

92. El-Kehdy, H., et al., *Immunoprofiling of Adult-Derived Human Liver Stem/Progenitor Cells: Impact of Hepatogenic Differentiation and Inflammation.* Stem Cells Int, 2017. **2017**: p. 2679518.

93. Todorova, D., et al., *Extracellular Vesicles in Angiogenesis.* Circ Res, 2017. **120**(10): p. 1658-1673.

94. Morales-Kastresana, A., et al., *Labeling Extracellular Vesicles for Nanoscale Flow Cytometry.* Sci Rep, 2017. **7**(1): p. 1878.

95. Shigemoto-Kuroda, T., et al., *MSC-derived Extracellular Vesicles Attenuate Immune Responses in Two Autoimmune Murine Models: Type 1 Diabetes and Uveoretinitis.* Stem Cell Reports, 2017. **8**(5): p. 1214-1225.

96. Nargesi, A.A., L.O. Lerman, and A. Eirin, *Mesenchymal stem cell-derived extracellular vesicles for renal repair.* Curr Gene Ther, 2017.

97. Severino, V., et al., *Extracellular Vesicles in Bile as Markers of Malignant Biliary Stenoses.* Gastroenterology, 2017.

98. McDaniel, K., et al., *Forkhead box A2 regulates biliary heterogeneity and senescence during cholestatic liver injury in micedouble dagger.* Hepatology, 2017. **65**(2): p. 544-559.

99. Eom, Y.W., K.Y. Shim, and S.K. Baik, *Mesenchymal stem cell therapy for liver fibrosis.* Korean J Intern Med, 2015. **30**(5): p. 580-9.

100. Omar, R., et al., *Hepatic Stellate Cells in Liver Fibrosis and siRNA-Based Therapy.* Rev Physiol Biochem Pharmacol, 2016. **172**: p. 1-37.

101. Zhou, L., et al., *Casticin attenuates liver fibrosis and hepatic stellate cell activation by blocking TGF-beta/Smad signaling pathway.* Oncotarget, 2017.

102. Barile, L. and G. Vassalli, *Exosomes: Therapy delivery tools and biomarkers of diseases.* Pharmacol Ther, 2017. **174**: p. 63-78.

103. Louvet, A. and P. Mathurin, *Alcoholic liver disease: mechanisms of injury and targeted treatment.* Nat Rev Gastroenterol Hepatol, 2015. **12**(4): p. 231-42.

104. McDaniel, K., et al., *The functional role of microRNAs in alcoholic liver injury.* J Cell Mol Med, 2014. **18**(2): p. 197-207.

105. Taura, K., et al., *Controversies over the Epithelial-to-Mesenchymal Transition in Liver Fibrosis.* J Clin Med, 2016. **5**(1).

106. Wang, Y.P., et al., *Lipocalin-2 negatively modulates the epithelial-to-mesenchymal transition in hepatocellular carcinoma through the epidermal growth factor (TGF-beta1)/Lcn2/Twist1 pathway.* Hepatology, 2013. **58**(4): p. 1349-61.

107. Mavila, N., et al., *Expansion of prominin-1-expressing cells in association with fibrosis of biliary atresia.* Hepatology, 2014. **60**(3): p. 941-53.

108. Pellicoro, A., et al., *Liver fibrosis and repair: immune regulation of wound healing in a solid organ.* Nat Rev Immunol, 2014. **14**(3): p. 181-94.

109. Bansal, M.B., *Hepatic stellate cells: fibrogenic, regenerative or both? Heterogeneity and context are key.* Hepatol Int, 2016. **10**(6): p. 902-908.

110. Senoo, H., N. Kojima, and M. Sato, *Vitamin A-storing cells (stellate cells).* Vitam Horm, 2007. **75**: p. 131-59.

111. Karin, D., et al., *The characteristics of activated portal fibroblasts/myofibroblasts in liver fibrosis.* Differentiation, 2016. **92**(3): p. 84-92.

112. Chen, Y., et al., *MicroRNAs as key mediators of hepatic detoxification.* Toxicology, 2016. **368-369**: p. 80-90.

113. Meng, F., et al., *Epigenetic regulation of miR-34a expression in alcoholic liver injury.* Am J Pathol, 2012. **181**(3): p. 804-17.

114. Han, Y., et al., *miR-34a-dependent overexpression of Per1 decreases cholangiocarcinoma growth.* J Hepatol, 2016. **64**(6): p. 1295-304.

115. McDaniel, K., et al., *Lin28 and let-7: roles and regulation in liver diseases.* Am J Physiol Gastrointest Liver Physiol, 2016. **310**(10): p. G757-65.

116. Yu, J., et al., *Induced pluripotent stem cell lines derived from human somatic cells.* Science, 2007. **318**(5858): p. 1917-20.

117. Hurteau, G.J., et al., *Stable expression of miR-200c alone is sufficient to regulate TCF8 (ZEB1) and restore E-cadherin expression.* Cell Cycle, 2009. **8**(13): p. 2064-9.

118. Hurteau, G.J., et al., *Overexpression of the microRNA hsa-miR-200c leads to reduced expression of transcription factor 8 and increased expression of E-cadherin.* Cancer Res, 2007. **67**(17): p. 7972-6.

119. Choi, S.S. and A.M. Diehl, *Epithelial-to-mesenchymal transitions in the liver.* Hepatology, 2009. **50**(6): p. 2007-13.

120. Viswanathan, S.R., et al., *Lin28 promotes transformation and is associated with advanced human malignancies.* Nat Genet, 2009. **41**(7): p. 843-8.

121. Zhang, J., et al., *The polymorphism in the let-7 targeted region of the Lin28 gene is associated with increased risk of type 2 diabetes mellitus.* Mol Cell Endocrinol, 2013. **375**(1-2): p. 53-7.

122. Mathews, S., et al., *Animals models of gastrointestinal and liver diseases. Animal models of alcohol-induced liver disease: pathophysiology, translational relevance, and challenges.* Am J Physiol Gastrointest Liver Physiol, 2014. **306**(10): p. G819-23.

123. Francis, H., et al., *Regulation of the extrinsic apoptotic pathway by microRNA-21 in alcoholic liver injury.* J Biol Chem, 2014. **289**(40): p. 27526-39.

124. Shell, S., et al., *Let-7 expression defines two differentiation stages of cancer.* Proc Natl Acad Sci U S A, 2007. **104**(27): p. 11400-5.

125. Lee, S.H., et al., *The ubiquitin ligase human TRIM71 regulates let-7 microRNA biogenesis via modulation of Lin28B protein.* Biochim Biophys Acta, 2014. **1839**(5): p. 374-86.

126. Viswanathan, S.R., G.Q. Daley, and R.I. Gregory, *Selective blockade of microRNA processing by Lin28.* Science, 2008. **320**(5872): p. 97-100.

127. Van Wynsberghe, P.M., et al., *LIN-28 co-transcriptionally binds primary let-7 to regulate miRNA maturation in Caenorhabditis elegans.* Nat Struct Mol Biol, 2011. **18**(3): p. 302-8.

128. Cheng, S.W., et al., *Lin28B is an oncofetal circulating cancer stem cell-like marker associated with recurrence of hepatocellular carcinoma.* PLoS One, 2013. **8**(11): p. e80053.

129. Song, J., et al., *Aberrant DNA methylation and expression of SPDEF and FOXA2 in airway epithelium of patients with COPD.* Clin Epigenetics, 2017. **9**: p. 42.

130. Ding, B., et al., *Forkhead Box A2 (FOXA2) inhibits the invasion and tumorigenesis in glioma cells.* Oncol Res, 2016.

131. Smith, B., et al., *The mutational spectrum of FOXA2 in endometrioid endometrial cancer points to a tumor suppressor role.* Gynecol Oncol, 2016. **143**(2): p. 398-405.

132. Jansen, F., G. Nickenig, and N. Werner, *Extracellular Vesicles in Cardiovascular Disease: Potential Applications in Diagnosis, Prognosis, and Epidemiology.* Circ Res, 2017. **120**(10): p. 1649-1657.

133. Kolhe, R., et al., *Gender-specific differential expression of exosomal miRNA in synovial fluid of patients with osteoarthritis.* Sci Rep, 2017. **7**(1): p. 2029.

134. Gao, J., S. Wang, and Z. Wang, *High yield, scalable and remotely drug-loaded neutrophil-derived extracellular vesicles (EVs) for anti-inflammation therapy.* Biomaterials, 2017. **135**: p. 62-73.

135. Choi, H.I., et al., *Helicobacter pylori-derived extracellular vesicles increased in the gastric juices of gastric adenocarcinoma patients and induced inflammation mainly via specific targeting of gastric epithelial cells.* Exp Mol Med, 2017. **49**(5): p. e330.

136. Wei, Y.B., et al., *Elevation of Il6 is associated with disturbed let-7 biogenesis in a genetic model of depression.* Transl Psychiatry, 2016. **6**: p. e869.